Global Acoustic Mapping of Ocean Temperatures

GAMOT

°C

Original contains color plates: All DTIC reproductions will be in black and white.

Woods Hole Oceanographic Institution
The Pennsylvania State University
Naval Research Laboratory–Stennis
The Florida State University
University of Alaska
University of Texas at Austin

DTIC QUALITY INSPECTED 2

QUARTERLY PROGRESS REPORT
January–March 1994

94 6 8 085

DISCLAIMER NOTICE
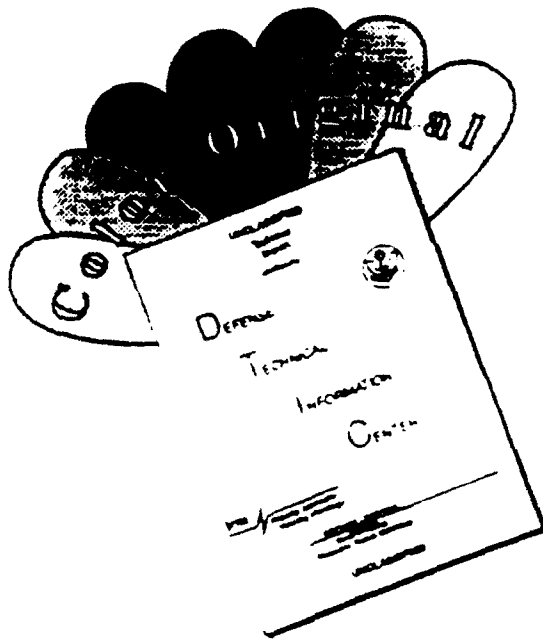
THIS DOCUMENT IS BEST QUALITY AVAILABLE. THE COPY FURNISHED TO DTIC CONTAINED A SIGNIFICANT NUMBER OF COLOR PAGES WHICH DO NOT REPRODUCE LEGIBLY ON BLACK AND WHITE MICROFICHE.

GAMOT

May 10, 1994

Dr. Ralph Alewine
Advanced Research Projects Agency
3701 North Fairfax Drive
Arlington, VA 22203-1714

Dear Dr. Alewine,

The attached report fulfills the fourth quarterly progress report requirement for the period from January 1, 1994 to March 31, 1994 as contained in the ARPA Grant No: MDA972-93-1-0004 entitled "Real Time System for Practical Acoustic Monitoring of Global Ocean Temperature" issued by the Contracts Management Office. The United States Government has a royalty-free license throughout the world in all copy rightable material contained herein. This report is approved for unlimited distribution and public release. Additional copies of this report will be mailed to the distribution list contained in Attachment Number 2 of the Grant.

Financial status reports will be submitted separately from this report. Woods Hole Oceanographic Institution, as the Grantee, will submit all financial reports directly to you.

The information contained in this report represents the inputs and opinions of the entire GAMOT team; the Woods Hole Oceanographic Institution, the Pennsylvania State University, the Applied Research Laboratory, the Florida State University, University of Alaska, University of Texas at Austin and NRL-Stennis. If this report generates any questions, please do not hesitate to direct your questions or comments to the Principal Investigators or the Program Manager.

John L. Spiesberger
Principal Investigator
WHOI/PSU

Daniel E. Frye
Principle Investigator
WHOI

John M. Kenny
Program Manager
ARL

GAMOT EXECUTIVE SUMMARY

Work continues on all GAMOT Tasks as described in ARPA Grant No: MDA972-93-1-0004.

• **Task A.** Task A work is on schedule. We are continuing the investigation of the acoustic thermometry data taken in 1987 along fifteen basin scale sections in the northeast Pacific. We have completed a number of tomographic inverse simulations using Cornuelle's inverse software. Incorporation of the ray trace software into the tomography program is proceeding smoothly and nearing completion. We are at the midpoint of automating the tomography process and have completed all interface definitions.

Work is nearing completion on the development of the signal processing package for the SSAR. System integration will start next quarter.

• **Task B.** The FSU tasks and deliverables are on schedule. We are continuing to analyze the results of our estimates of acoustic travel time anomalies on our reduced gravity model of the northeastern Pacific Ocean. These results clearly demonstrate that the interannual variability of the anomalies is dominated by the large scale Rossby waves propagating off the coast of North America. Additionally, we are developing an adjoint code to assimilate acoustic results into a layered model.

This report includes the accomplishments and activities of NRL-Stennis. A $1/8°$ 6-layered Pacific Ocean simulation north of 20° S with realistic bottom topography was driven by a monthly ECMWF wind climatology averaged over 1981-1991. A $1/4°$ 6-layered global simulation with realistic topography was run from 1981 to 1993 driven by ECMWF 1000mb winds. The 81-91 ECMWF mean was replaced by the annual mean from the Hellerman-Rosenstein wind stress climatology. The model had been spun up to statistical equilibrium using the Hellerman-Rosentstein wind stress climatology prior to the 81-93 integration. The model output was saved at 3.05 day intervals.

• **Task C.** Development of the SSAR is nearing completion and fabrication of the operational units has begun. No significant delays or problems have been encountered. The long-term, free drifting test of the Standard SSAR prototype was terminated following a failure of the conductor assembly in the hose section. The buoy was retrieved on March 10, 1994 about 120 miles north of Bermuda. It was deployed for a total of four months. The failure mode was abrasion of the conductors where they came into contact with the hose wall. A new combined stop rope/conductor assembly has been designed to eliminate this problem, similar to what was originally used in the Snubber SSAR prototype, which has not experienced the abrasion failure.

Laboratory fatigue testing of short hose sections has continued at TMT. A successful long term test of the third test hose has been completed. The test has run for 10^6 cycles without hose failure, where 5×10^5 cycles was the goal of the tests. These tests were designed to mimic maximum forcing in the operational

systems. The test section with conductors built into the hose wall, however, failed after 140,000 cycles and the decision was made to delay development of this design. The integrated stop rope/conductor assembly design will be used instead.

Two tests of the ultra short baseline acoustic navigation system have been completed. In the first, the acoustic array was carefully calibrated in an acoustic test facility to document the accuracy, sensitivity, and resolution of the array. Following these tests, a field trial at the AUTEC range in the Bahamas was performed using a SSAR equipped with two acoustic pingers that were tracked by the range. A direct and independent measurement of array location relative to the surface float was the result. This result combined with the GPS tests conducted previously in Bermuda provide unambiguous verification of the accuracy of the SSAR positioning.

Schedules for the complete system test are on hold because the ATOC source schedule is up in the air. We are looking at alternatives to the ATOC sources for conducting the final SSAR at-sea tests.

• **TASK D.** A draft version of the 70 Hz source procurement proposal was discussed with ARPA at a meeting on March 7, 1994. The final proposal has been prepared and is presently undergoing institutional review. It will be submitted within a few weeks to ARPA. It presents two options for source procurement and testing with an 18 month schedule. Because there have been no changes to the status of Task D, the Task D section has not been included in this report.

• **Meetings.** An ATOC/GAMOT Science workshop was hosted by Dr. J. O'Brien in March at Florida State University.

• **Issues and Concerns.** In the previous quarterly reports, two issues were addressed:
• Acoustic interaction of cabled sources with the bottom slope, and
• Identification of a source for the autonomous mooring.
These issues have not been resolved and there is no new information to report.

There is one new issues:
• Final SSAR acoustic/processing tests need to be performed at sea with a suitable source transmitting M sequences. Rather than wait for the ATOC sources to go on line, the SSARs should be tested with another source which will give us time to correct problems during the hiatus. The AUTEC range operates a suitable source at 160 dB source level that could be used for these tests. In fact we ran this source during the navigation tests in April with an M-sequence signal. An Operational Test Plan is in preparation which will outline the tests to be performed with the AUTEC source in August.

GAMOT Review: John Spiesberger
TASK A

15 May 1994

All Task A work is on schedule. In the last quarter we have accomplished the following tasks.

1. Programs for semi-automating the comparison between forward models and acoustic thermometry data have been written and are in use. The forward model is based on ray tracing using the algorithm called ZRAY (Spiesberger, Terray, and Prada, 1994). These algorithms are being used to identify the acoustic multipaths measured in the acoustic thermometer experiments taken in the northeast Pacific in 1987. Fifteen sections are under investigation, ranging between 1000 and 3000 km. To date, most of the sections have been successfully understood with the ray trace model.

2. A theoretical investigation has been conducted which has found that it is possible that ray theory can be extended to acoustic frequencies below 100 Hz. Previously, it has been believed by the acoustic oceanography community that ray theory was not an accurate method for computing travel times below 100 Hz. A manuscript draft will soon be submitted for publication (Draganov and Spiesberger, 1994).

3. A new parabolic approximation to the acoustic wave equation has been developed. This new approximation has much less error in absolute acoustic phase than previous approximations. Thus, it can be used to accurately compute absolute times of travel of sound without the user having to specify a reference speed of sound. This new parabolic approximation also is valid for high grazing angles. A manuscript describing these findings will be submitted for publication soon (Tappert, Spiesberger, and Boden, 1994). Tappert's involvement in this project was funded through Task A, under subcontract to Penn State University.

4. We have computed travel times of sound through the Florida State and Naval Research Lab models and compared these times with those measured in the Kaneohe source experiment in the 1980's. The Kaneohe source experiment found that,

    (a) Travel times changed by about ± 0.2 s at interannual time scales (Spiesberger et al., 1993).

(b) The spatially averaged temperature of the northeast Pacific is structured. Thus, stations separated by only 500 km detected different changes in the spatially averaged temperature to the Kaneohe source at 4000 km distance (Spiesberger et al., 1993).

The travel times through the FSU and NRL models both predict travel times which change by about ±0.2 s. The NRL model predicts that receivers separated by 500 km along the coast have different changes in section averaged temperature. Thus the NRL model produces many of the observed characteristics observed from the Kaneohe source experiment. The NRL model has been run with slightly different initial condition to investigate limits of predictability. Our conclusion to date is that the class of models used by GAMOT resemble the Kaneohe source data, and thus appear to be an effective approach toward understanding interannual and interdecadal variability in the ocean. This natural variability is necessary to quantify to detect global warming.

5. The acoustic multipaths from the Kaneohe source have been identified at one SOSUS station using a ray tracing algorithm called ZRAY. This was a breakthrough since this is the furthest, 4000 km, that ray theory has been successfully used to understand acoustic propagation in the ocean. The acoustic source was centered at 133 Hz. Travel times from this section are being compared to an eddy resolving section taken in July 1988 by NAVOCEANO. These findings will be prepared for publication later this year.

6. Numerical simulations have begun which will demonstrate the improved resolution obtained with drifting receivers compared with fixed receivers.

7. Numerical simulations have begun which will demonstrate that drifting receivers suppress the "noise" from the mesoscale field better than stationary receivers. The mesoscale is probably the biggest source of noise when looking for climate change in the ocean.

8. We have started feasibility studies to investigate how to map climate changes in the Southern Ocean using autonomously moored sources and SSARs. The idea is to put the sources and receivers south of the Antarctic convergence to avoid the acoustic problems related to crossing that front.

9. We have begun automating the inverse model.

REFERENCES

1. Draganov, A. and Spiesberger, J., Diffraction and modelling pulse delays in structured media, in preparation, (1994).

2. Spiesberger, J.L., Frye, D., O'Brien, J., Hurlburt, H., McCaffrey, J., Johnson, M., Global Acoustic Mapping of Ocean Temperatures (GAMOT), proceedings, Oceans 93', (1993).

3. Spiesberger, J.L., Terray, E., and Prada, K., Successful ray modelling of acoustic multipaths over a 3000 km section in the Pacific, in press, J. Acoust. Soc. Am., (1994).

4. Tappert, F., Spiesberger, J., New full-wave approximation for ocean acoustic travel time predictions, (1994).

NUM	TASK A	Start Date	Finish Date
A.1	ESTIMATE IMPROVED RESOLUTION FROM SSAR BY NUMERICAL SIMULATION	1/15/94	1/15/95
A.2	DETERMINE THE OPTIMUM :		
	SSAR ARRAY DEPTH	5/1/93	6/30/93
	SOURCE LOCATION AND DEPTH	5/1/93	11/30/93
A.3	ESTIMATE THE INFLUENCE OF FREQ, INCLINATION, DISTANCE AND SVP ON MULTIPATH STABILITY	5/1/93	6/30/95
A.4	DEVELOP ALGORITHMS AND COMPUTATIONS WHICH:		
	DO NOT GENERATE EXTRANEOUS EIGEN RAYS	5/1/93	5/15/93
	CALC LOSS FOR GEOMETRIC RAYS	5/1/93	5/15/93
	CALC LOSS FOR SHADOW ZONES OF CAUSTICS	5/1/93	5/15/93
A.5	INCORPORATE THE RAY TRACE ALGORITHM INTO THE INVERSE PROGRAM	7/15/93	5/15/94
A.6	ASSIMILATE TOMO DATA INTO O'BRIEN OCEAN MODEL	9/15/94	4/1/95
A.7	AUTOMATE THE PROCEDURE TO CHANGE SPATIAL COORDS OF MULTIPATHS DUE TO SEASONAL CYCLE	5/1/93	6/30/95
A.8	DEMO REAL TIME TOMOGRAPHY:		

Gantt chart timeline spanning 1993, 1994, and 1995 (months A M J J A S O N D J F M A M J J A S O N D J F M A M J J).

NUM	TASK A	Start Date	Finish Date
	USING DATA FROM SS4R	1/15/95	6/30/95
	USING DATA FROM FIXED RCVRS	3/15/95	6/30/95
A.9	ANALYSIS OF 1987 TOMO DATA TO DETERMINE SEASONAL CYCLE INFLUENCES ON ACOUSTIC TRAVEL TIMES:		
	FORWARD PROBLEM	7/15/93	6/30/94
	INVERSE PROBLEM	9/15/93	8/30/94
A.10	SIMULATION OF OCEAN CLIMATE TEMPS FROM AN O'BRIEN OCEAN MODEL USING SSARS	5/1/94	5/30/95

1993 1994 1995
A M J J A S O N D J F M A M J J A S O N D J F M A M J J

GAMOT QUARTERLY REPORT
FIRST QUARTER 1994

FLORIDA STATE UNIVERSITY
PROFESSOR JAMES J. O'BRIEN

SUMMARY

We are continuing to analyze the results of our estimates of acoustic travel time anomalies in our reduced gravity model of the northeast Pacific ocean. These results clearly demonstrate that the interannual variability of the anomalies is dominated by the large-scale Rossby-waves propagating off the coast of North America. Additionally, we are developing an adjoint code to assimilate acoustic results into a layered model.

TASK-B STATUS

B4 (update). Two model runs will be compared below. Both contain a Kelvin wave from a wind-driven equatorial model input at the southeastern boundary (described in previous reports). Case (i) is only forced by the Kelvin wave. Case (ii) includes local windstress. The model was spun-up for 20 years with climatological winds and a climatological Kelvin wave from the equatorial model. Observed winds and the raw Kelvin signal were then used to run the model from 1961-1989.

The model circulation for (i) and (ii) and method of computing travel time anomaly (TTA) was discussed in the previous quarterly report.

The paths over which TTAs are estimated are shown in Fig. 1 and the TTAs for (i) and (ii) are in Fig. 2. A strong correlation exists between (i) and (ii); the linear correlation c is found to vary from 0.6 to 0.8 and are shown in Fig, 2. There are two types of differences between the TTAs for the two cases. The first difference is due to the seasonal variations of the winds, driving a strong annual signal which does not appear in the remote-only case, as seen in Fig. 2. There are also times when the signal in case (i) appears to lag the signal in case (ii). For example, across path #1 the TTA for (ii) reaches a maximum in late 1976 and for (i) the maximum is in late 1977. However, the maxima during 1982-1983 coincide. The mechanism behind this lag remains to be resolved in detail, but it is clearly related to the effects of wind-forcing.

Spectral analysis of the TTAs for case (ii) is shown is Fig. 3. The annual signal is the only clear peak. The lack of other peaks is probably the result of the nonstationary properties of the signals and the significant power in the lowest frequencies. A different perspective on the spectral characteristics is obtained by examining their wavelet transform.

Figure 4 not only reveals the annual signal as does Fig. 3., but its amplitude variation is also indicated. For path #1 the annual signal lessens during the early 1970s, 1976 and 1984-85. The amount of variation depends on the particular path and, as in Fig. 3, path #9 and #10 show no annual variations.

Following the local modulus maximum indicates the flow of energy in the signal and simplifies the comparisons between case (i) and (ii). Figure 5 shows the local modulus maximum of Fig. 4. Lots of similarity is seen at the longer periods between the winds only and winds plus remote cases, as expected from the visual impression of Fig. 2. Interpreting the wavelet transform deep within the cones of influence is problematic as the transform loses accuracy as one penetrates these regions.

B5. Design of new models. Part of this work is being done in collaboration with researchers at the Naval Research Laboratories (NRL). Ocean models very similar to the FSU model have been developed, but with additional complexity. Details of the NRL models are discussed in the previous report. We are also developing an optimal control method to assimilate oceanic tomography data into the upper layer of an ocean model. The goal is to obtain an improved estimate of the time independent density field. The optimal spatial structure based on the best fit of the model to observations is determined. The variational cost function measures two "distances": i) between the acoustic tomography data and the model counterpart which can be expressed in terms of model variables, and ii) the discrepancy between the model density and Levitus density data. At this time no long-term tomographic data is available; therefore, several identical twin experiments will be performed in order to test the assimilation technique.

FIGURES

Fig 1. Great circle paths used for calculations of travel time.
Fig 2. Travel time anomolies. Blue is case (i) and black is case (ii). The TTA values are adjustable by an unknown coefficient. The linear correlation coefficient between the two cases is shown. The final latitude of the path ⁃ indicated.
Fig.3. The power spectrum for the TTA's for case (ii). The linear trend and mean were removed before analysis. Four forward and backward Hanning passes were applied to the spectrum.
Fig.4. The wavelet transform modulus for cases (i) and (ii). The modulus is related to the energy density. The path number is indicated at the top of the page. The upper plot is for case (ii) and the lower is case (i). The horizontal axis is time, the left vertical axis is wavelet-scale and the right vertical axis is actual period in years. Colors are from blue (minimum) to white (maximum) and the diagonal lines represent the "cones of influence" where the transform begins to lose accuracy.
Fig. 5. The lines of local maximum for Fig.4. Blue is case (i) and black is case (ii). The vertical axis is time period in years.

Great Circle Paths

path # 1; c= 0.79

(a)

latitude: 21.230

path # 2; c= 0.79

(b)

latitude: 22.840

path # 3; c= 0.72

latitude: 24.660

path # 4; c= 0.67

latitude: 26.460

path #1

path #2

path #3

path #4

path #5 path #6 path #7 path #8

path #9

path #10

2

SCALE (YEARS)

SCALE (YEARS)

S
F

SCALE (YEARS)

SCALE (YEARS)

SCALE (YEARS)

SCALE (YEARS)

SCALE (YEARS)

#

8

SCALE (YEARS)
1970 1975 1980 1985 1990
10 8 6 4 2 1

SCALE (YEARS)
1970 1975 1980 1985 1990
10 8 6 4 2 1

SCALE (YEARS)

SCALE (YEARS)
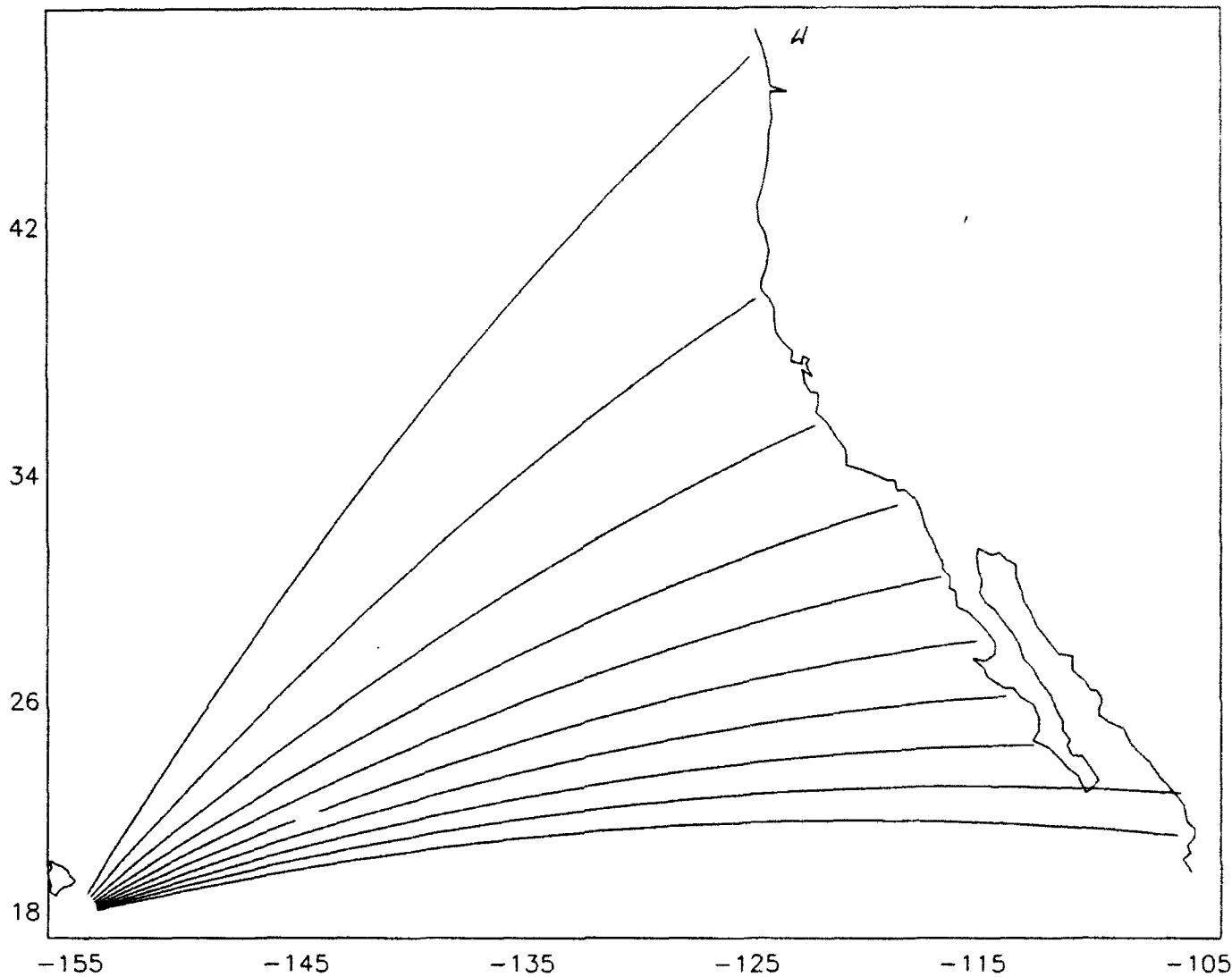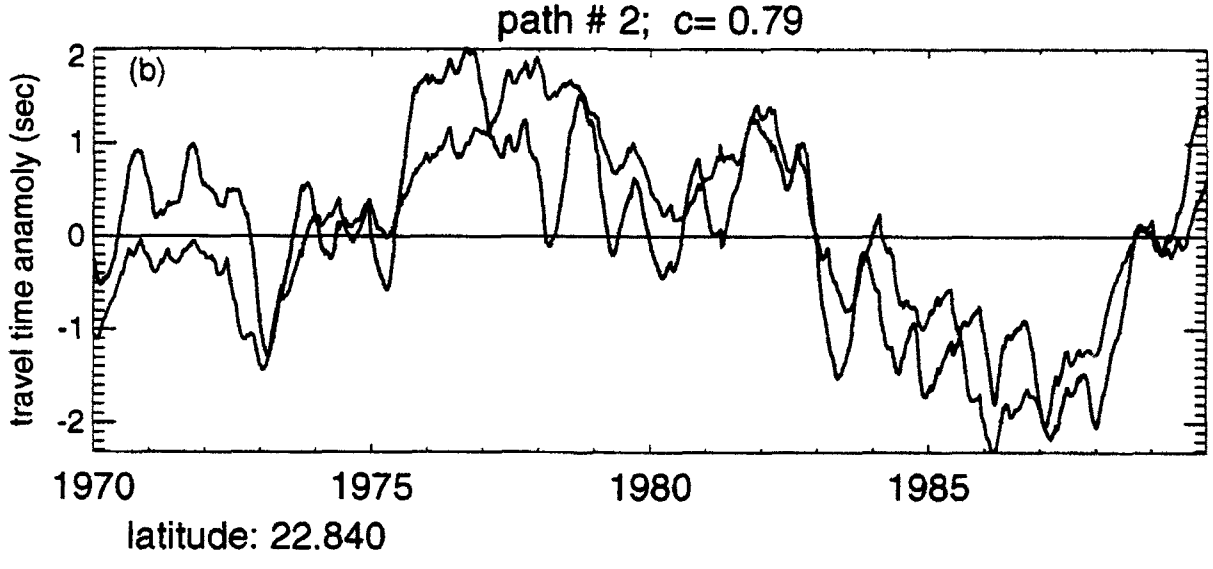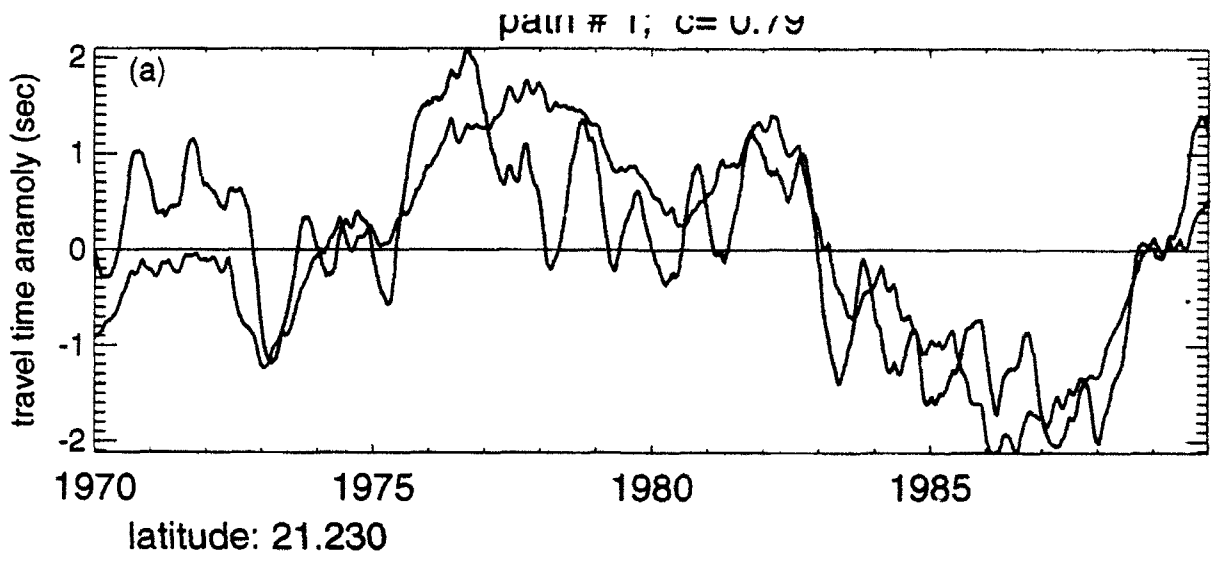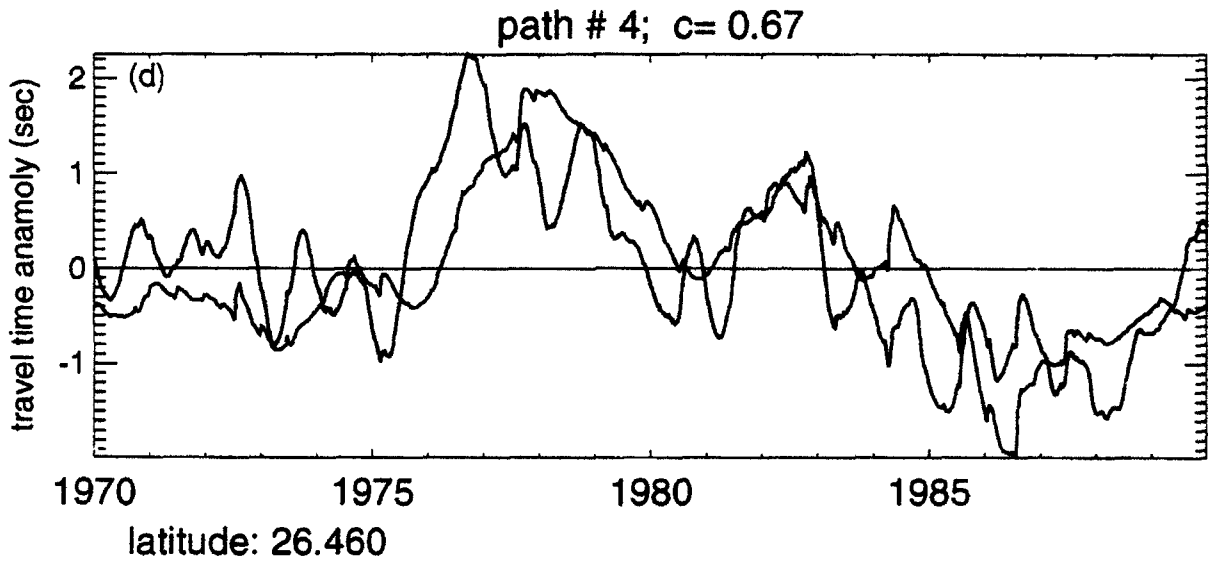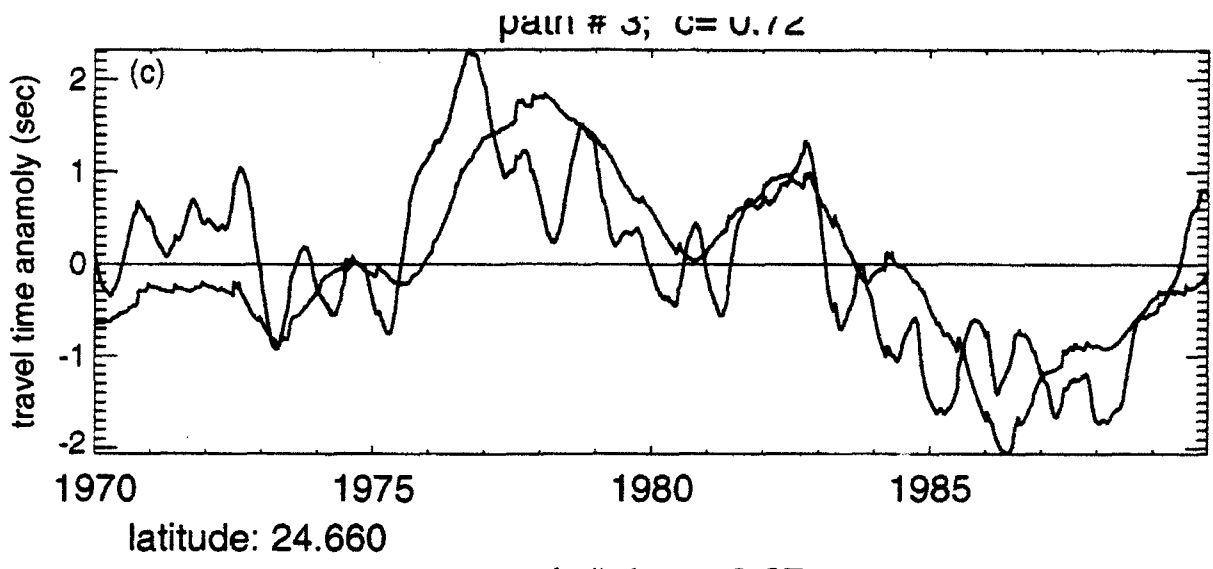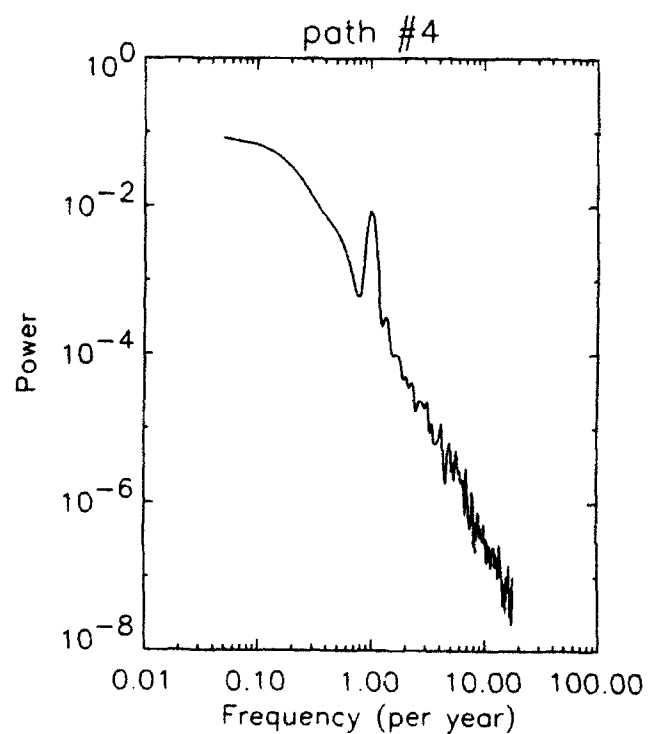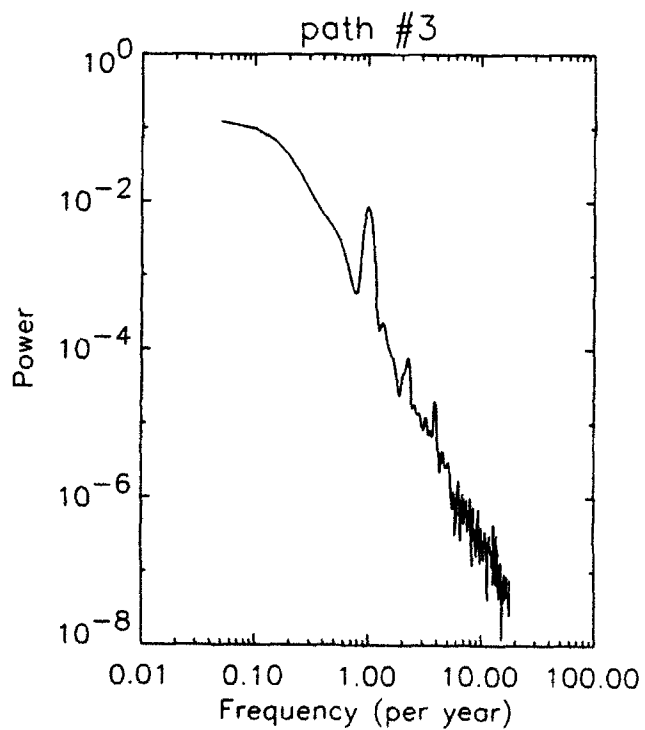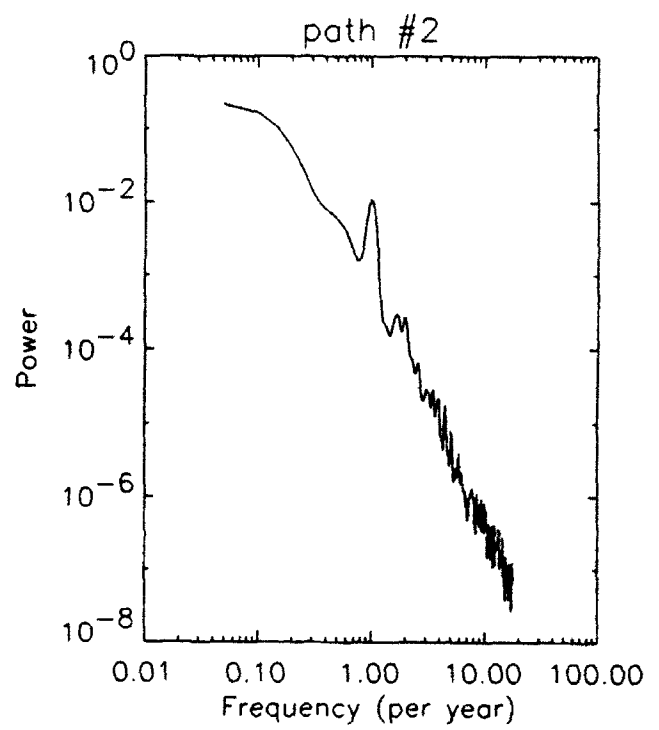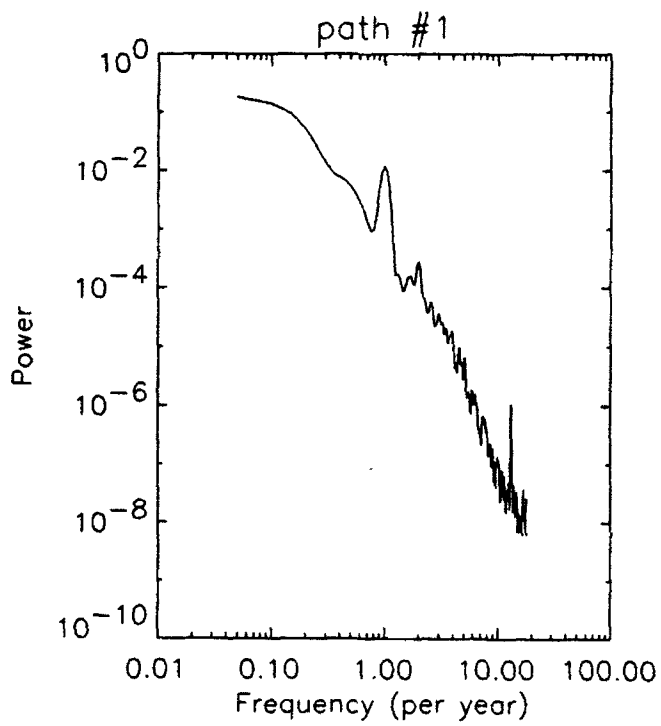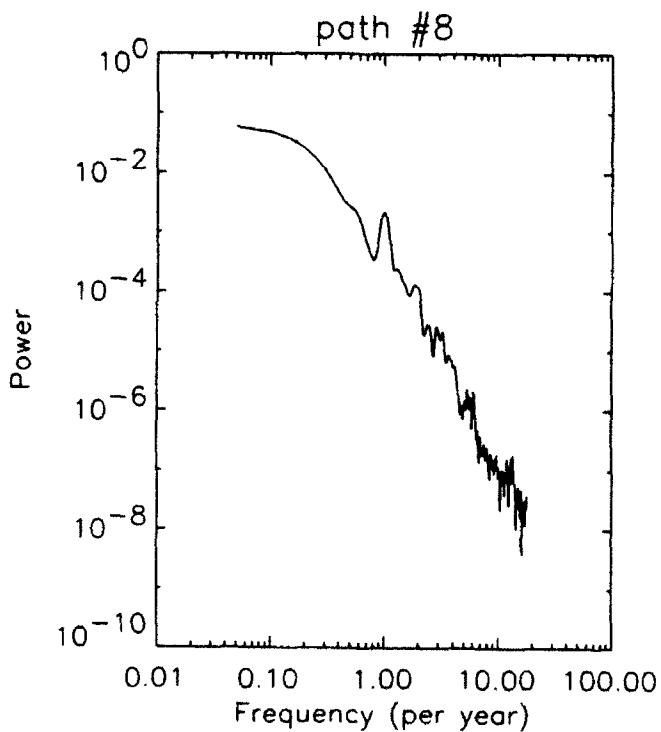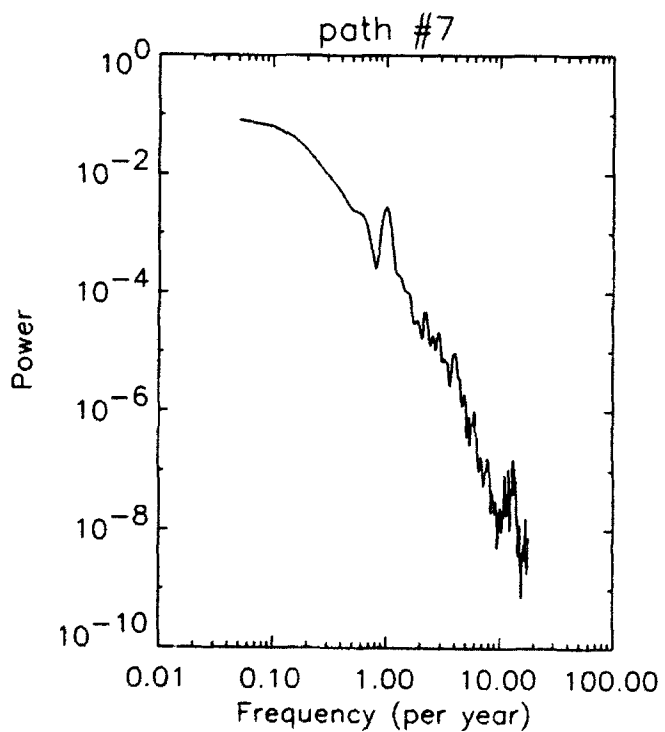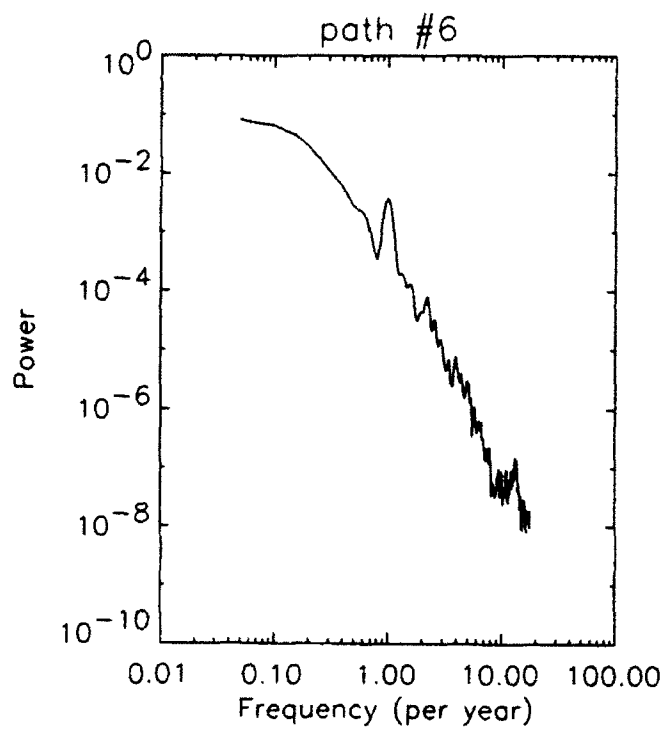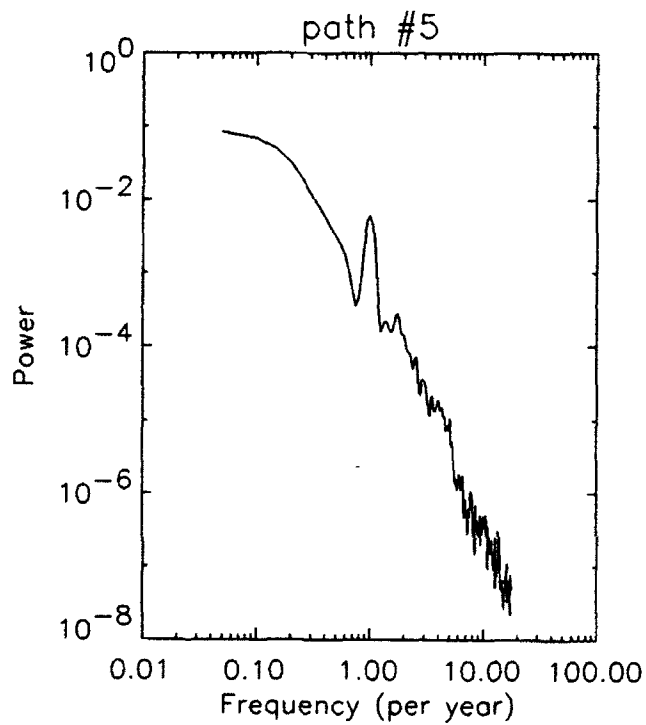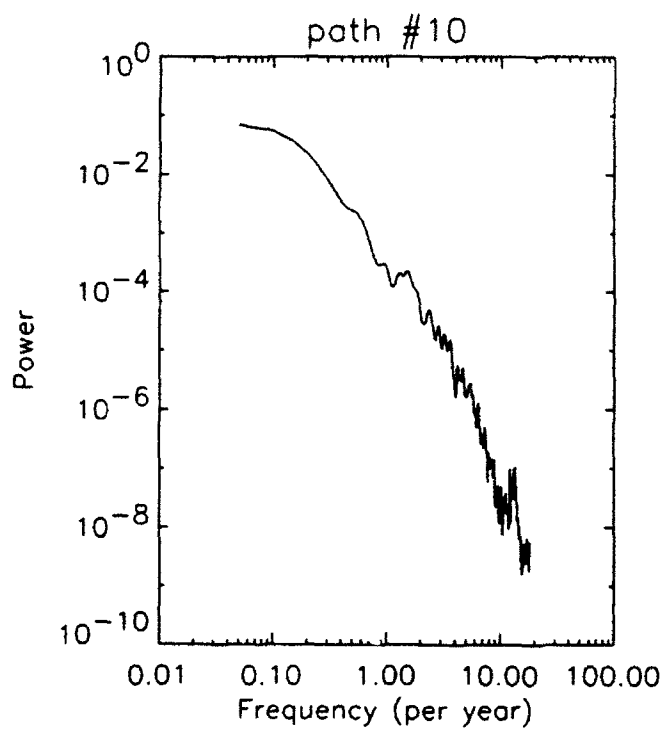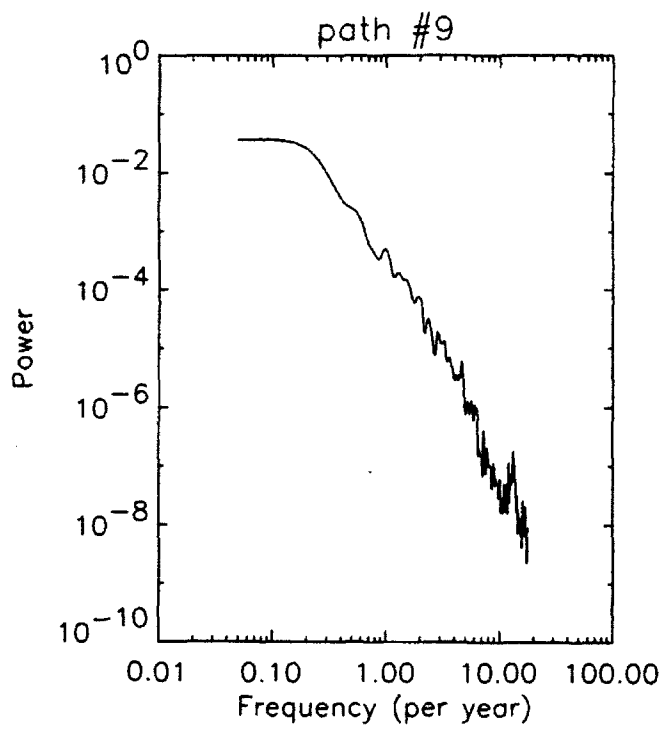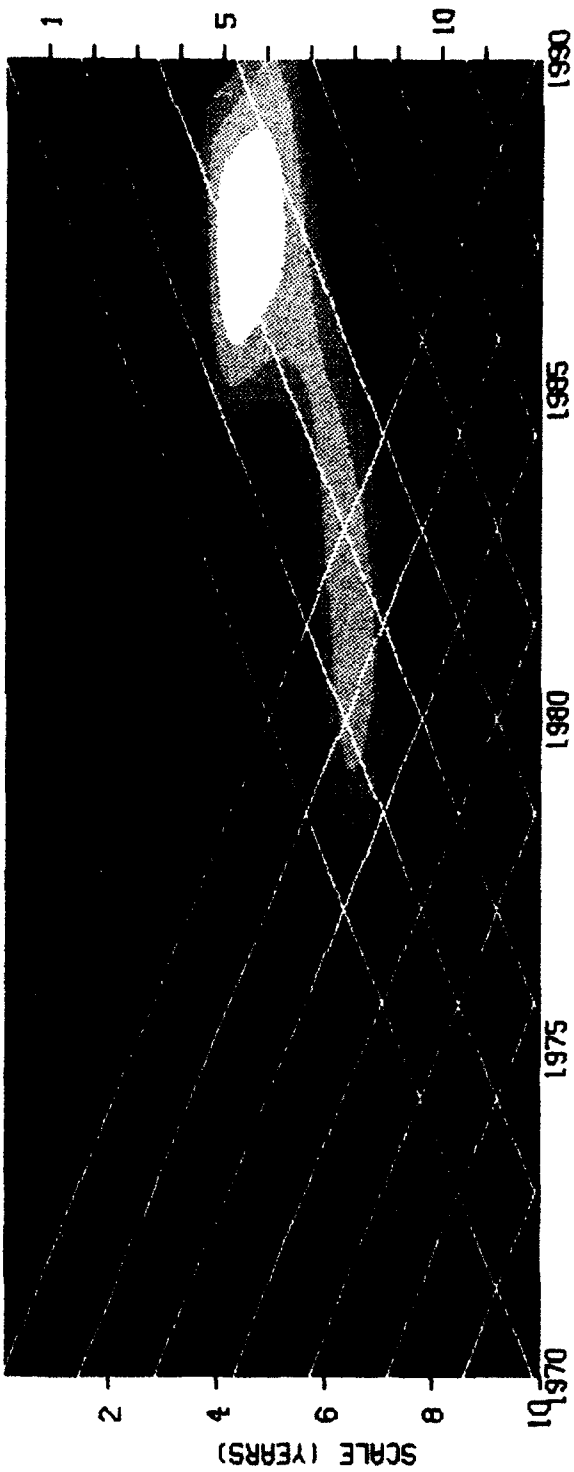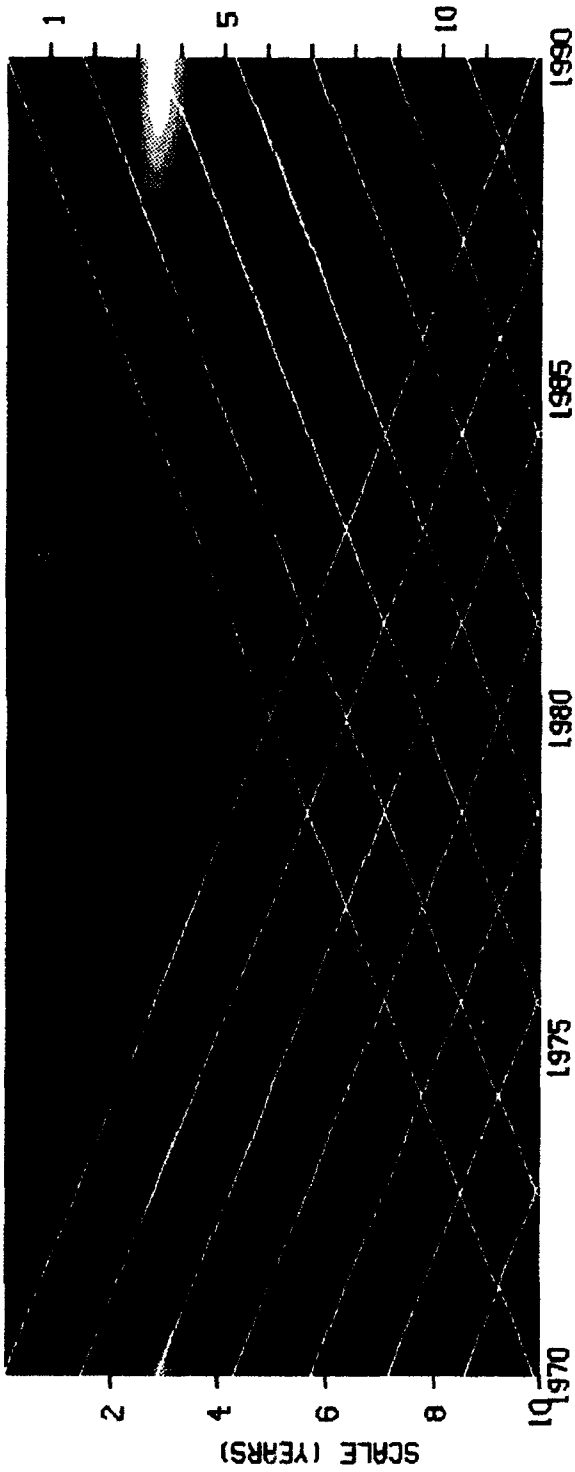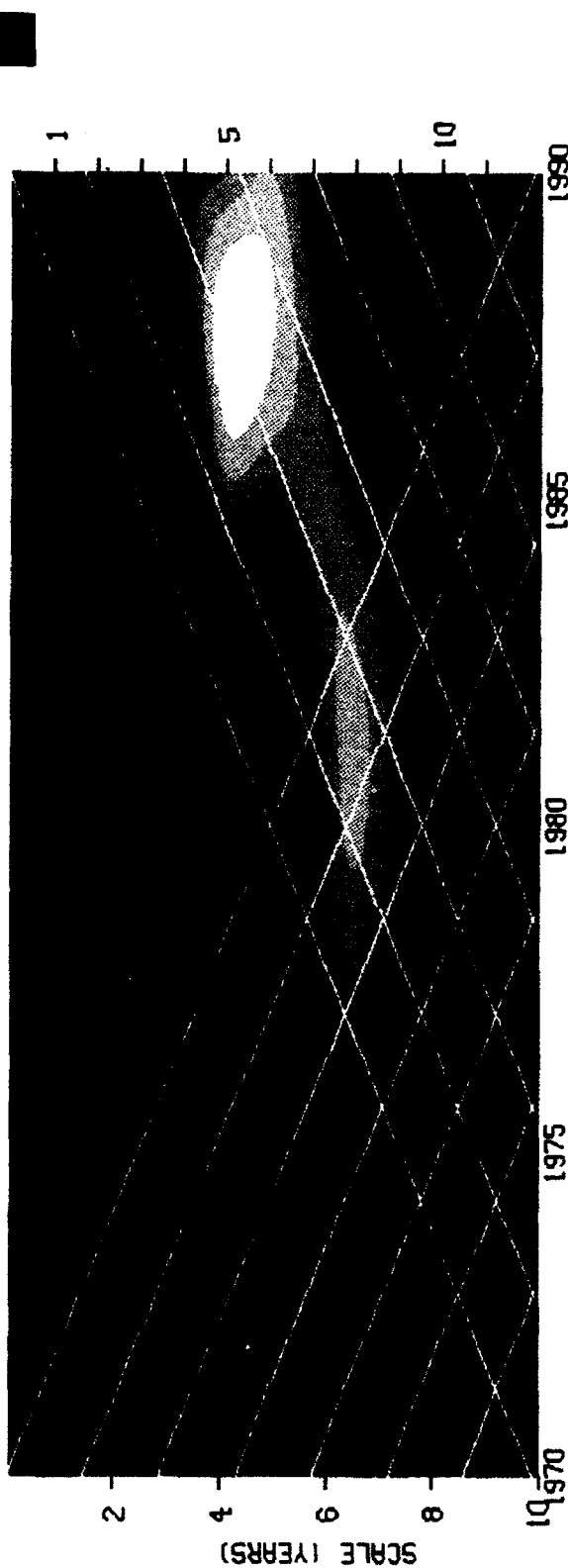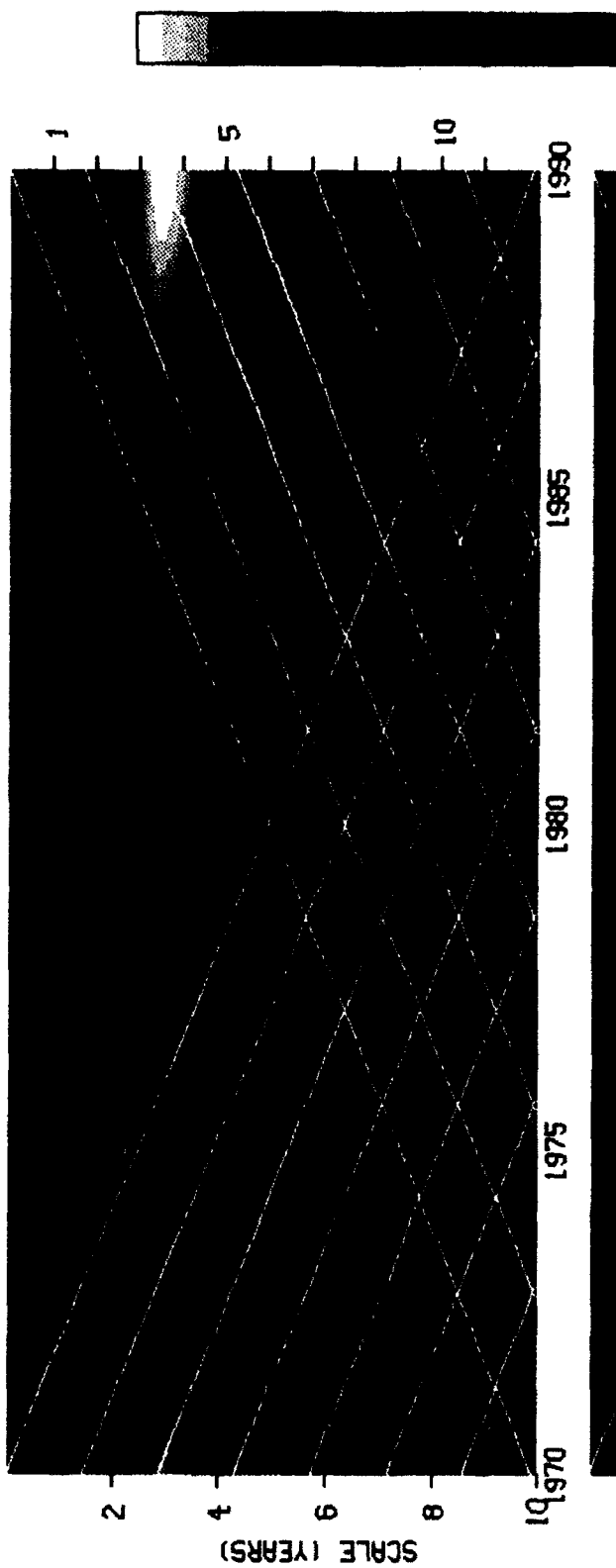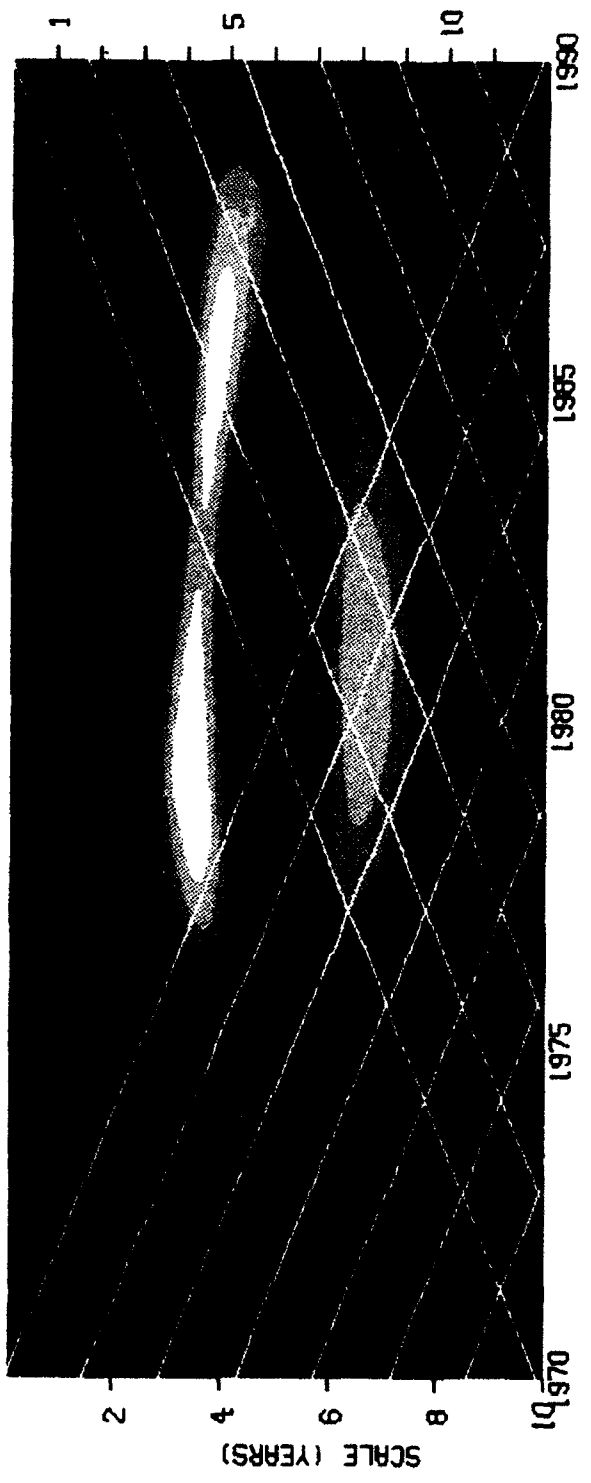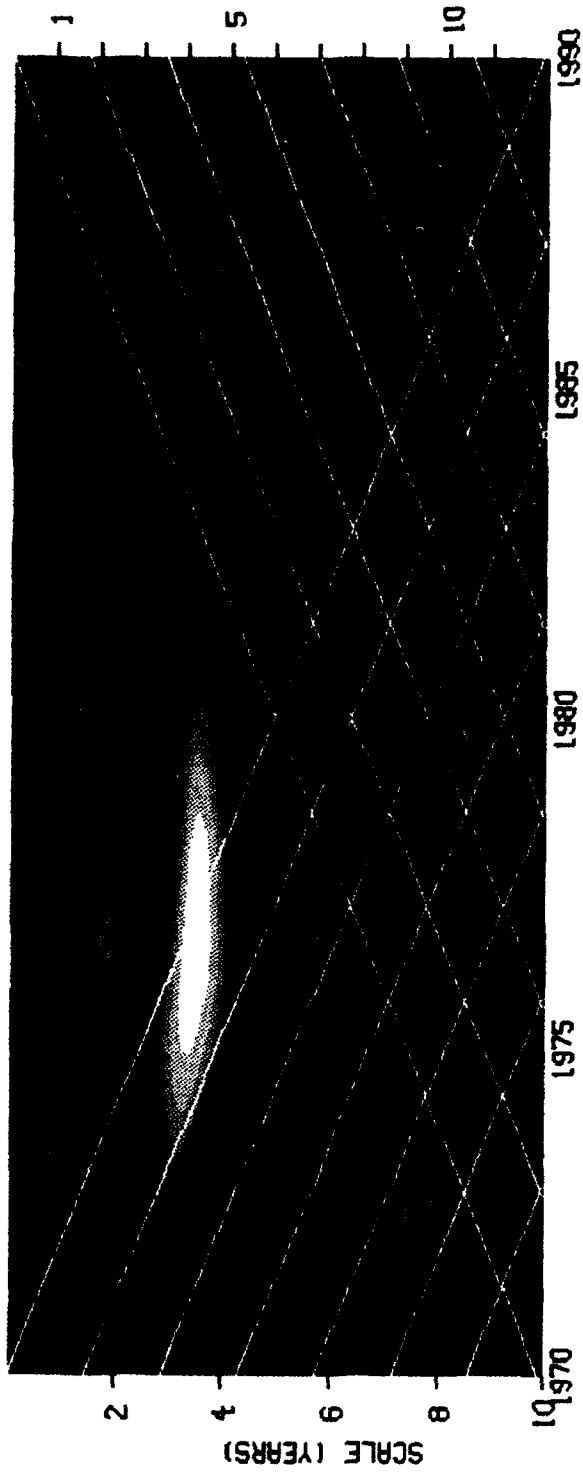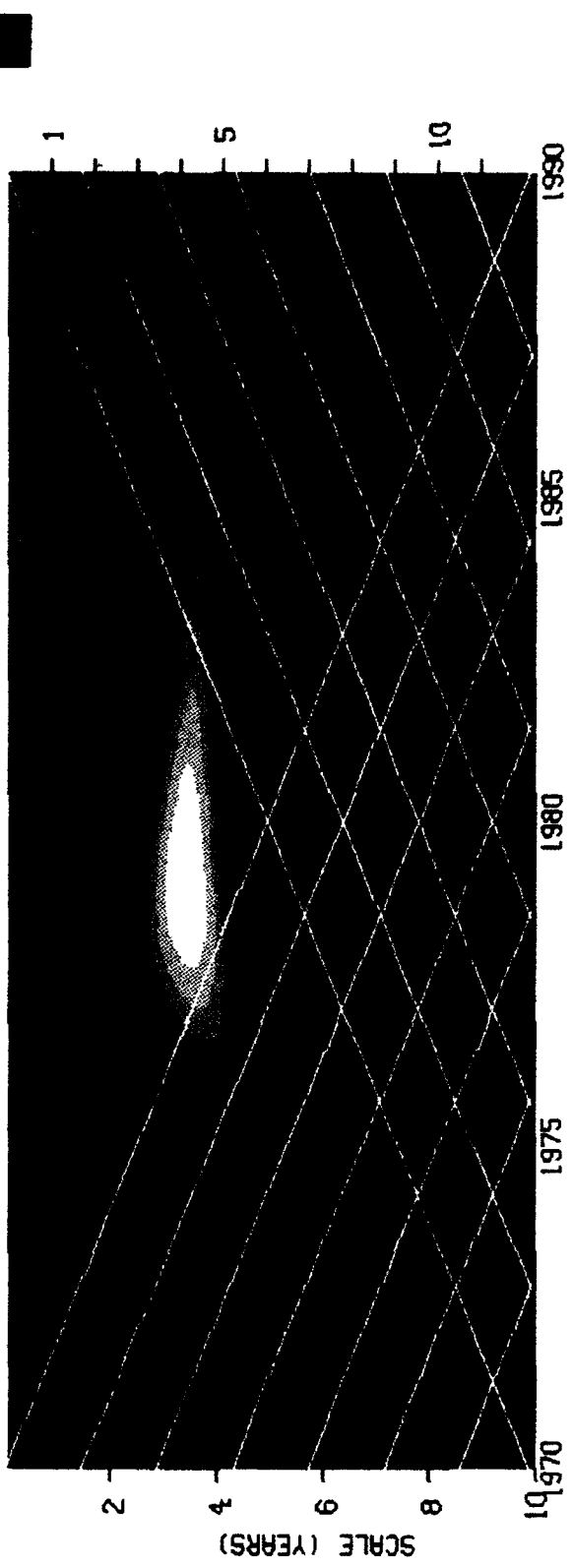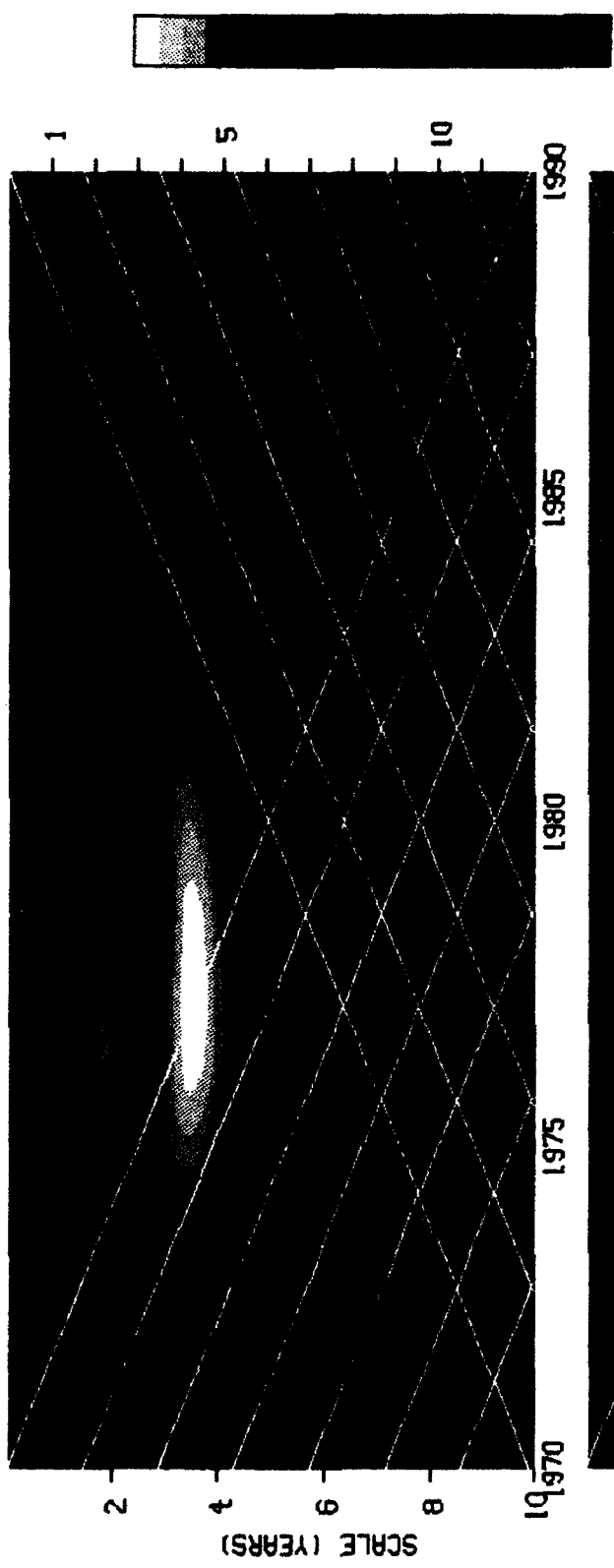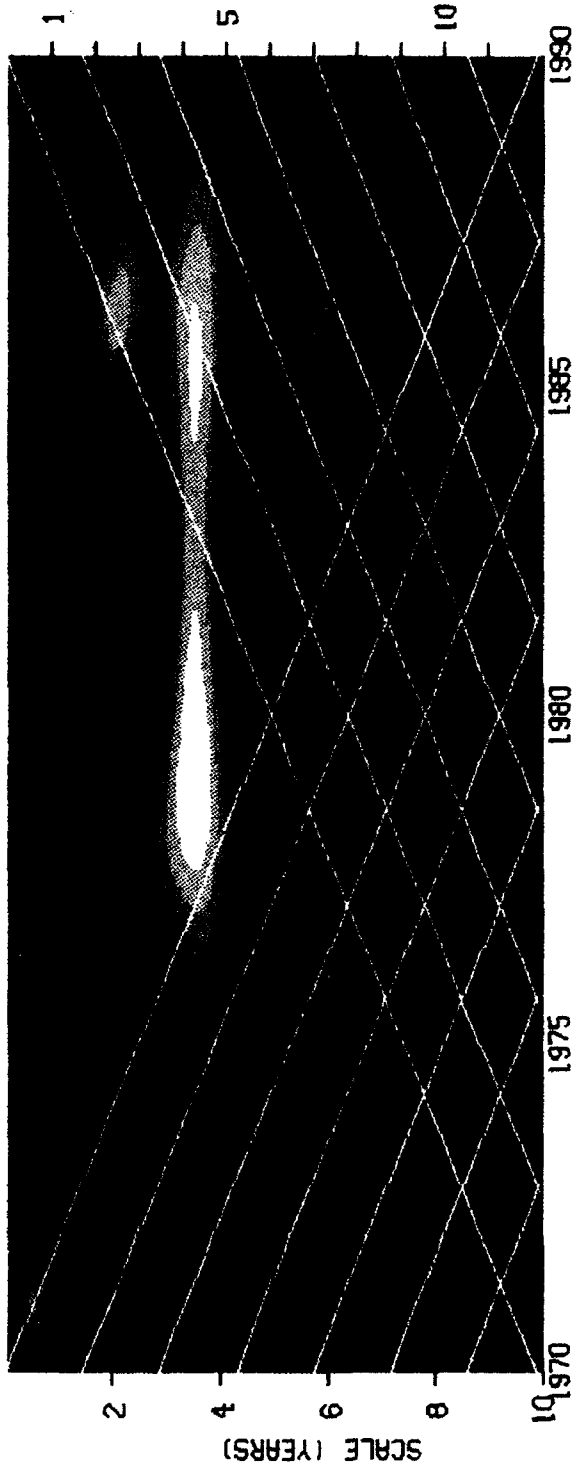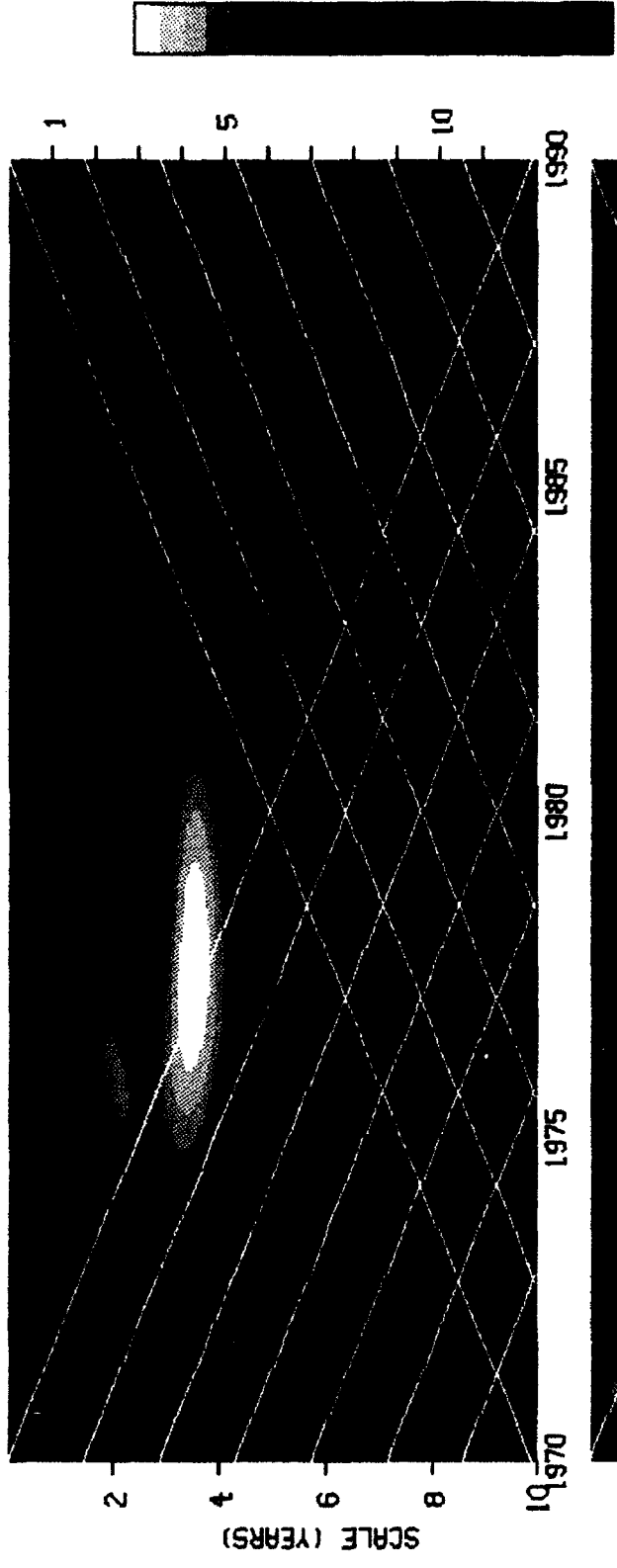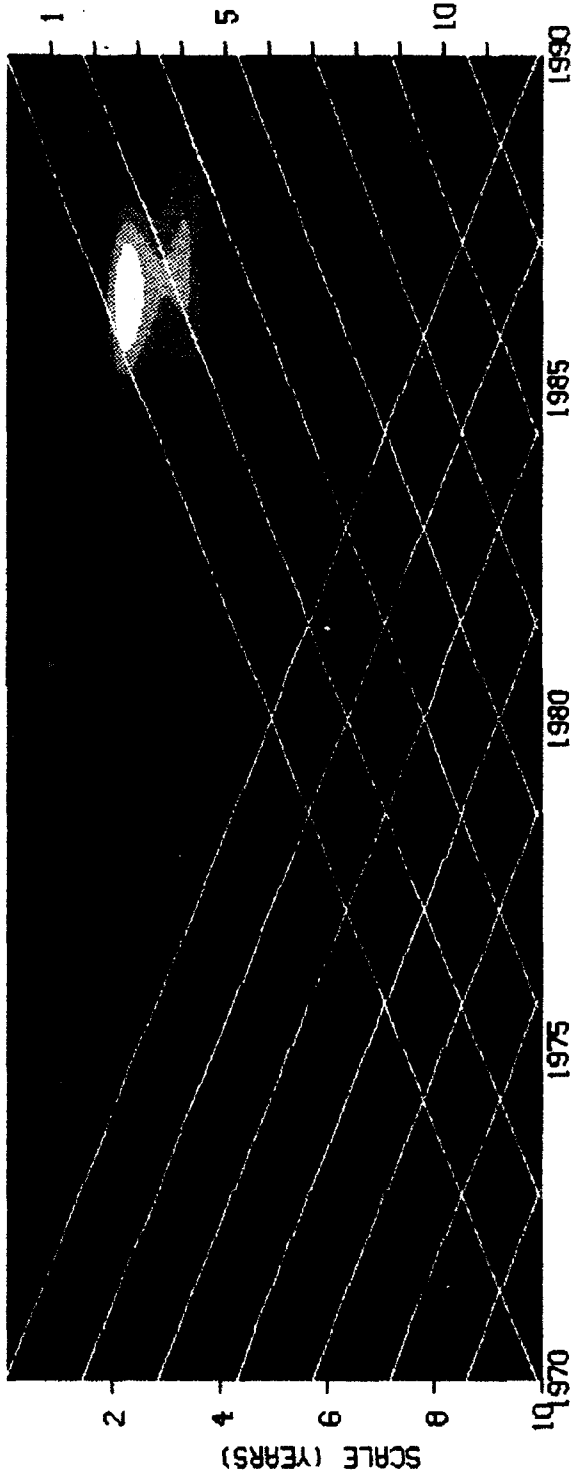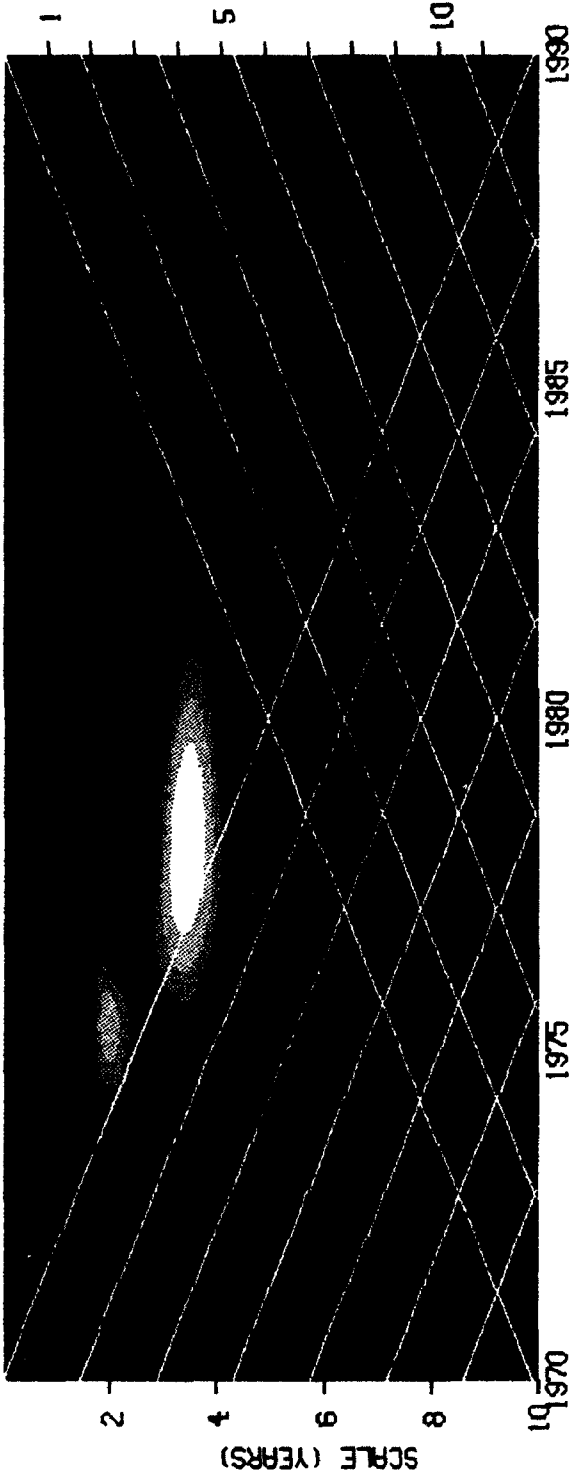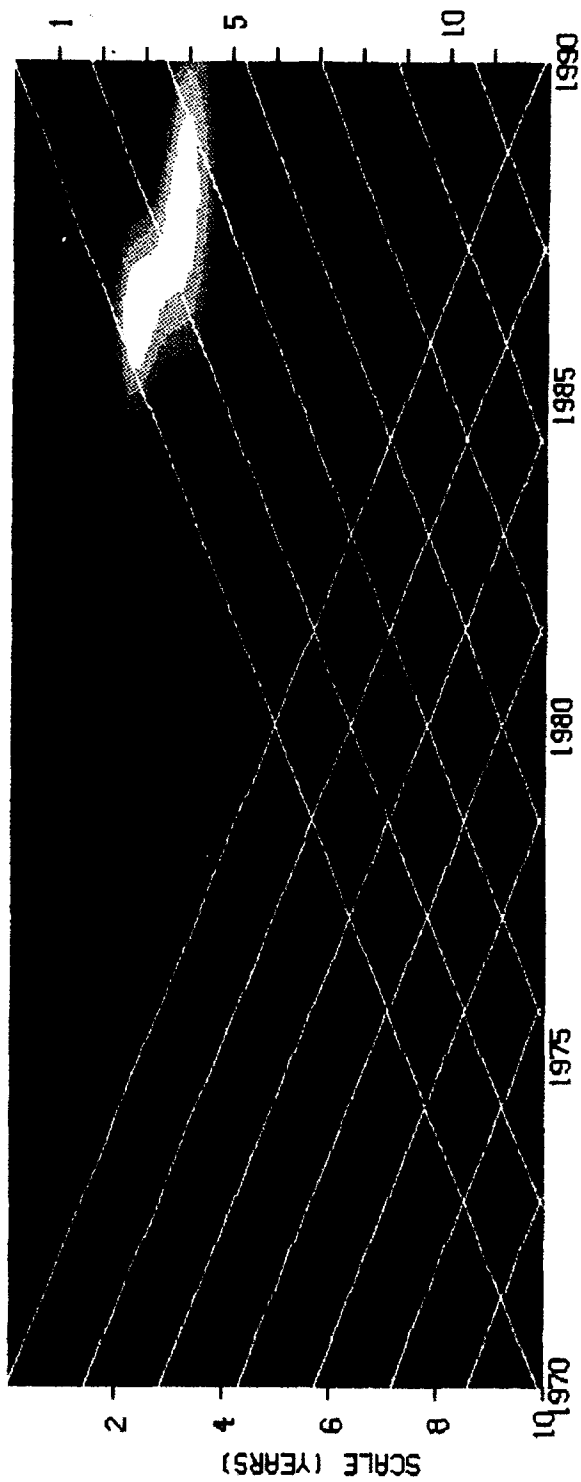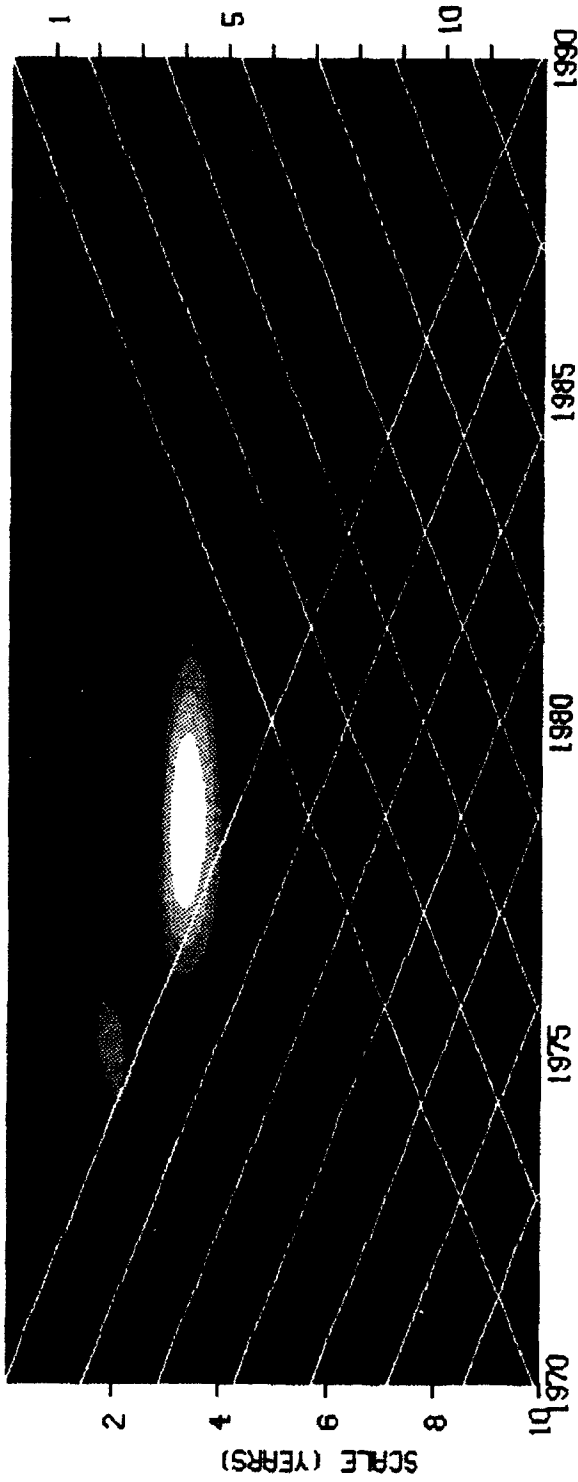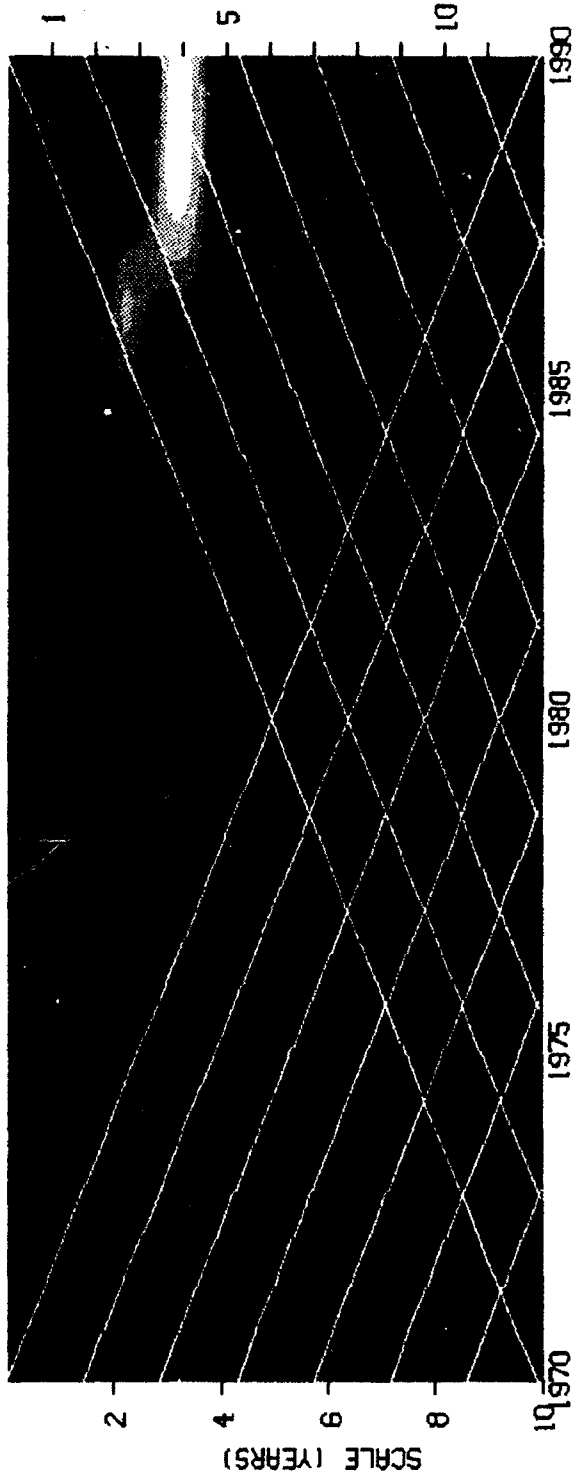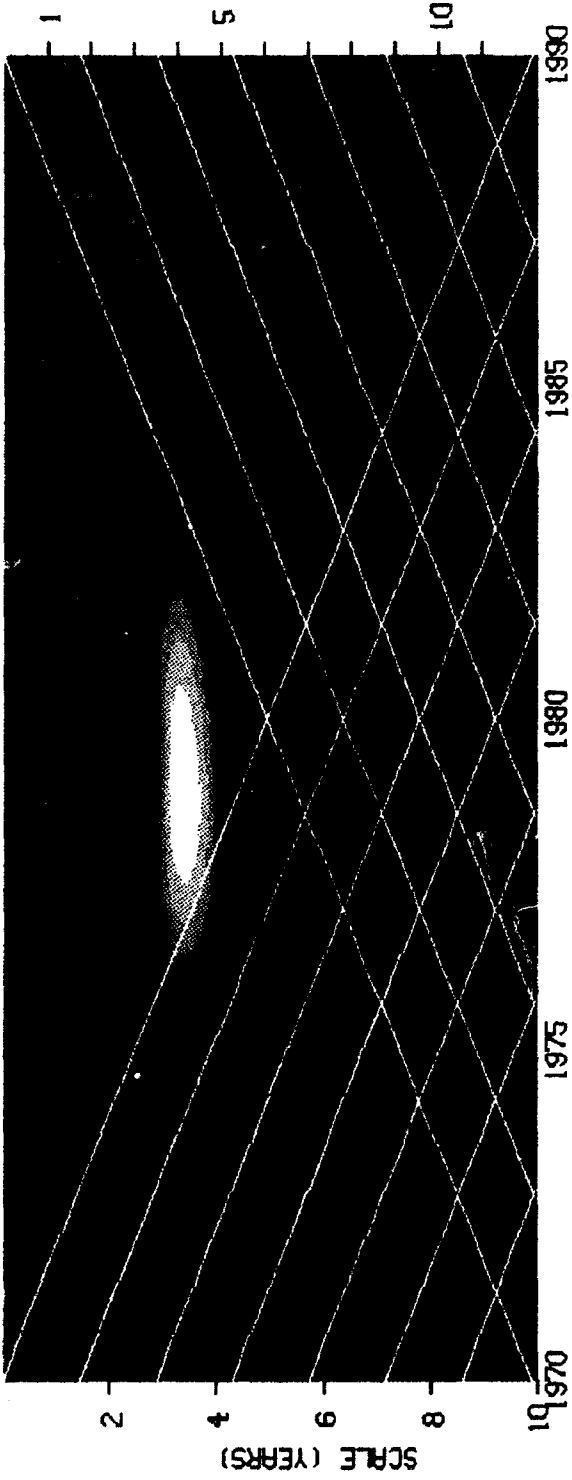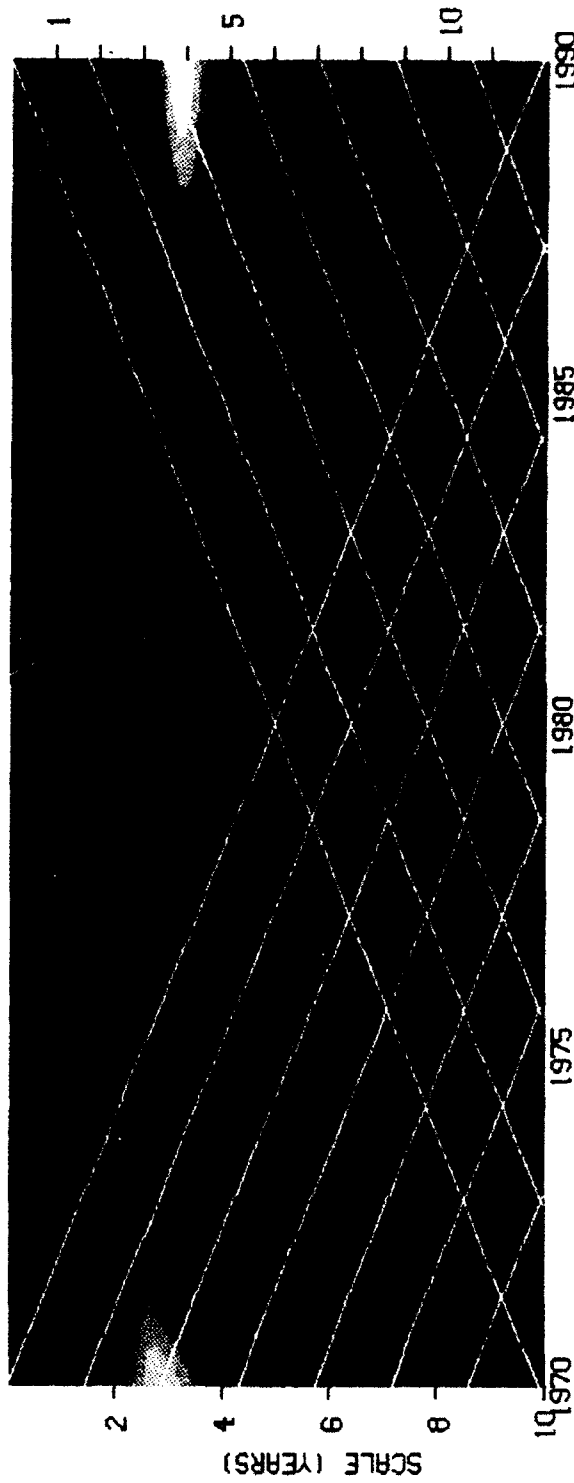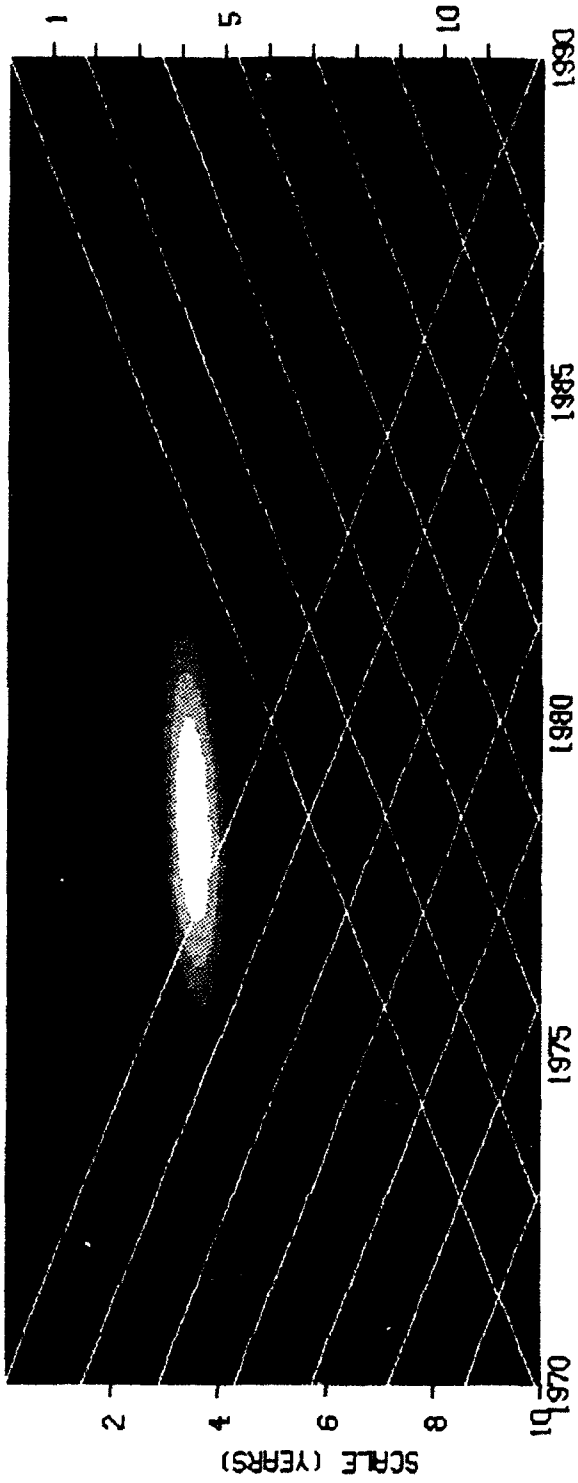
#10
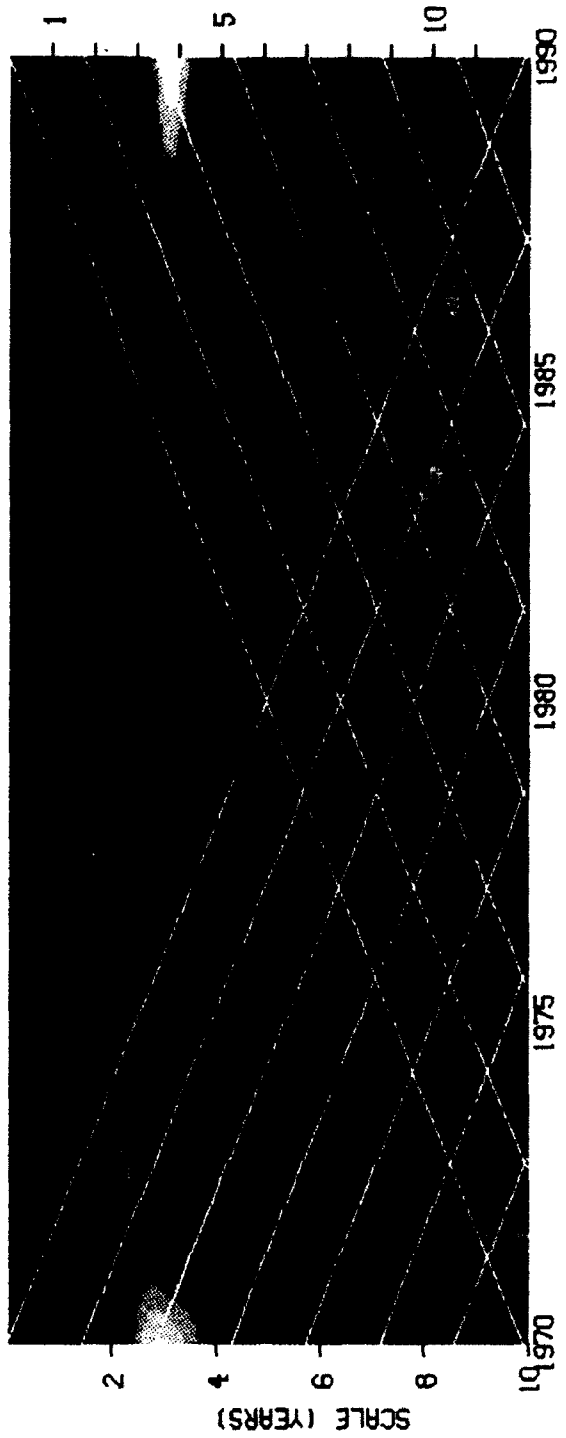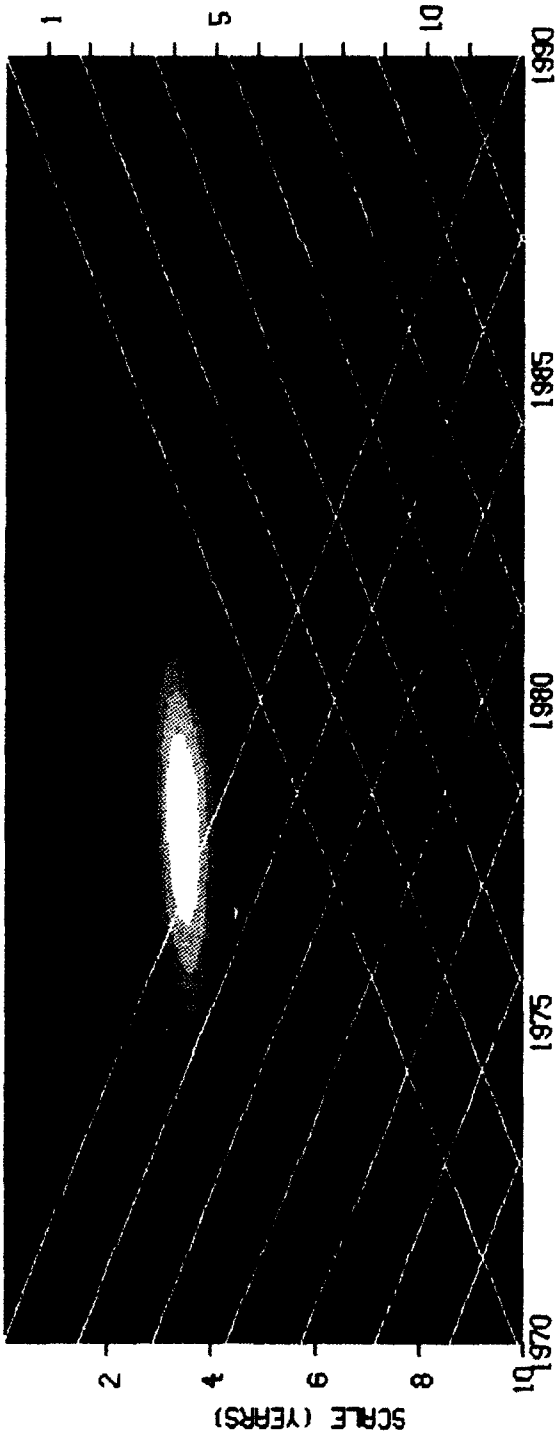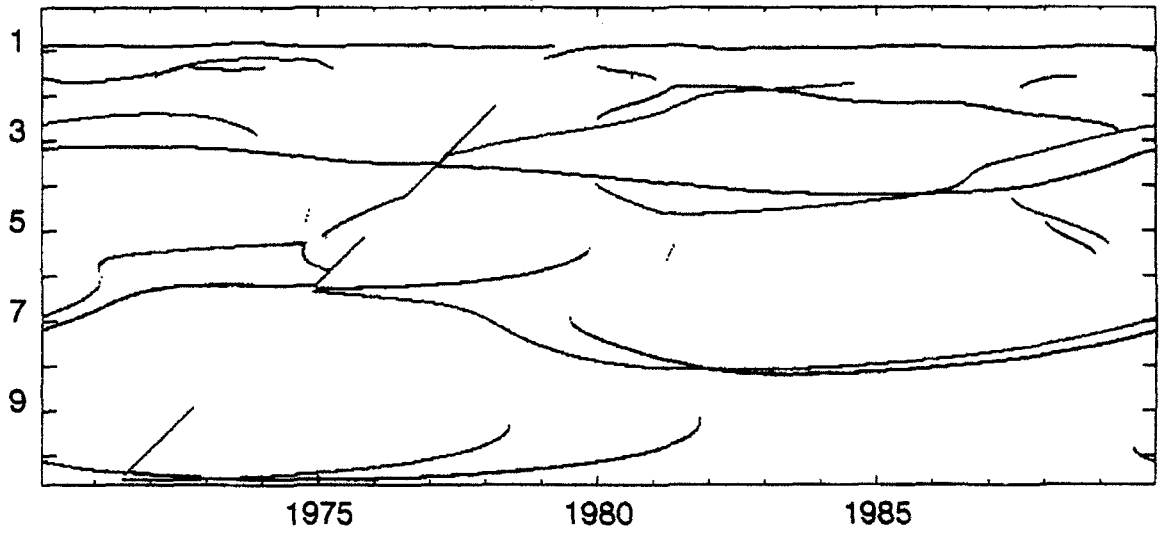
path # 1

path # 2
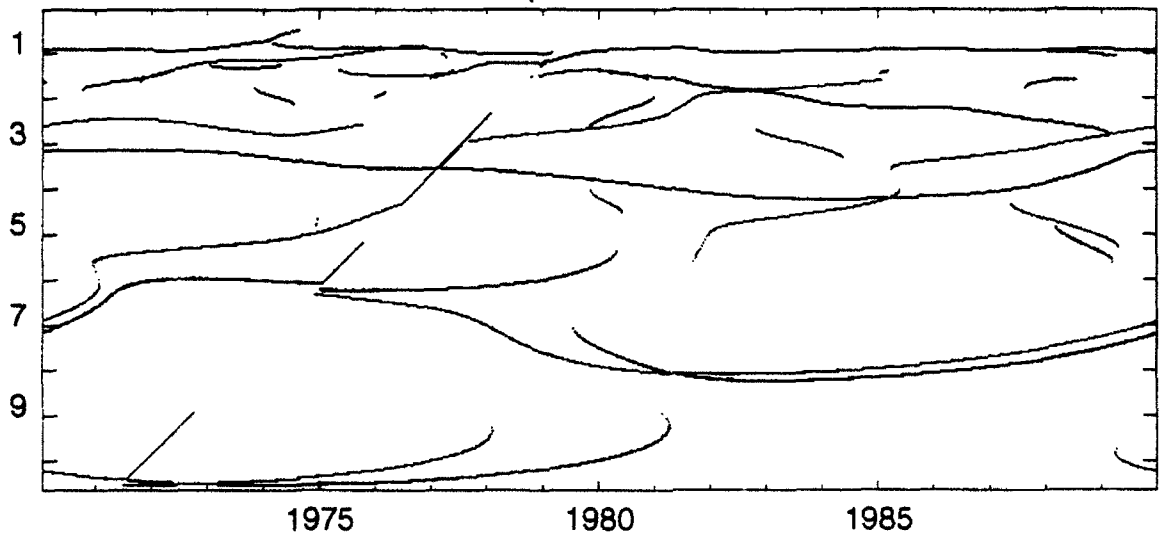
path # 3
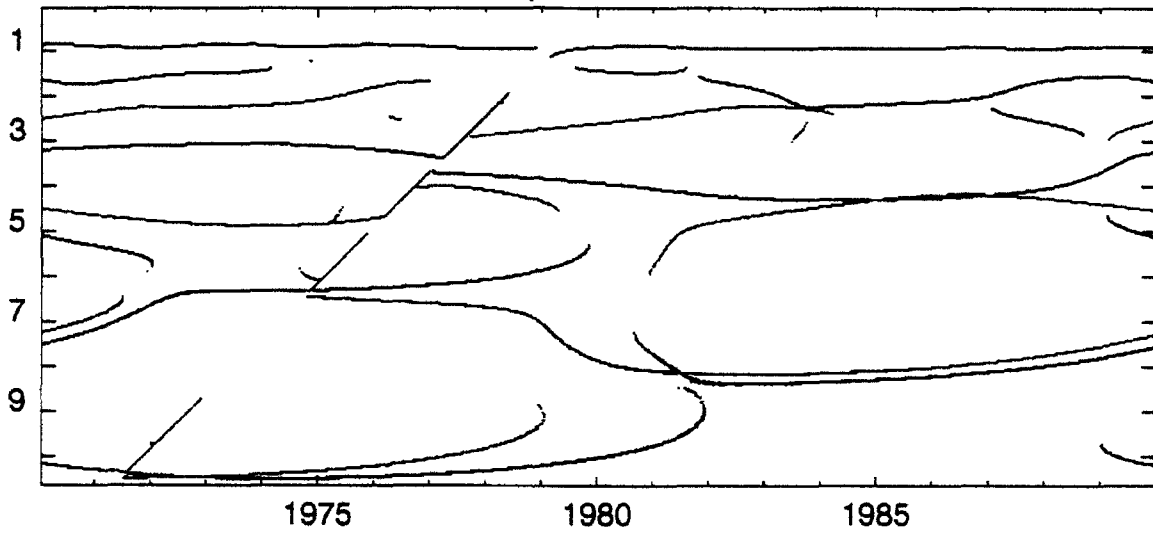
path # 4
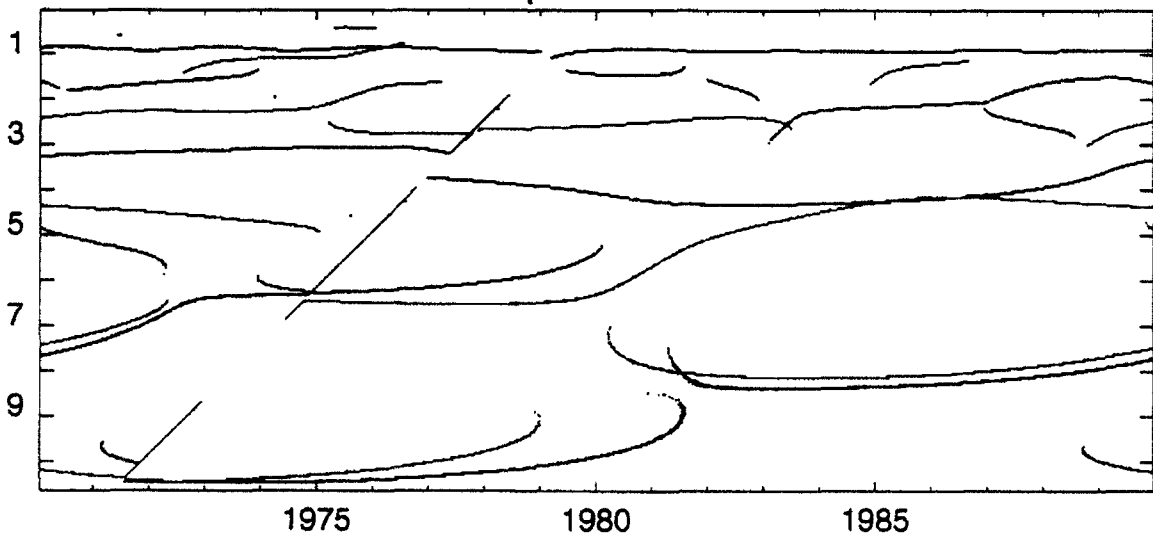
path # 5
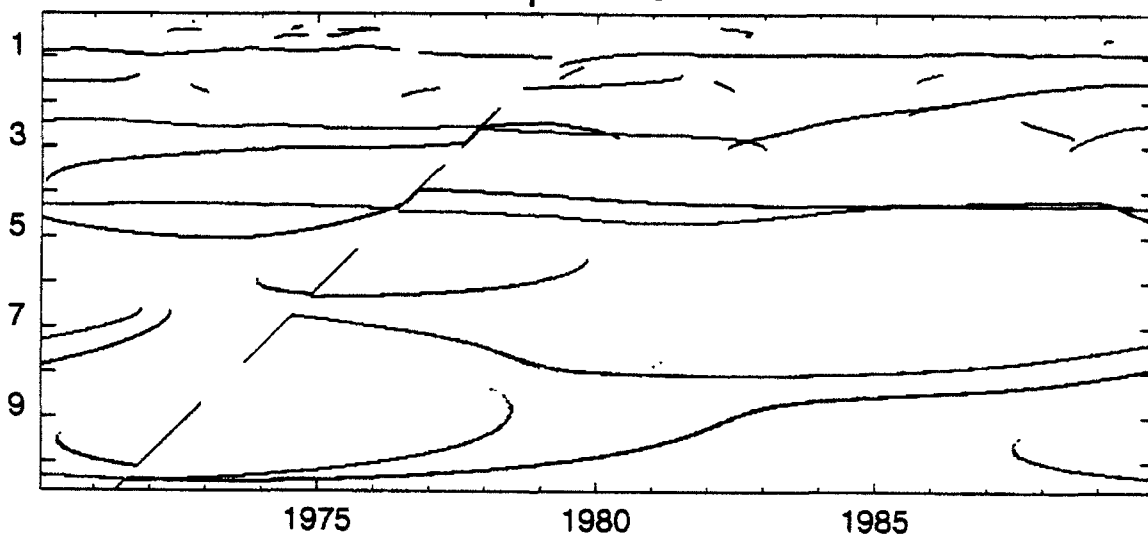
path # 6
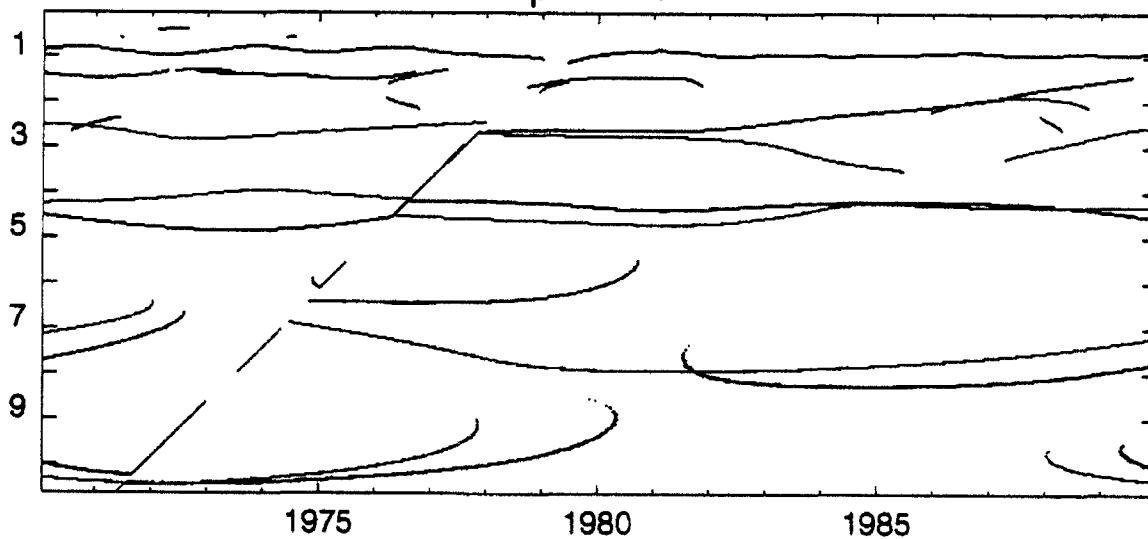
path # 7
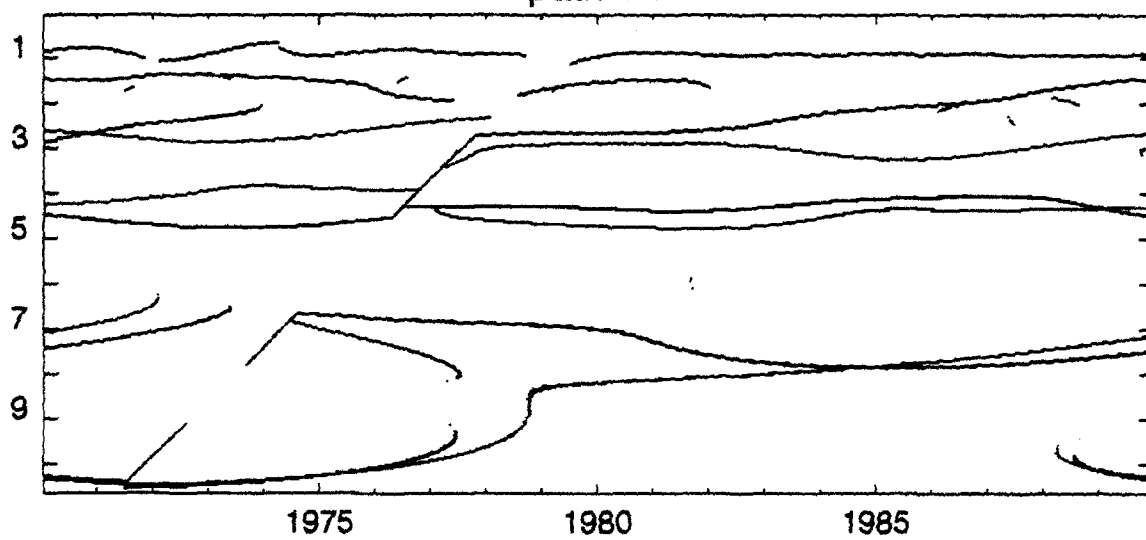
path # 8
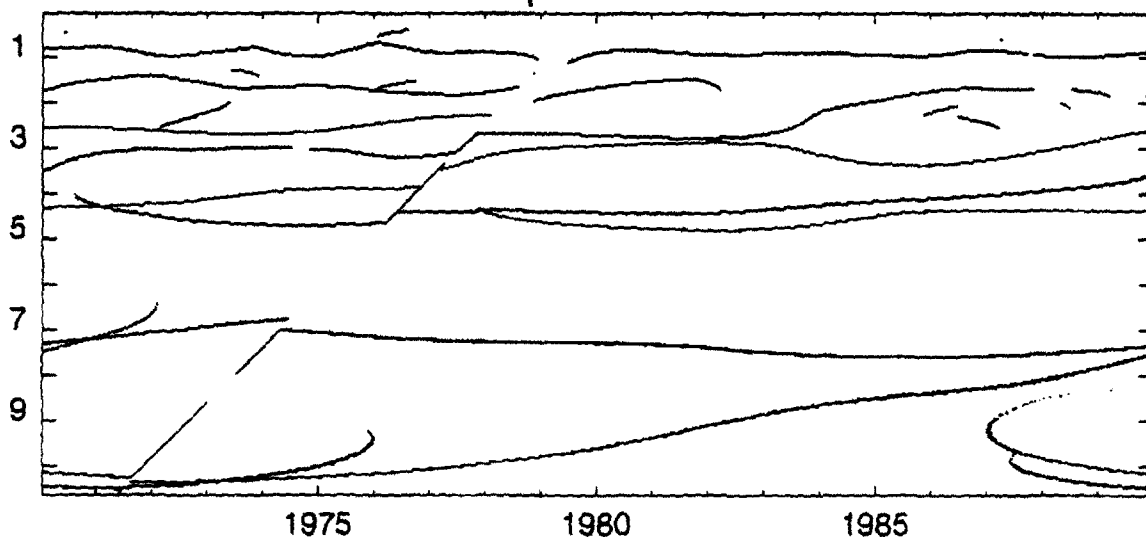
path # 9
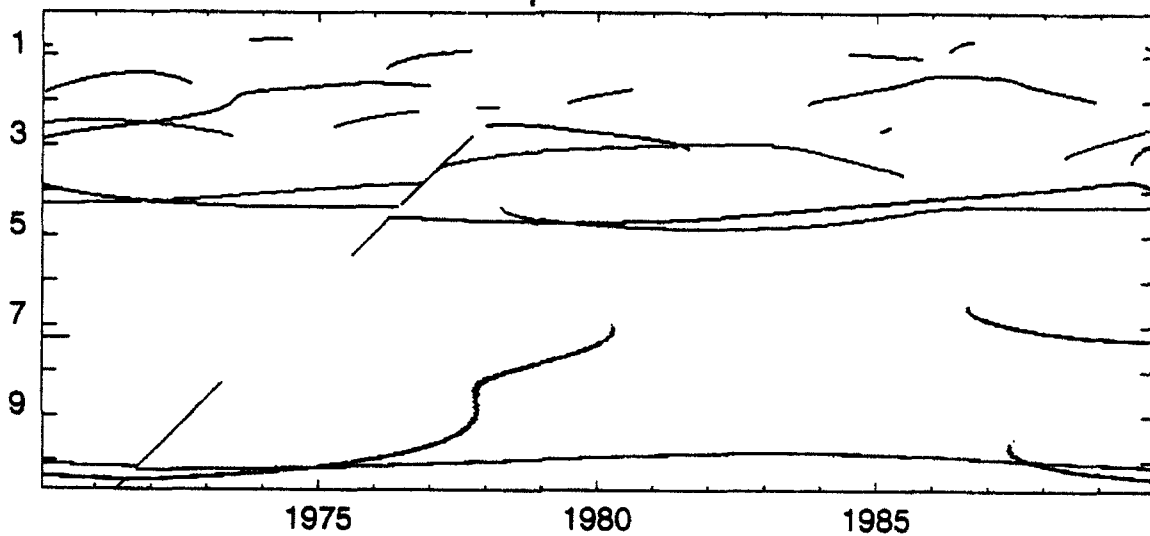
path # 10
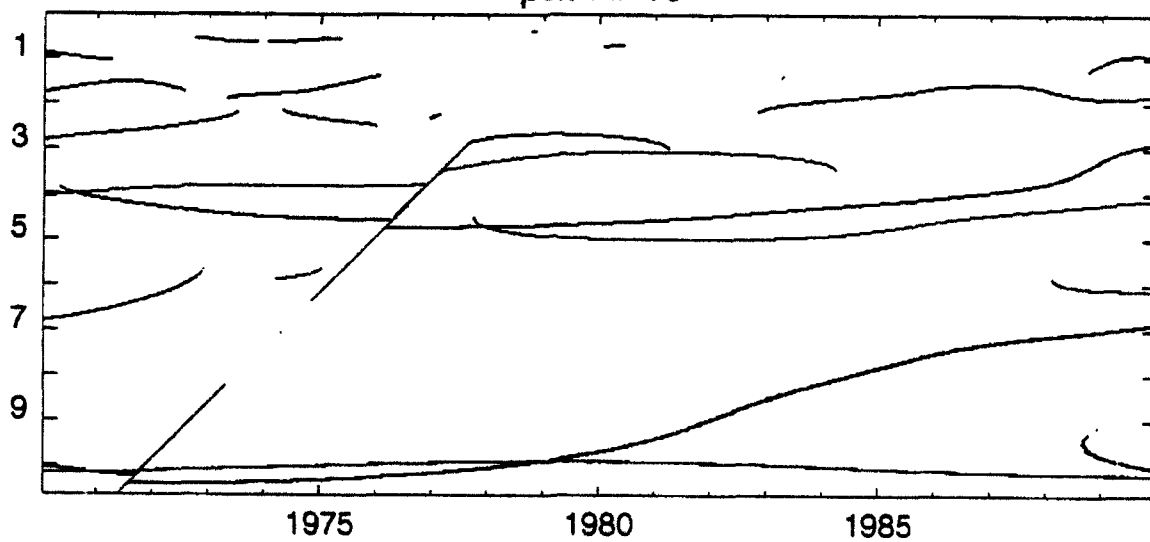
A Decadal Impact of the 1982-83 El Niño

G. A. Jacobs, H. E. Hurlburt, J. C. Kindle, E. J. Metzger,

J. L. Mitchell, W. J. Teague, and A. J. Wallcraft

April 22, 1994

We present evidence which indicates that the effects of equatorial El Niño episodes are more far-reaching than previously believed. Recent (1991) significant anomalies in both ocean circulation and Sea Surface Temperature (SST) over the North Pacific Ocean are linked with this century's largest such episode, the 1982-83 El Niño. This decadal link is provided by a Rossby wave which propagated across the entire Pacific Basin.

The effects of the 1982-83 El Niño at the Peru and Ecuador coasts were almost immediate: the Sea Surface Height (SSH) rose and SST increased [1]. The subsequent reduction in fish populations [2, 3] and the increased rainfall [4] severely impacted the regional economies [5]. These local effects, which last from 1 to 2 years, are normally associated with El Niño events with varying degrees of intensity.

Recently observed oceanic anomalies in SSH and SST indicate that during 1991 to

1

1993, a portion of the Kuroshio Extension transport was routed to a more northern latitude. In this paper we present evidence that the 1982-83 El Niño is responsible. The Kuroshio is a strong current which flows from the Philippines to the southern coast of Japan and then separates from the coast at 35°N. After separation, it flows eastward as the Kuroshio Extension, advecting an enormous amount of heat in the form of warm water into mid-latitude regions. The anomalous northward routing of a portion of the Kuroshio Extension advected warm waters further north than normal, resulting in extremely warm SST anomalies across the North Pacific during the early 1990's.

The observational evidence for this rerouting of a portion of the Kuroshio Extension comes from satellite altimeter and infrared data. Significant changes in SSH are seen in a combined analysis of altimeter data from the Geosat-Exact Repeat Mission satellite (Geosat-ERM) [6] and the European Remote Sensing satellite (ERS-1). The resulting change in SSH (Fig. 1a) represents a change in ocean circulation over the interval from 1988 to 1993. Similar results are obtained by a combination of TOPEX/POSEIDON and Geosat-ERM altimeter data.

In Figure 1a, a positive SSH anomaly centered just south of 40°N at 175°E lies north of the Kuroshio Extension. The anomaly indicates that a portion of the current is routed to a path that follows the northern slope of the anomaly. The circulation changes imply changes in SST as warm waters are advected further north. A consistent set of global SST has been compiled since 1985 by Reynolds [7]. A warm SST anomaly north of the Kuroshio Extension is clearly seen in Figure 1b extending from Japan to North America at 40°N. This SST anomaly is just north of the SSH anomaly as expected (Fig. 1). Thus,

2

both satellite-sensed SSH and SST strongly suggests a northward shift of a portion of the Kuroshio Extension and a subsequent anomalous northward transport of warm waters.

Concurrent with the recent abundance of satellite data is a revolution in our ability to numerically model the dynamical processes in the oceans. From a numerical model simulation, we use results which cover the decade from 1981 to 1993. The model simulation and observational data provide independent results. This synergy is very important as results from one source alone may be inconclusive due to errors or assumptions. SSH changes in the model simulation (Fig. 1c) indicate an anomaly from Japan to Alaska similar to that of the altimeter data. This suggests that the events which give rise to this ridge are realistically simulated in the model. The decadal simulation provides a unique, continuous, high-resolution data set which is used to identify the sequence of events which generate the observed trans-Pacific ridge. An animation of the model SSH variations from 1981 to 1993 clearly reveals that these events began in 1982 as a result of the El Niño.

The 1982-83 El Niño was initiated by the relaxation and subsequent reversal of easterly winds over the western and mid-Pacific [9] which generated an eastward propagating equatorial Kelvin wave. A Kelvin wave is a special class of shallow-water waves which occurs along the equator or along coastlines [10]. The Kelvin wave was reflected from the American continents as a westward propagating Rossby wave, a class of waves which depend on the sphericity and rotation of the Earth (Fig.s 2 and 3). The Rossby wave reflection process and initial westward propagation in response to the 1982-83 El Niño have been simulated by other ocean models [11]. The subsequent propagation of the El Niño-generated Rossby wave across the entire North Pacific is summarized in the panels of Figure 3.

3

The implications of these results are far reaching and unanticipated. Up to now, propagation of a Rossby wave across the Pacific Ocean at these high latitudes has never been demonstrated. Comparison of the Geosat altimeter data at 30°N with model results verifies the wave's trans-basin journey (Fig. 4). Rossby waves, observed at the coast of the American continents [12, 13], were not anticipated to propagate an appreciable distance into the basin as coherent structures. The energy of the wave was expected to cascade to smaller scales (i.e., the wave would dissipate into eddies) and not to propagate as far as Hawaii at this latitude. However, our observations and simulations indicate that the Rossby wave not only remained intact as far as Hawaii, but continued across the basin and is coherent well over a decade later. The Rossby wave generated by the 1982-83 El Niño exists today in the northwest corner of the Pacific Ocean.

Additional evidence of the wave is indicated by a positive dynamic height anomaly observed in hydrographic data south of Japan at 137°E [14]. The anomaly moves from 18°N in 1984 to almost 30°N in 1989 which agrees well with the movement of the Rossby wave in Figures 3 and 4. Thus, the Rossby wave propagating from North America to the Kuroshio Extension is observed in both the model and the ocean. Two additional ocean model simulations were performed to help isolate the decadal effects of the 1982-83 El Niño. One simulation was initialized in 1984 after the El Niño and shows the absence of the El Niño-generated Rossby wave at 30°N (Fig. 4c). The other experiment starts in 1981, includes the 1982-83 El Niño, but wind forcing reverts to climatology in 1984 to exclude subsequent wind forced anomalies. It shows the Rossby wave (Fig. 4d), and because no knowledge of the ocean or atmosphere after 1982 was used, it demonstrates the potential

4

for decadal predictions of El Niño-generated Rossby waves and their effects.

In the model, the Rossby wave produces a significant geostrophic velocity anomaly of approximately 10 cm/sec in the upper ocean as the wave passes through the Kuroshio Extension in 1991. The geostrophic flow induced by the trailing edge of the Rossby wave reduces the flow of the Kuroshio Extension along 35°N. The leading edge of the Rossby wave induces an eastward velocity perturbation near 40°N. The result is a routing of a portion of the Kuroshio Extension transport to about 40°N during 1991 and subsequent years. During 1991 the largest SST anomalies are found north of the Kuroshio Extension coincident with the maximum Rossby wave effects on the current. These anomalies reach a peak of over 1°C above climatology. After the Rossby wave propagates to the northwest, the geostrophic perturbations on the Kuroshio Extension abate, the Kuroshio Extension returns to its climatological latitude, and the anomalous SSTs begin to disappear.

Corroboration of these events is provided by satellite IR frontal analyses [15] which indicate a northward displacement of the Kuroshio Extension in 1990-91 and a southward displacement from 1991-93. In 1992-93 the Rossby wave forms a ridge of high SSH from Japan to Alaska (Fig. 3c). The results presented here indicate that the events giving rise to the trans-Pacific SSH ridge and SST anomaly in 1991-92 originated with the 1982-83 El Niño. Thus, the oceanographic effects of a major El Niño have extratropical and decadal components.

Climatological effects associated with warm, tropical SST anomalies during major El Niño events are well-documented [16]. Surprisingly, the SST anomalies which we observe

5

at much higher latitudes across the North Pacific are of the same amplitude and temporal-spatial extent as those observed in the tropics during major El Niño events. At higher latitudes, significant statistical relationships between SST anomalies in the Pacific ocean and weather patterns over the North American continent have been found [17]. Thus, it is possible that the 1982-83 El Niño still has important effects on the climate in 1993. Stated succinctly, the 1982-83 El Niño is not over: its effects have moved from South America to the northwest across the Pacific Basin. This Rossby wave should continue to propagate across the far northwest corner of the North Pacific Basin for at least another decade and continue to affect the circulation of the North Pacific.

The deterministic nature of the processes which we report indicates that the ocean is not wholly chaotic and unpredictable even over basin and decadal scales. Relatively simple planetary wave dynamics, the numerical models which include them, and global satellite data sets provide the necessary and timely tools for long-term oceanic predictions (Fig. 4). Finally, we note that these long time scale events imply that attempts to determine the climatological or average state of the oceans (a major component of Earth's climate) will require monitoring of the ocean circulation over decadal time scales. This is indeed a major task which will require synergistic use of numerical ocean models and continuous satellite monitoring for a complete understanding.

1   Figure Captions

Fig. 1: (a) Change in SSH from the Geosat-ERM (Nov 86 - Oct 89) to ERS-1 (Apr 92 - Mar 93). The color bar indicates changes from -15 to 15 cm. The climatological position of the Kuroshio Extension [18] is plotted so that the positions of the features may be compared. Large scale circulation in the oceans is approximated by the geostrophic relation which implies that water flows along lines of constant height with higher SSH to the right when facing downstream. Thus, changes in SSH are related to changes in ocean circulation. The high SSH anomaly north of the Kuroshio Extension at 175°E indicates a northward shift of a portion of the Kuroshio Extension's transport. (b) Deviation of SST averaged over Apr 92 - Mar 93 from a mean over 1985-92. Data are supplied by infrared radiometer satellites [7]. The color bar indicates anomalies from -1 to 1°C. The high SST anomaly extending from Japan eastward at about 40°N is just north of the SSH anomaly in 1a as would be expected by the circulation changes implied by 1a. (c) Change in model SSH from the time of the Geosat-ERM (Nov 86 - Oct 89) to the ERS-1 time frame (Apr 92 - Mar 93). These are the same time periods as covered by the altimeter satellites in (a) A ridge of SSH extends from Japan to the Gulf of Alaska. Figure 1c is provided by a 6-layer, 1/4°resolution, primitive equation ocean model [19, 20, 21] of the global ocean circulation. This model is based upon conservation of momentum and mass and has current velocity, ocean pressure, and SSH as variables. The boundary follows the 200 m isobath. This simulation is forced only be winds and is spun up to statistical equilibrium by forcing with the Hellerman and Rosenstein wind stress climatology [22]. Subsequently, the model is forced from 1981 to 1993 with daily 1000 mb winds derived from the European Centre for

Medium-Range Weather Forecasts (ECMWF) with the annual mean replaced by that of Hellerman and Rosenstein[21]. The model reproduces all of the major current systems of the North Pacific including the equatorial currents and the Kuroshio Extension [21].

Fig. 2: (a) Model SSH deviation in Aug 1982 from a mean over Jan 81 - Dec 92. The SSH high along the equator and along the coast of the American continents is a signature of the 1982-83 El Niño event caused by an eastward propagating equatorial Kelvin wave. The initial equatorial Kelvin wave at the onset of El Niño has been studied analytically [23] and numerically [24, 25]. The trans-basin eastward propagation of the equatorial wave requires about 2 months to reach the South American coast, leaving in its wake the positive SSH anomaly extending westward to the central Pacific. (b) Model SSH deviation 5 months after the time of Figure 2a. Upon reaching South America, the equatorial Kelvin wave generates poleward propagating coastal Kelvin waves along the western coasts of the Americas. The SSH high along the equator diminishes significantly, but coastal Kelvin waves, which propagated up the North American coast, leave a high in SSH along the entire coast. The increase in SSH along the coast, associated with the passage of the coastal Kelvin waves, is visible as far as the Gulf of Alaska. Historically, in response to other El Niño events, coastal Kelvin waves have been observed to propagate along the coast of North America as far as the Aleutian Islands [26]. (c) Model SSH deviation 9 months after the time of Figure 2a. The high SSH along the North American continent begins to peel away from the coast as a westward propagating Rossby wave.

Fig. 3: Model SSH is averaged over one year to reduce short time-scale variability (a: over Mar 84 – Feb 85, b: over May 87 – Apr 88, c: over Apr 92 – Mar 93), and the

8

11 year model mean SSH is subtracted. The Rossby wave SSH ridge is indicated by the dashed line. (a) Model SSH deviation 2 years after the 1982-83 El Niño. The Rossby wave shown in Figure 2c has propagated away from shore. (b) Model SSH deviation 5 years after the 1982-83 El Niño. The Rossby wave extends from Taiwan to the Gulf of Alaska. The decrease in Rossby wave phase speed with increasing latitude causes bending of the wave front [12]. At the northern end, the wave propagates very slowly. Five years after the 1982-83 El Niño high SSH is still observed near the northwest coast of North America. At the same time, the southern end of the wave has already swept past the Hawaiian Islands. (c) Model SSH deviation 10 years after the 1982-83 El Niño. The Rossby wave has moved to a position extending from Japan to Alaska.

Fig. 4: SSH variations along 30°N from Japan to north of Hawaii (a) from the Geosat altimeter mission and (b) from the model over November 1986 to July 1989. The mean SSH from 140°E to 160°W at each point in time has been removed to reduce the effects of the annual steric anomaly due to seasonal heating and cooling of the ocean surface. The dashed line indicates the propagation of the Rossby wave generated by the 1982-83 El Niño across the Pacific Ocean. The propagation speed at 30°N for the wave is 4.9 cm/s which is very close to the theoretical value of approximately 5 cm/s for a non-dispersive, internal Rossby wave. (c) In another model experiment, the wind anomalies which cause the equatorial Kelvin wave associated with the 1982-83 El Niño are removed. The equatorial Kelvin wave and subsequent Rossby wave never occur in the model simulation. (d) In another model experiment, the predictive skill of the model is demonstrated by forcing with observed winds only over the period 1981-84 and climatological winds afterward. The equatorial

9

Kelvin wave results and the Rossby wave chain of events occurs. Thus, this phenomena is

predictable on decadal scales.

References

[1] Cane, M. A., *Science, 16*, pp. 1189-1194, (1983).

[2] Barber, R. T. and F. P. Chavez, *Science, 16*, pp. 1203-1208, (1983).

[3] Barber, R. T. and F. P. Chavez, *Nature, 319*, pp. 279-285 (1983).

[4] Rasmusson, E. M., and J. M. Wallace, *Science, 16*, pp. 1195-1202, (1983).

[5] Goldberg, R. A., G. Tisnado M., and R. A. Scofield, *J. Geophys. Res., 92*, pp. 14,225-14241, (1987).

[6] Born, G.H., J.L. Mitchell, and G.A. Heyler, *J. Astron. Sci., 35*, pp. 119-134, (1987).

[7] Reynolds, R. W. and D. C. Marsico, *J. Climate, 6*, pp. 768-774 (1993).

[8] Hurlburt, H. E., A. J. Wallcraft, Z. Sirkes, E. J. Metzger, *Oceanography, 5, (1)*, pp. 9-18.

[9] Wyrtki, K., *J. Phys. Oceanogr., 5*, pp. 572-584, (1975).

[10] Gill, A. E., Acedemic Press, pp. 662.

[11] Johnson, M. A., and J. J. O'Brien, *J. Geophys. Res., 95*, pp. 7155-7166, (1990).

[12] White, W. B., and J. F. T. Saur, *J. Phys. Oceanogr., 13*, pp. 531-544, (1983).

[13] Jacobs, G. A., W. J. Emery, and G. H. Born, *J. Phys. Oceanogr. 23*, pp. 1155-1175, (1991).

[14] Qiu, Bo, and T. M. Joyce, *J. Phys. Oceanogr., 9*, pp. 1062-1079, (1992).

[15] Szczechowski, C., Naval Oceanographic Office, Kuroshio Position Reports, unpublished.

[16] Glantz, M. H., R. W. Katz, and N. Nicholls, Cambridge University Press, pp. 535.

[17] T. P. Barnett and R. Preisendorfer, *Monthly Weather Rev., 115*, pp. 1825-1850, (1987).

[18] Teague, W. J., Carron, M. J., and P. J. Hogan, *J. Geophys. Res., 95*, pp. 7167-7183, (1990).

[19] Hurlburt, H. E. and J. D. Thompson, *J. Phys. Oceanogr. 10*, pp. 1611-1651, (1980).

[20] Wallcraft, A. J., *NOARL Report 35., Naval Research Lab, Stennis Space Center, MS*, 21 pp., (1991)

[21] Metzger, E. J., H. E. Hurlburt, J. C. Kindle, Z. Sirkes, and J. M. Pringle, *Mar. Technol. Soc. J., 26 (2)*, pp. 23-32, (1992).

[22] Hellerman, S., and M. Rosenstein, *J. Phys. Oceanogr., 13*, pp. 1093-1104, (1983).

[23] McCreary, J., *J. Phys. Oceanogr., 6*, pp. 632-645, (1976).

[24] Hurlburt, H. E., J. C. Kindle, and J. J. O'Brien, *J. Phys. Oceanogr., 6*, pp. 621-631, (1976).

[25] Kindle, J. C. and P. A. Phoebus, *J. Geophys. Res.*, accepted, in press.

[26] Chelton, D. B., and R. E. Davis, *J. Phys. Oceanogr., 12*, pp. 757-784, (1982).

[27] This work was sponsored by the Office of Naval Research (ONR) and the Advanced Research Projects Agency (ARPA).

12

[28] This document, NRL contribution number NRL/JA/7323–93-0025, has been reviewed and is approved for public release.

(a)

(b)

(c)

(a)

(b)

(c)

-15   cm   15
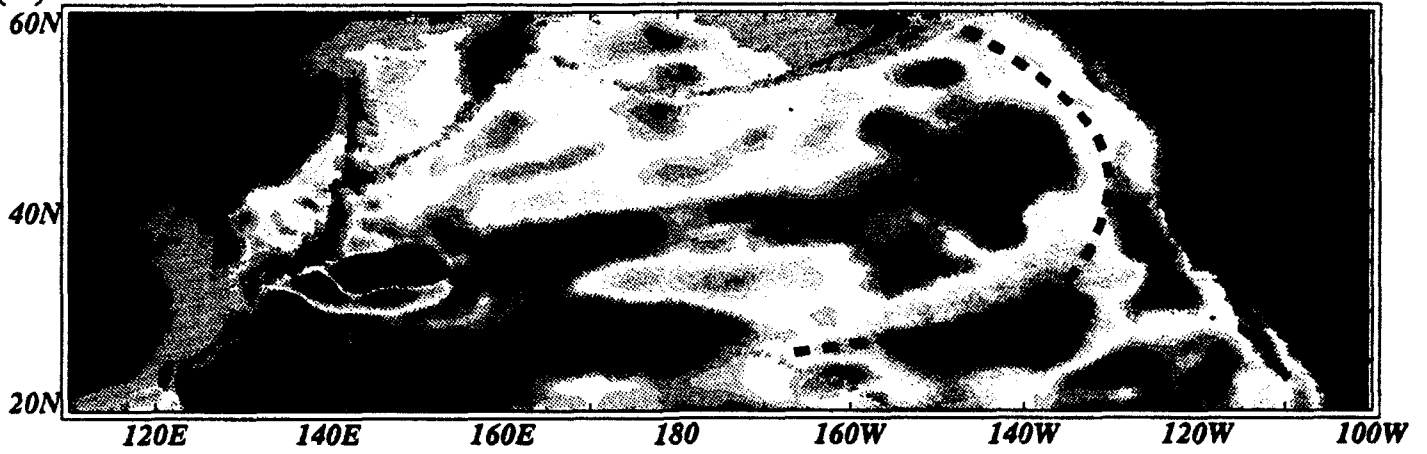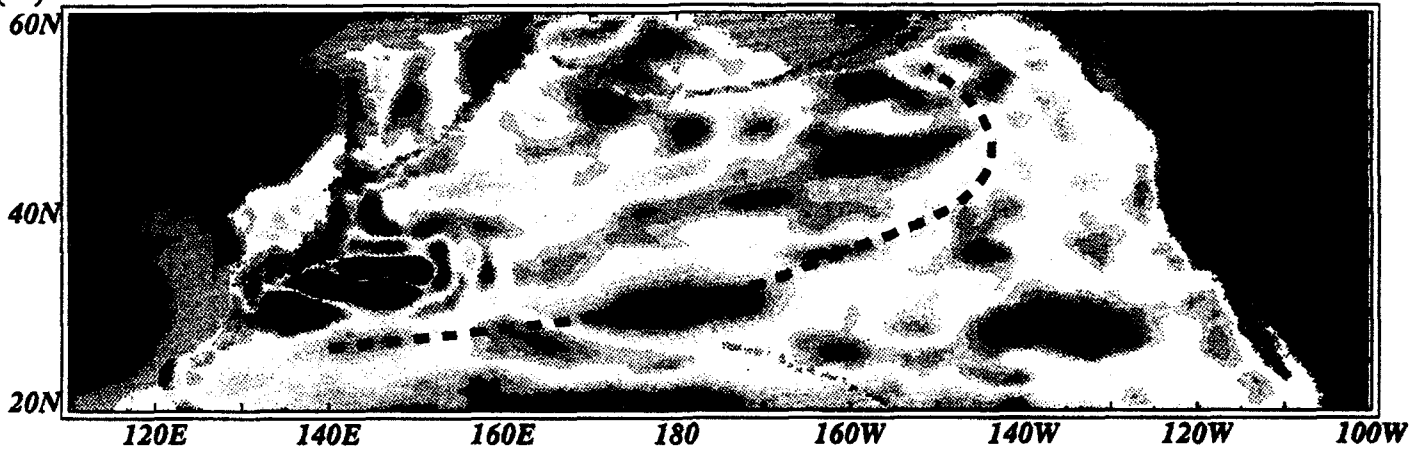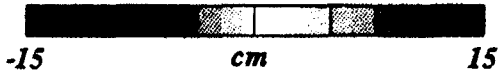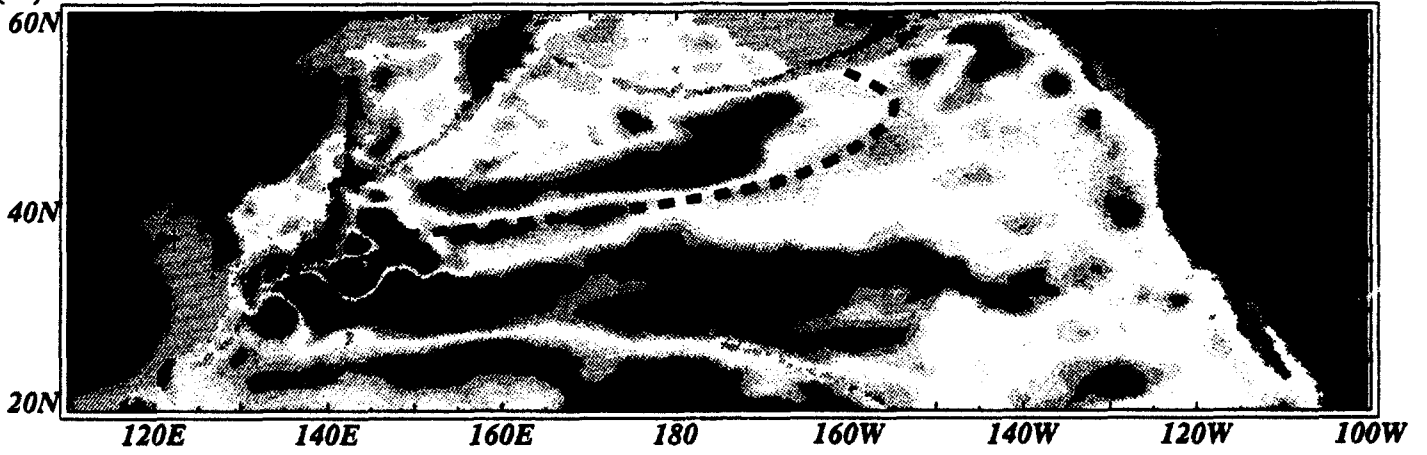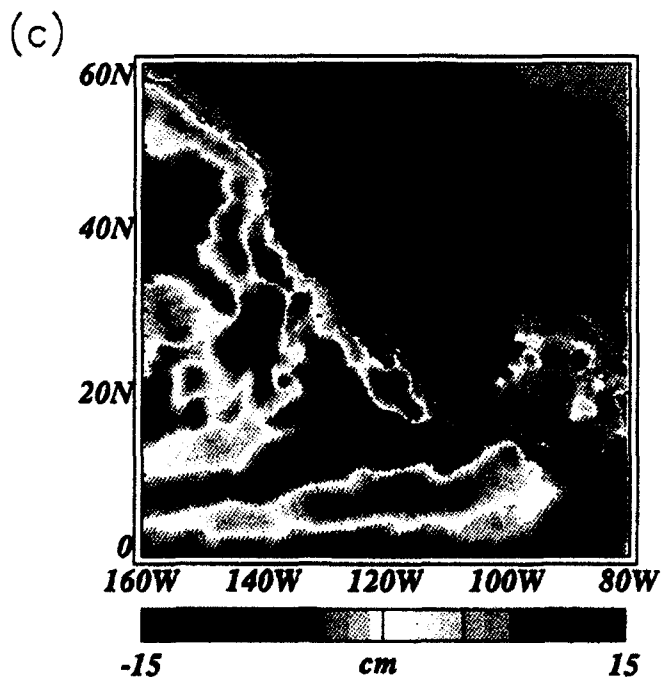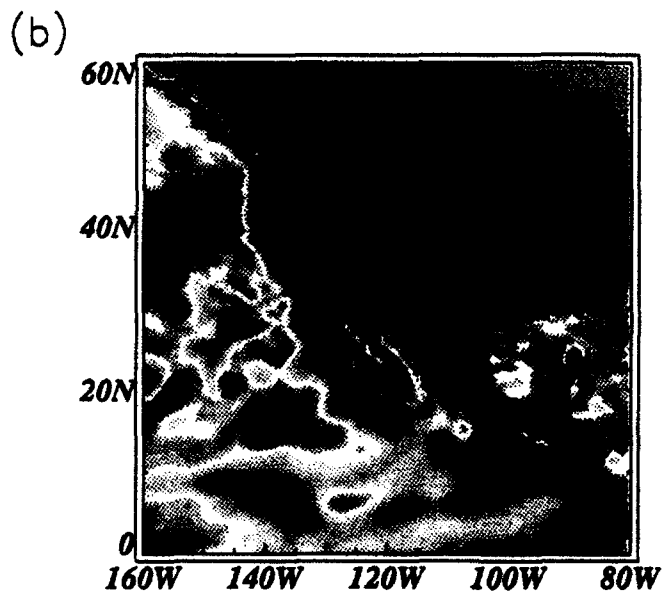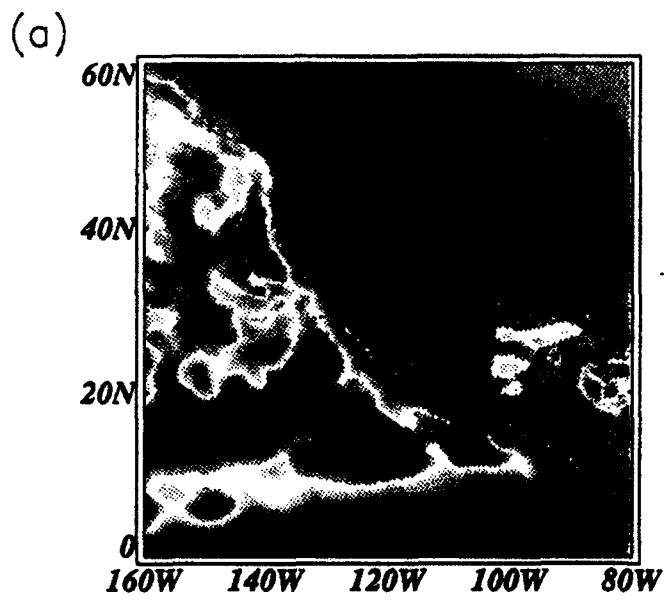
(a)
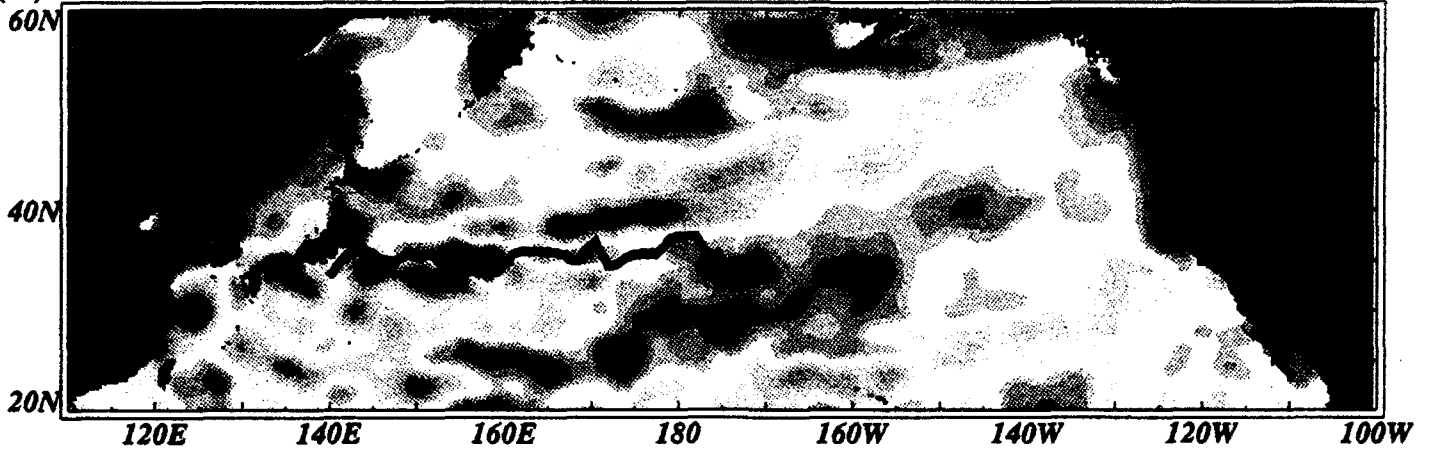
(b)
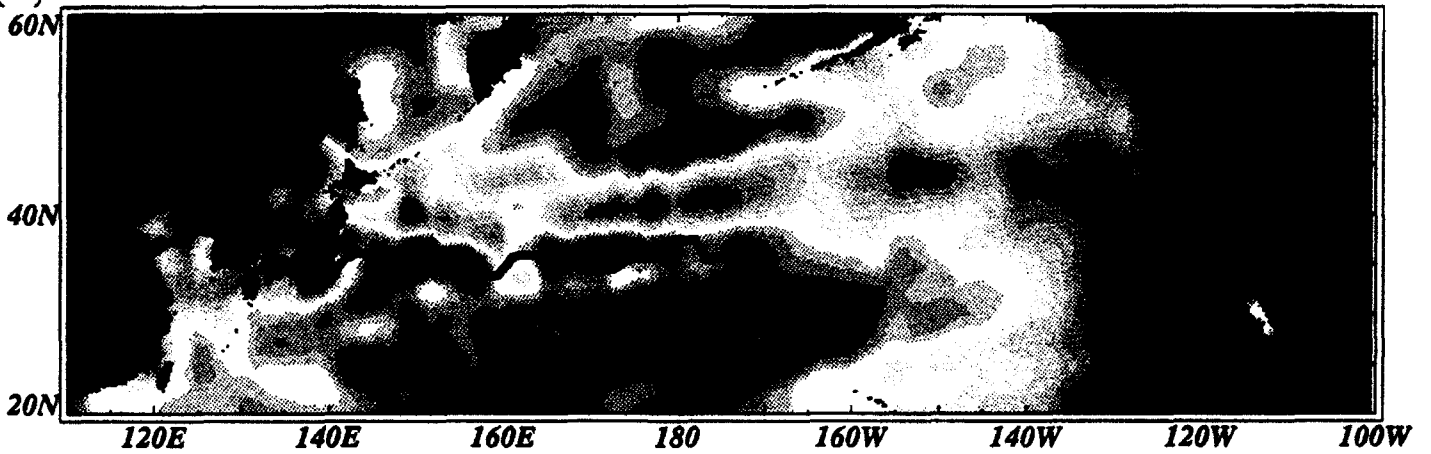
(c)
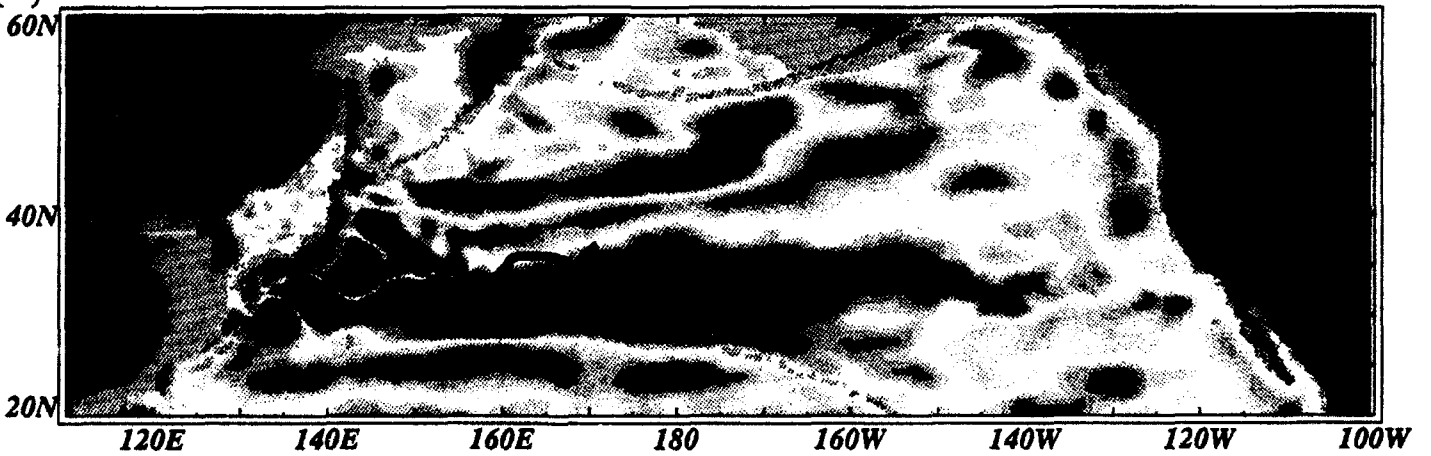
Time-longitude plot at 30N

(a)   (b)   (c)   (d)

-10   cm   10

NUM	TASK B	Start Date	Finish Date
B.1	OBTAIN EQUATORIAL PAC WIND FIELDS FROM 80-91 AND DRIVE THE EQUATOR MODEL	4/14/93	5/31/93
B.2	EXTRACT THE COASTAL KELVIN SIGNAL FROM THE EQUATOR MODEL AND DRIVE THE MID LATITUDE MODEL	6/1/93	6/30/93
B.3	INTEGRATE THE MODEL SOLUTIONS BETWEEN HAWAII AND WEST COAST RCVRS	6/1/93	6/30/93
B.4	COMPARE WITH OBSERVATIONS AND IDENTIFY VARIABILITY IN ACOUSTIC TRAVEL TIMES	7/1/93	9/1/93
B.5	DESIGN FUTURE EXPERIMENTS	9/15/93	4/10/94
B.6	ADD MODEL COMPLEXITY AND VERTICAL STRUCTURE TO IMPROVE ESTIMATES OF TRAVEL TIME	4/15/94	9/1/94
B.7	RUN NRL MODELS	9/15/94	4/1/95
B.8	USE REAL DATA TO ASSIMILATE INTO OCEAN MODELS OF THE NORTH PACIFIC	9/15/94	4/1/95
B.9	SUBMIT FINAL REPORT	4/15/95	6/30/95

TASK C:
SSAR DEVELOPMENT

March Retrieval Cruise

The Standard version of the SSAR prototype was deployed for a long term test on November 5, 1993 about 50 miles offshore Bermuda. It made a big loop to the south and then drifted close to the island about a month later. It was retrieved on December 5, checked for damage, and re-deployed 70 miles east of Bermuda on December 9. Figure C.1 shows the drift track for November 5, 1993 to March 10, 1994 when it was retrieved following a failure in the conductors in the hose section. Figures C.2a and 2b show some of the data telemetered during this period. These results confirm our earlier analytical analysis of the forces experienced by the Standard SSAR where maximum tensions are of the order of 1500 lbs.

Following retrieval of the SSAR, the system was inspected for damage, corrosion, or other problems. The conductor failure was caused by abrasion of the conductor assembly by the inner hose wall where the conductors were attached to the stop rope (Figure C.3). The conductor assembly was longer than the stop rope and this excess length caused hockles to form at the attachment points which led directly to the abrasion problem. There was no noticeable abrasion on the stop rope itself. In hindsight, had we been less conservative on the length of the conductor assembly, this problem would not have occurred. The conductor assemblies for the operational units have been re-designed and are described below. The only other damage to the SSAR during the 4-month test was caused by fish or shark bites on the hose section. These bites were in the form of cuts a few inches long or punctures. None were deep enough to penetrate the hose, but some did cut deep enough to damage the Kevlar cords designed to help protect against fishbite (Figure C.4). No loss of internal pressure resulted from the cuts nor were the hoses weakened since the Kevlar cords act to prevent the propagation of cuts.

Final Hose Designs

The final design for the stop rope/conductor assembly is shown in Figure C.5. It is used in both Standard and Snubber designs. It consists of an inner strength member of Vectran line (RBS=16,000 lbs), 8-24 gauge conductors helically wound around this core and held in place with a polyester braid, and a thick, abrasion resistant Spectra braid covering the entire assembly. It is terminated by eye-splicing around a thimble at each end of the hose with the conductors led out of the assembly below the splice. The stop rope is made so that the hoses can stretch 20% before the rope begins to take the load. Eight conductors are used to provide redundancy for the three signal wires and for a temperature sensor located at the bottom of the hose.

Figure C.6 shows the final designs for the Snubber hose. The Standard hose is similar but has an ID of 4 inches and a length of 50 feet. Three hoses of each type have

been ordered for the initial SSAR production with a decision on additional hoses put off u
we collect acoustic data in the ocean and determine if one design is significantly better tha
the other. Figures C7 and C8 show the final SSAR designs for the production units.

Fatigue Testing of Hose Assemblies

The fatigue testing of short hose assemblies has continued at TMT's tests facility.
These hoses are Snubber designs, but the results are applicable to the Standard design witl
appropriate scaling. Following the early failure of the first two test hoses, a third short h
was built with increased wall thickness near the ends and more carefully tapered cord
segments to minimize stress concentrations. This hose also incorporated the required
electrical conductors within the rubber hose wall as a way of providing protection for the
conductors. This design required a new design for the end fittings so that the conductors
could safely exit the hose at the ends. The new design covered the steel end fittings with
vulcanized rubber and ran the conductors inside this rubber layer.

A test plan for this hose was prepared after an analysis of the SSAR forces that ar
expected under severe sea conditions. This analysis concluded that maximum tensions in
Snubber hose would be about 800 lbs. A test that alternately tensioned the hose from 50-
lbs every 4 seconds was then begun. At the bottom end the hose end was flexed $\pm 30°$
every three seconds. A test success was defined as 500,000 cycles without serious damag
this being about 10% of the number of cycles a SSAR will see in one year, but perhaps 1
times the number of times a tension maximum will be experienced.

The test was begun on March 9, 1994 and 500,000 cycles were completed on Apr
(Tables C1 and C2). At this time, tension was increased to cycle from 30-1300 lbs. At
640,000 cycles, the stop rope was removed to more fully stress the hose. At 710,000 cy
the hose suffered a sudden non-catastrophic 1/4 inch length increase. As of April 20, the
hose had successfully survived 950,000 cycles in flex and 630,000 cycles in tension with
failure with almost half of these cycles at tensions 60% higher than the maximum anticip:
loads. Unfortunately, the conductor in the wall design did not fare as well. Complete
conductor failure occurred at 144,000 cycles with partial failure as early as 3500 cycles.
Conductor failure mode is not well understood at this time and will await x-ray analysis :
dissection of the test hose. The most likely cause of conductor failure is z-kinking of the
copper during the tension cycle. The use of a more compliant conductor construction sh(
eliminate this problem. Our conclusion, however, is that design improvements will have
wait and that to be safe we should stick with the combined stop rope/conductor assembly
design for the first operational SSARs.

Testing of the Ultrashort Baseline Acoustic Navigation System

Two important test of the ultrashort baseline (USBL) acoustic navigation system v
completed this quarter. In the first the USBL acoustic array was calibrated in a special
acoustic calibration facility at O.R.E., Inc. The calibration measures the sensitivity and
accuracy of the array in determining the bearing and azimuth of a sound source. Figure
is an example of the test results which shows true angle versus measured angle for 360° ‹

TEST OF HOSE ASSEMBLY C1
Data Recorded During Normal Cycling

Date	Time of Day, hours	Total Tension Cycles	Total Bending Cycles	Tension Range, pounds	Elongation Range, inches	Pressure Range, psi	Comments
03-09-94	--	101	0	50 - 800			Start bend cycling
03-09-94	1610	136	632				Conductor resistance changing
03-09-94	1920	1,478	3,500				Conductor open at high tension
03-10-94	0700	6,426	17,021				All conductors but one intermittent
03-11-94	0734	16,513	42,951				
03-12-94	0242	25,152	64,060				Equipment failure and hose damage
03-17-94	--	25,152	64,060				Restart test
03-18-94	0944	41,960	89,465				
03-19-94	0811	55,285	114,310				
03-20-94	1100	70,980	143,920				All conductors open
03-21-94	0725	86,672	166,474				
03-22-94	0614	105,870	191,530				
03-23-94	0705	126,360	216,960				
03-24-94	0836	147,608	247,138				
03-25-94	0758	167,453	272,173				
03-26-94	0703	188,020	297,730				
03-27-94	0748	209,960	325,060				
03-29-94	0738	252,490	377,900				
03-30-94	1406	279,704	411,570				
04-01-94	0918	314,740	456,300				
04-02-94	0923	335,870	482,860				
04-03-94	1056 DST	357,640	510,000	50 - 800	- 14.4		End of first phase of test
04-03-94	1150	358,215	510,990	30 - 1300	- 15.4	3 - 46	Running at higher tension range
04-04-94	0657	368,760	532,080	30 - 1300	- 15.6	3 - 44	
04-05-94	0723	382,220	558,990	35 - 1340	12.9 - 15.6	3 - 44	
04-06-94	0739	395,600	585,745	35 - 1290	12.9 - 15.6	3 - 41	
04-07-94	0723	408,886	611,915	35 - 1285	13.0 - 15.8	3 - 42	
04-08-94	0952	423,296	641,100	40 - 1320	- 15.9	3 - 42	
04-08-94	1652	423,979	641,512	50 - 840	- 16.3	4 - 56	Stretch rope removed. Tension reduced.
04-09-94	0648	434,975	656,900	50 - 800	12.8 - 16.1	4 - 53	
04-09-94	0828	436,780	658,736	50 - 1000	13.2 - 17.2	5 - 65	Tension increased
04-09-94	0835	436,890	658,865	50 - 1210	13.2 - 17.8	5 - 79	Tension increased
04-09-94	0914	437,390	659,580	70 - 1300	13.4 - 18.9	6 - 84	Running at higher tension range
04-10-94	0732	453,535	684,185	60 - 1320	14.3 - 19.2	4 - 82	
04-11-94	0730	471,440	710,590	60 - 1320	14.6 - 19.4	3 - 80	Abrupt increase in hose length at 0750 hours
04-12-94	0834	490,795	738,242	40 - 1350	15.1 - 20.6	1 - 73	
04-13-94	0734	508,200	763,617	60 - 1340	15.5 - 21.1	1 - 71	
04-14-94	0734	526,390	790,095	50 - 1340	15.7 - 21.3	0 - 70	Test interrupted for 4 hours 24 minutes
04-15-94	0800	541,576	812,144	50 - 1340	16.1 - 21.5	0 - 69	
04-16-94	0710	559,320	837,772	60 - 1320	16.3 - 21.8	0 - 68	
04-18-94	0640	594,290	890,290	40 - 1240	16.4 - 22.0	-1 - 66	Test interrupted for 20 minutes
04-19-94	0622	612,390	916,060	40 - 1290	16.6 - 22.2	-1 - 65	
04-20-94	0715	631,470	943,530	40 - 1340	16.7 - 22.3	-1 - 66	

Table C2: Conditions and results of hose flex and
tension fatigue cycling tests.

TEST RESULTS	HOSE SAMPLE #1	HOSE SAMPLE #2	HOSE WITH CONNECTORS, SAMPLE #C1
Min and Max Load	0-1,800 lbs	0-1,300 lbs	50-800lbs 510,000 cycles; 50-1300$^+$ lbs 490,000 cycles
Load Cycle Duration	10 sec	9.5 sec	4 sec
Elongation* at Maximum Load	50%	42.5%	With Stop Rope: ~ 40%
Flex Angle	45°	25°	30°
Duration of Flex Cycle	3 sec	2.5 sec	2.5 - 3 sec
Fill Fluid Pressure at Max Tension	220 psi	105 psi	65 psi
Load Cycles till Failure	4,152	9,878	Still functioning at 631,470
Flex Cycles till Failure	13,761	39,546	Still functioning at 1,000,000 flex cycles
Failure Type and Localization	Burst failure at end of steel coupling. Reinforcement intact.	1/4" burst at taper of extra reinforcement; hose otherwise intact.	Test stopped conductor failure after 17,000-144,000 flex cycles

* Elongation measured in compliant section of test hoses at load cycle 100.
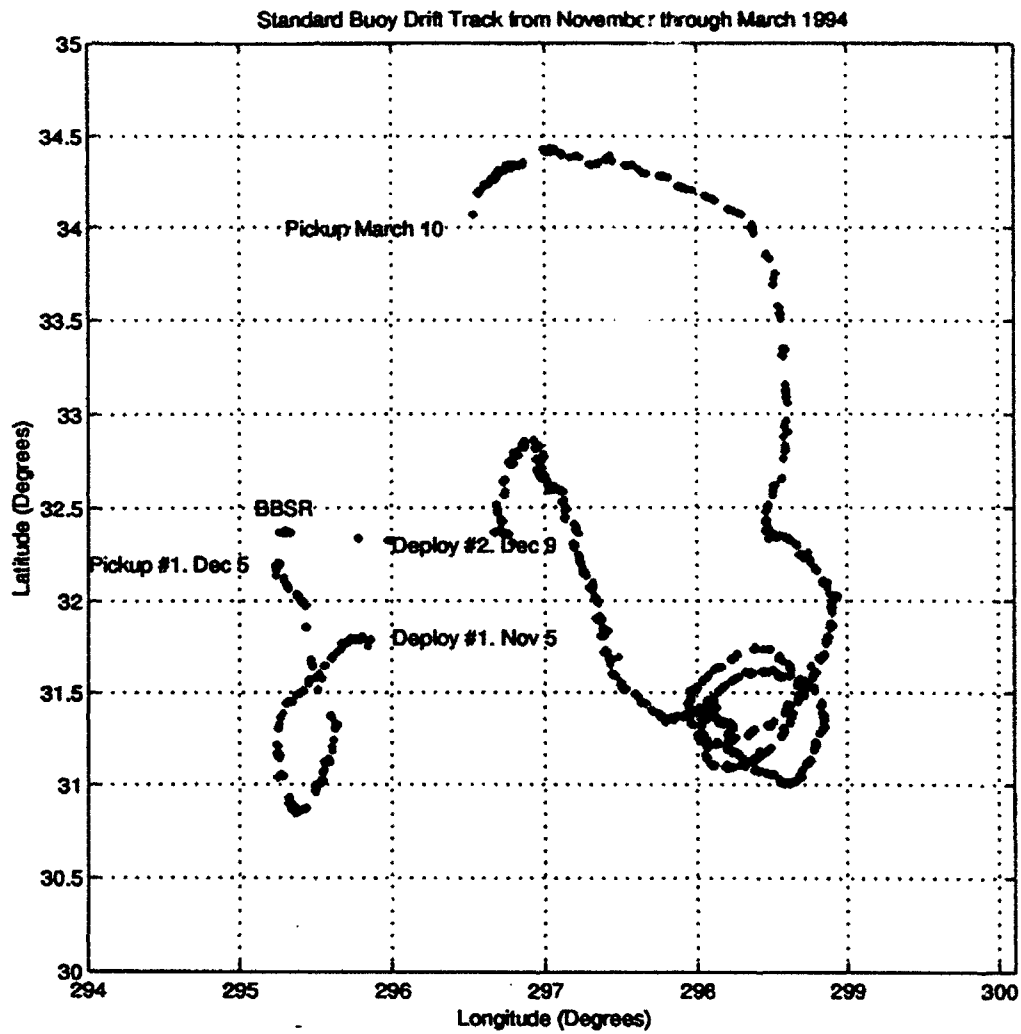
Figure C1   Drift track of the Standard SSAR prototype
from 5 November 1993 to 10 March 1994

Figure C2a: Data from the Standard SSAR during the long term drift test.

Figure C2b: Data from the Standard SSAR during the long term drift test.

Loop formation of
conductor rope due
to excessive length

Closeup of abraded rope
loop showing damaged braid,
insulation and conductors
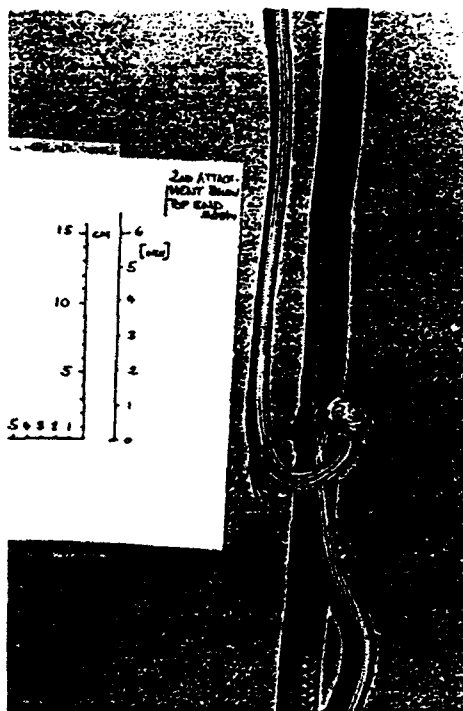
Formation of kinked
conductor rope loop

Closeup of kink loop
with abraded outer braid,
insulation, and conductors

Figure C3   Stop Rope/Conductor Rope Assembly, with conductor
rope abrasion damage after 4 months sea service.
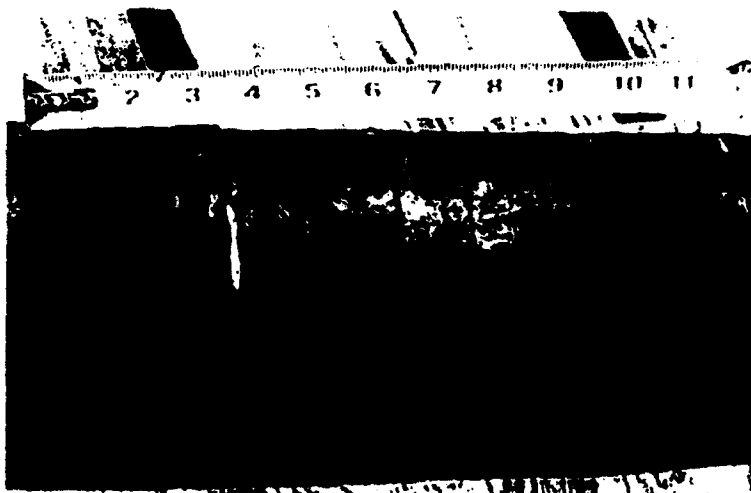
Upper jaw razor blade like teeth cuts, some penetrating into and stopped by embedded Kevlar fabric (parallel cuts 45° inclined)
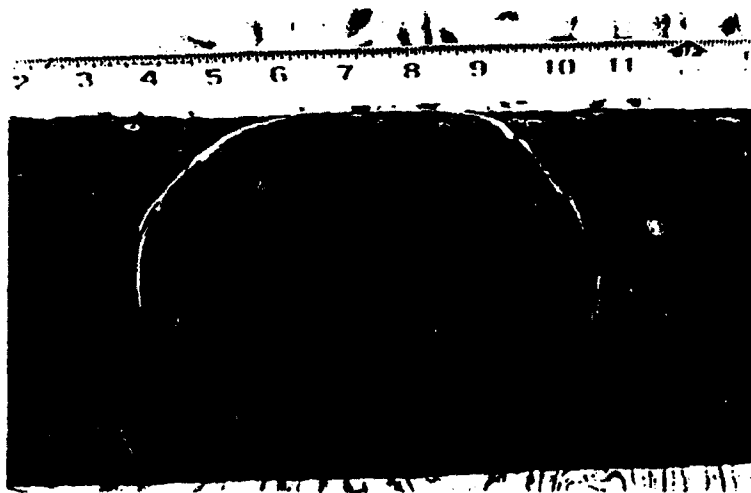
Lower jaw teeth impressions (random shape incisions, less deep than upper jaw cuts)

Figure C4 Hose from the Standard SSAR showing evidence of fishbite damage

1.0" DIA.

OUTER CONDUCTOR LAYER

INNER CONDUCTOR LAYER
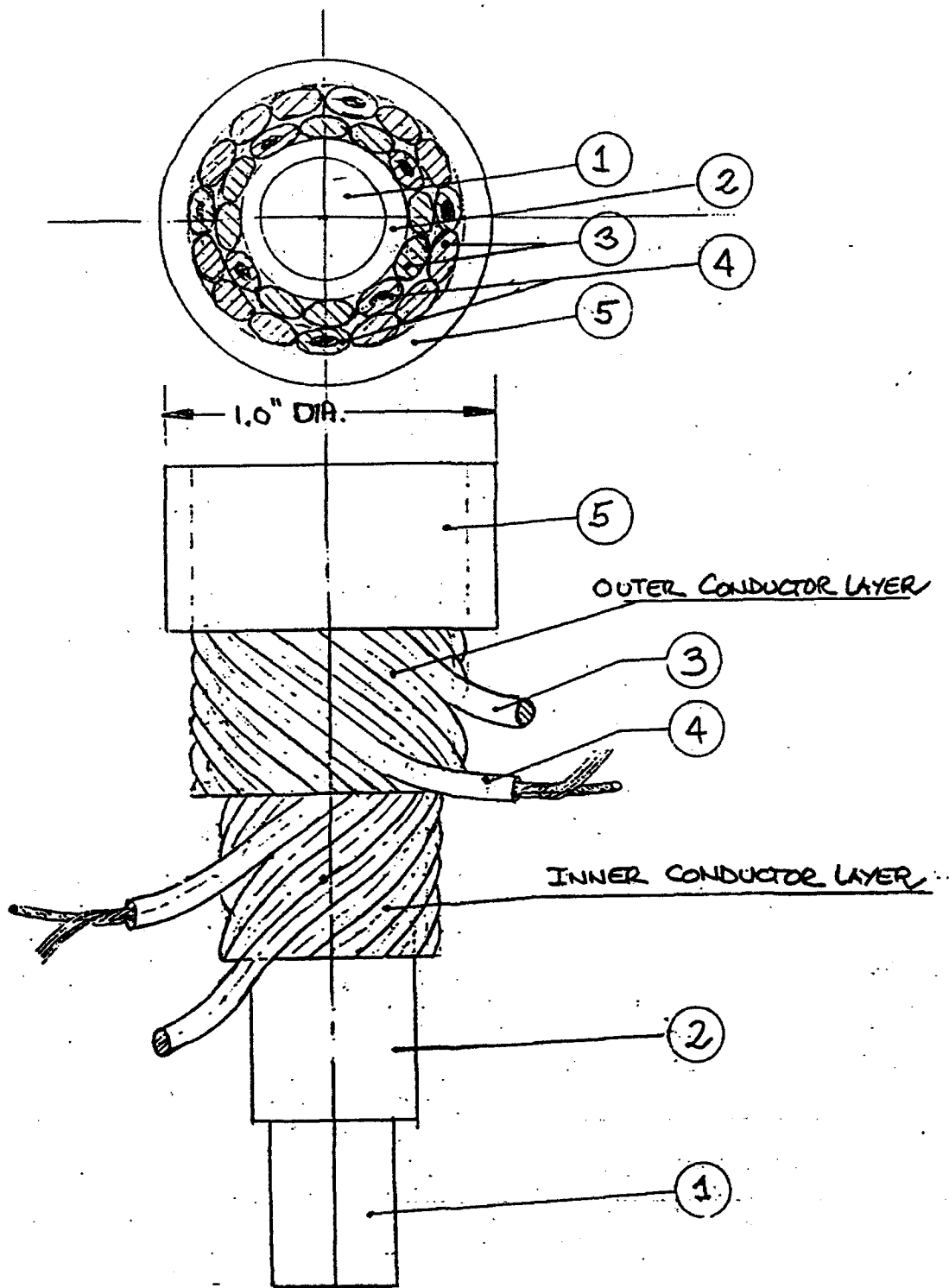
(1) VECTRAN HS ROPE, 16,000 LBS STRONG, 0.375" DIA.
(2) POLYESTER OVERBRAID (BEDDING SURFACE FOR CONDUCTOR LAYER)
(3) POLYETHYLENE EXTRUDED FILLER, 0.08" DIAMETER
(4) COMPLIANT AWG#24 COPPER CONDUCTORS [8] WITH HEAVY INSULATION
(5) HEAVY SPECTRA BRAIDED OUTER JACKET AS ABRASION PROTECTION

Figure C5   Redesigned conductor stop rope for SSAR *Snubber*
            and *Standard* production hoses
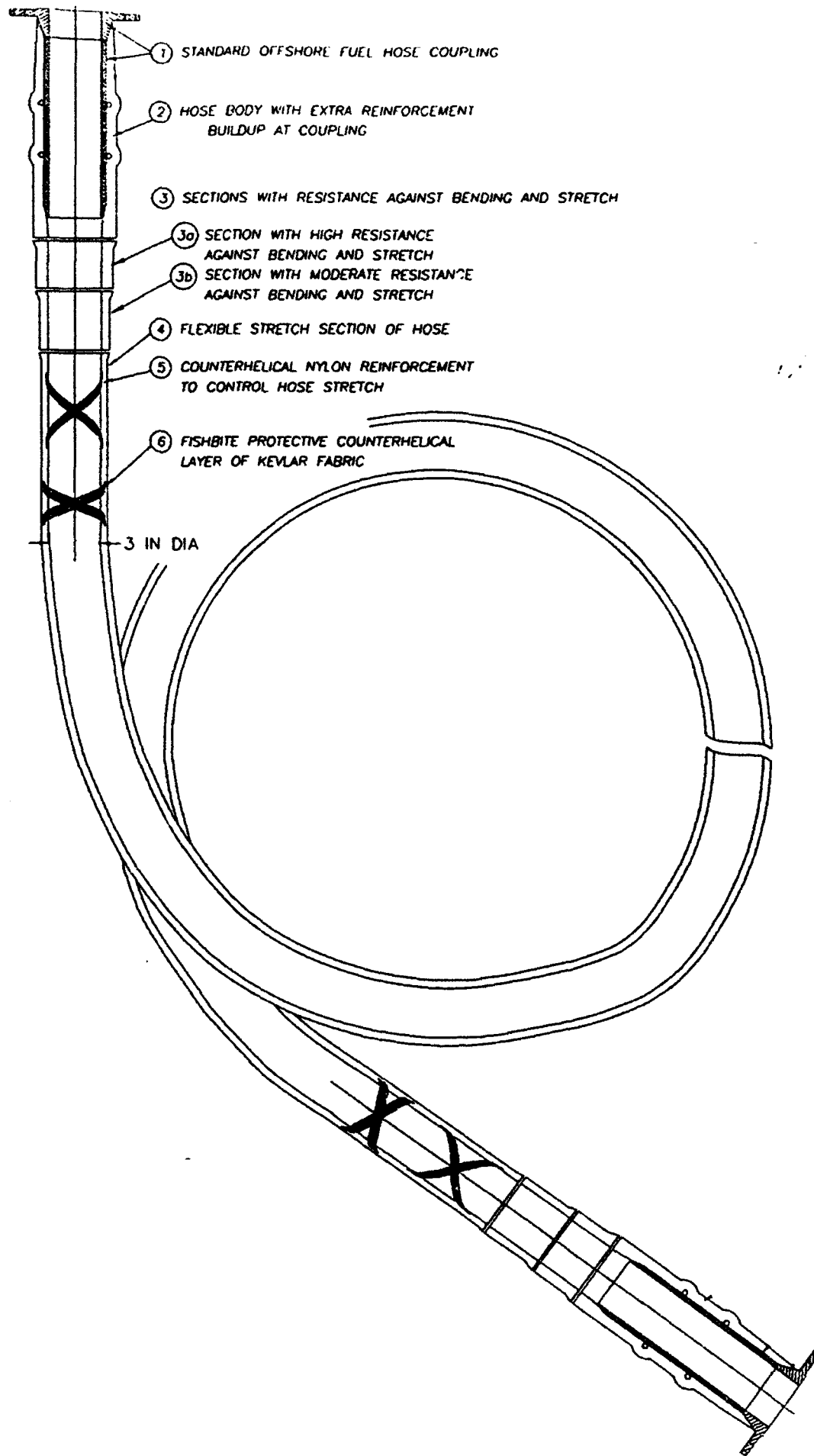
Figure C6   Final Design for Production *Snubber* Hose
(Outer diameter 4.0", length 98 ft)
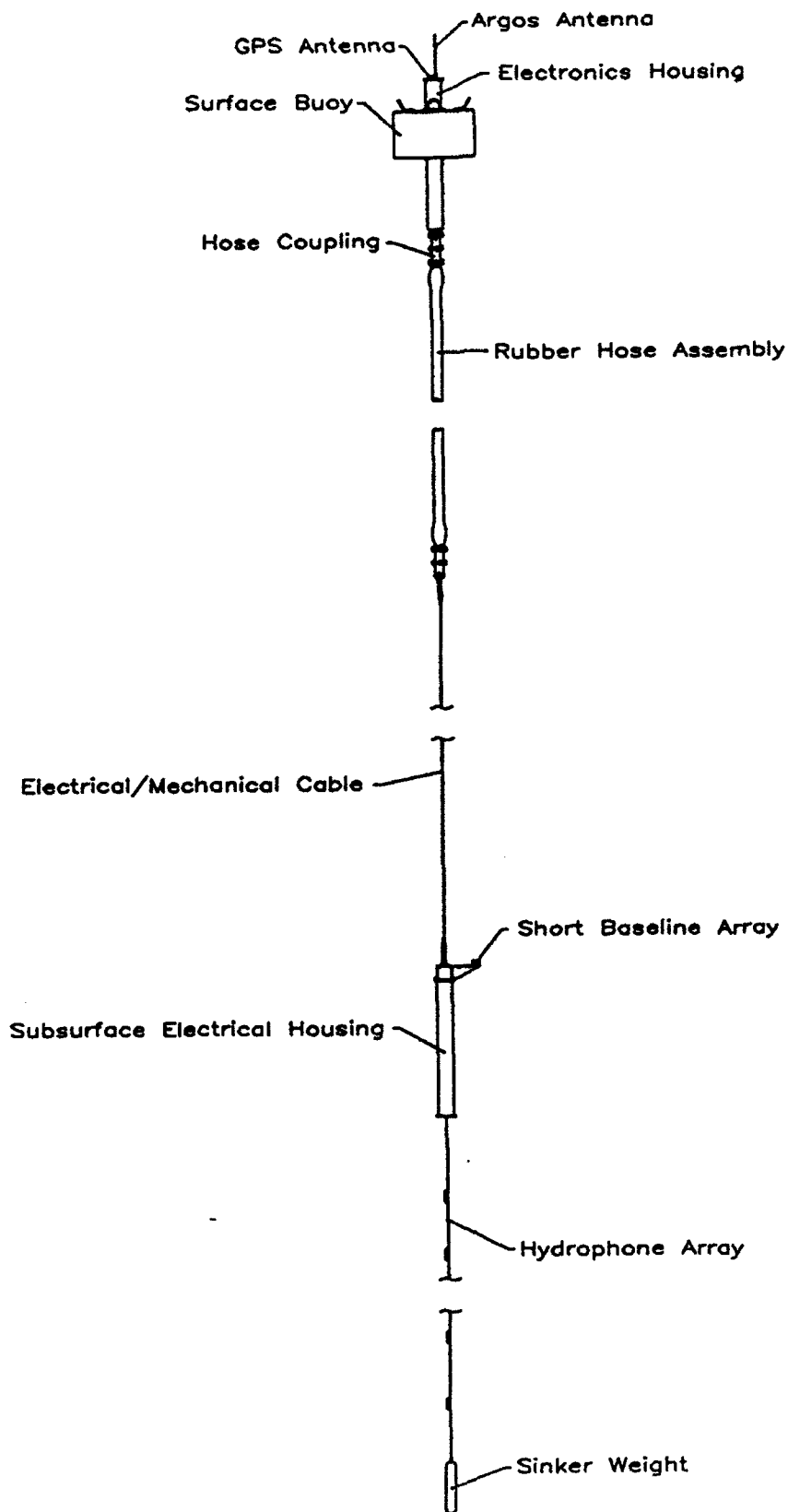
Figure C7   Final design for the Standard SSAR
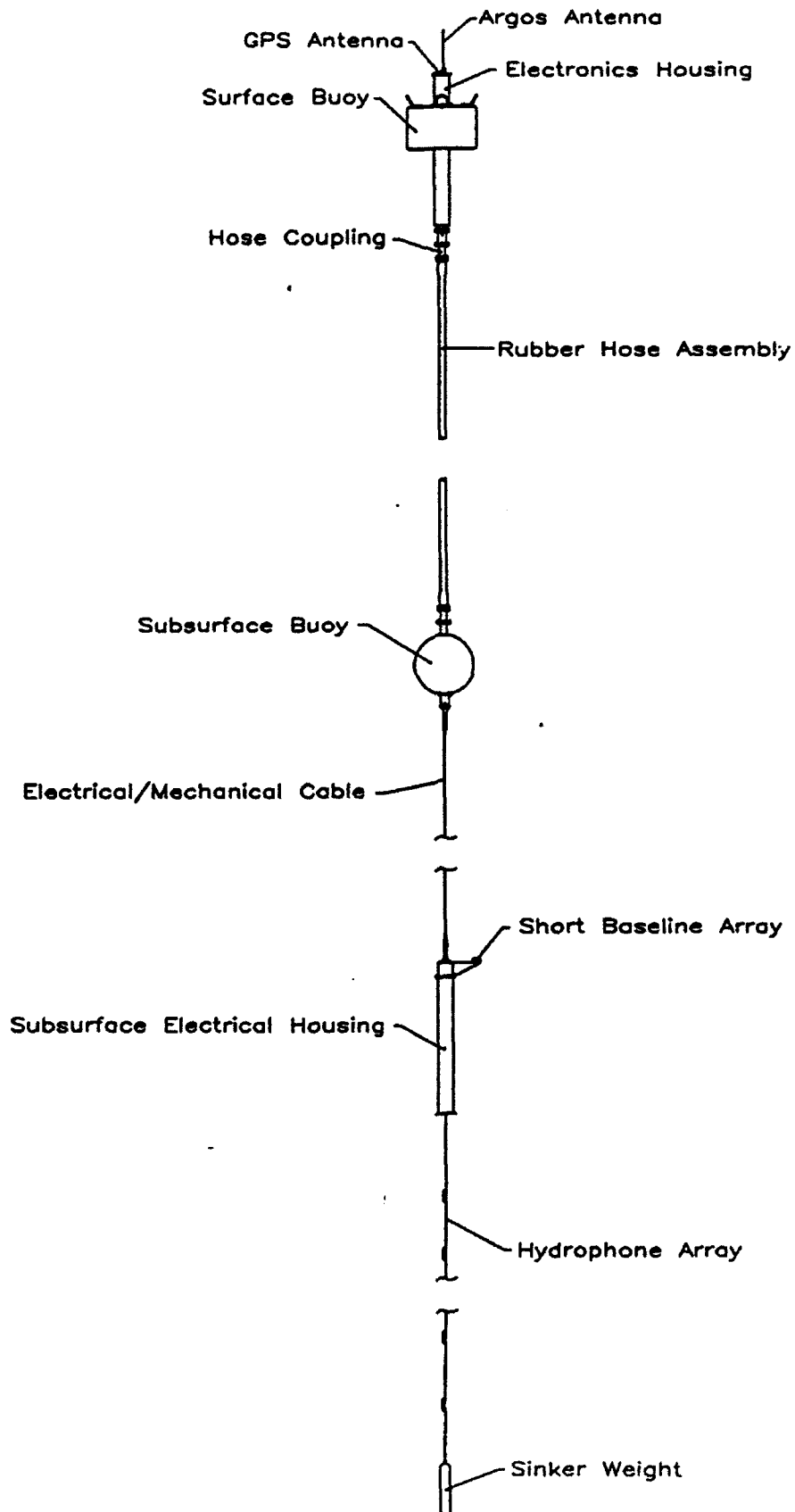
Figure C8   Final design for the Snubber SSAR

Raw xyz data converted to az-el
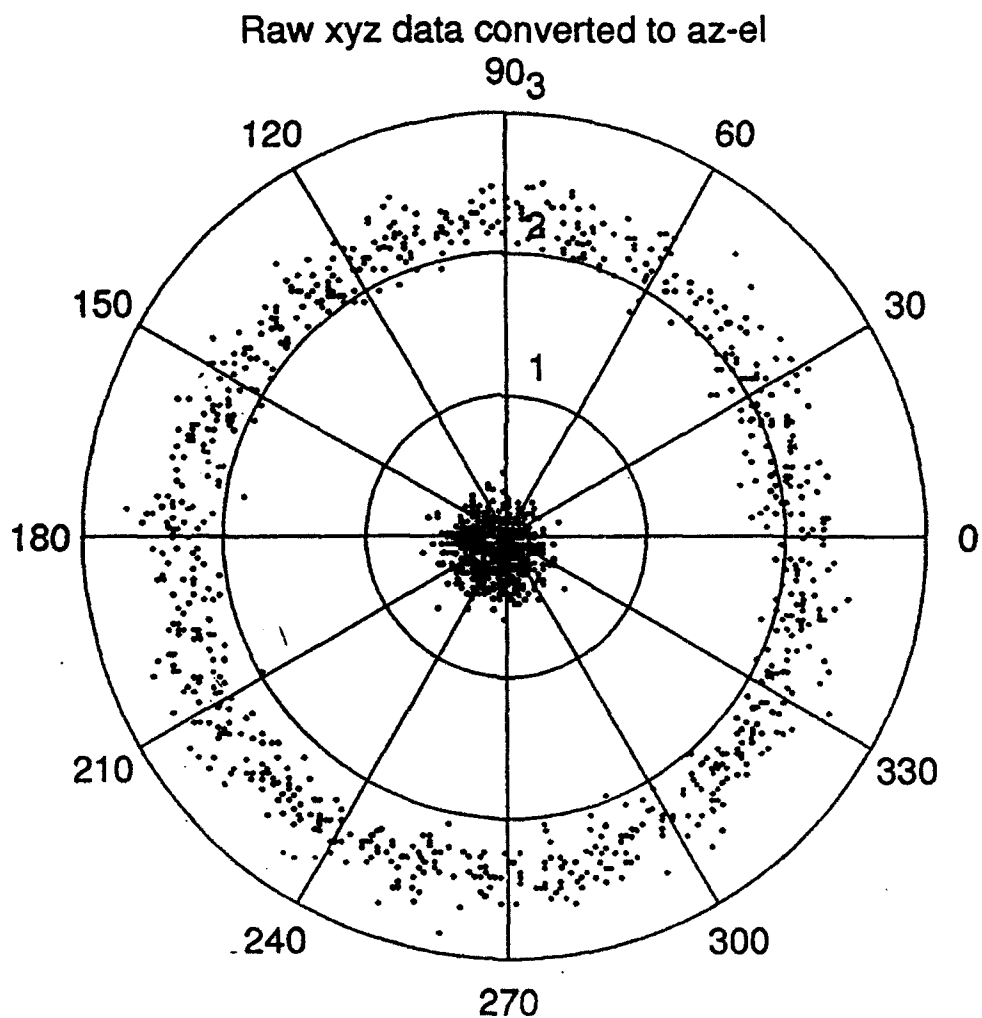
polplot(allpos(1:1850,1:3),-0.04,0.04,4,3);

Figure C9a: Calibration plot of first short baseline transducer. Two
                inclination angles are shown, 0 and 2 degrees. Sample
                points are taken at two degree increments around the
                circle from 0 to 358 degrees. The slight offset of the
                circles toward the lower left is due to a constant phase
                shift at the analog front-end which was not removed
                before this plot was made.

orecal2, sblcal3-6, New transducer
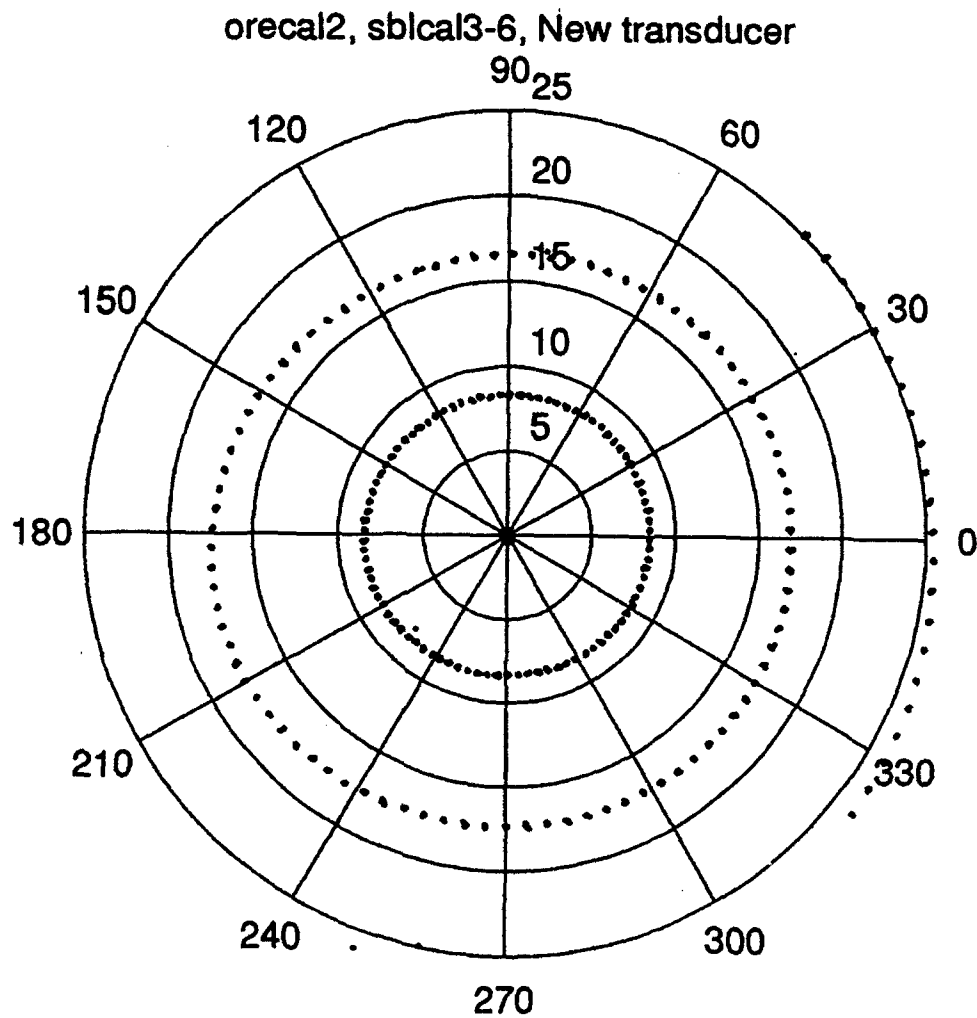
Figure C9b: Calibration plot of second short baseline transducer with an improved (lower noise) analog front-end. Data is taken at 4 degree increments from 0 to 356 degrees. This transducer has larger spacing between elements which increases system resolution.

Buoy and array positions in Range Coordinates
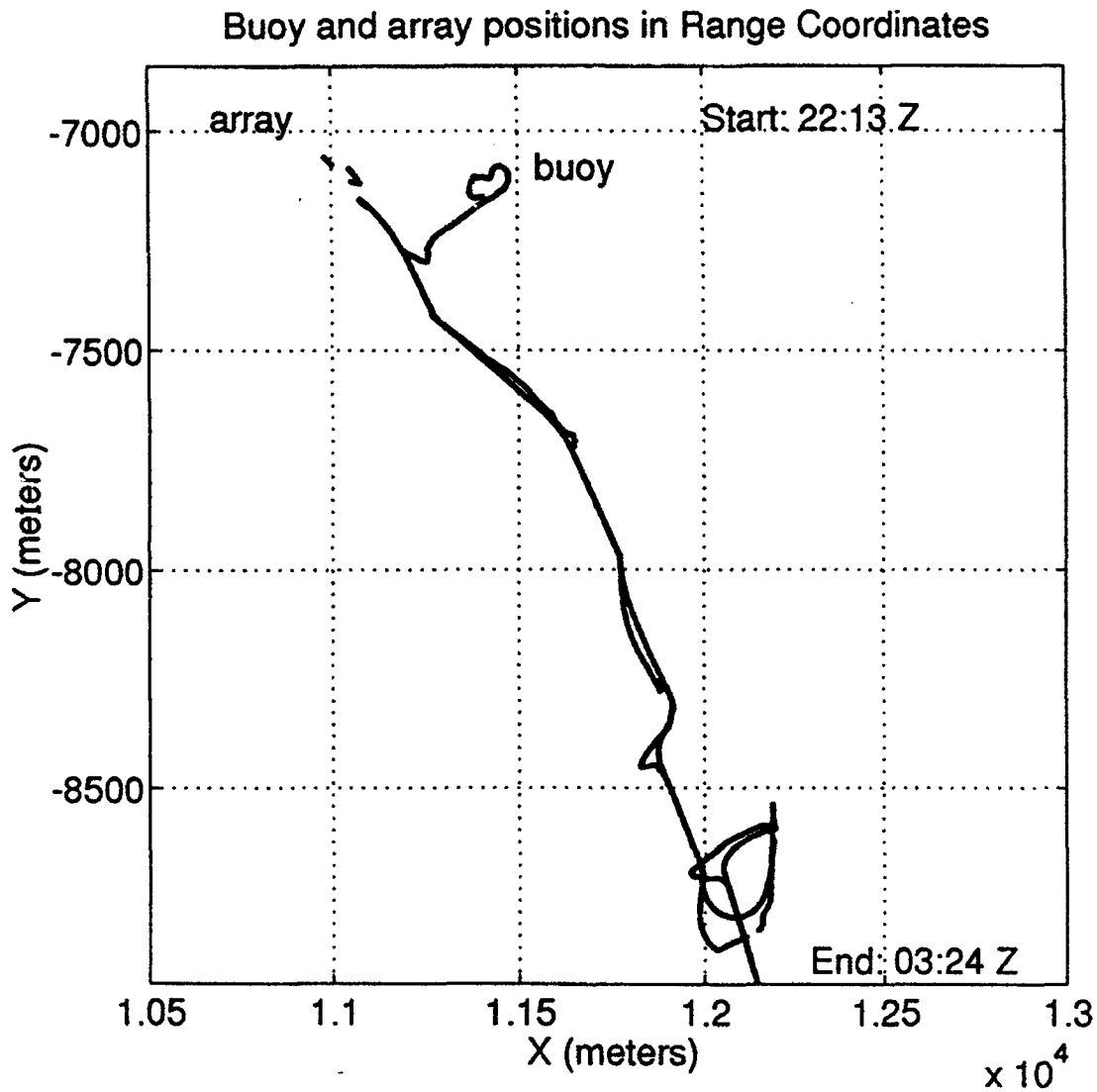
Figure C10:   Drift track for the SSAR buoy during the tracking
experiment at the AUTEC range. Buoy and array tracks
are shown. At the start, the array is tracked on the
surface until the floats holding it are removed and it is
allowed to fall into position below the buoy.

Relative x-y for Buoy-Array from Range Track data
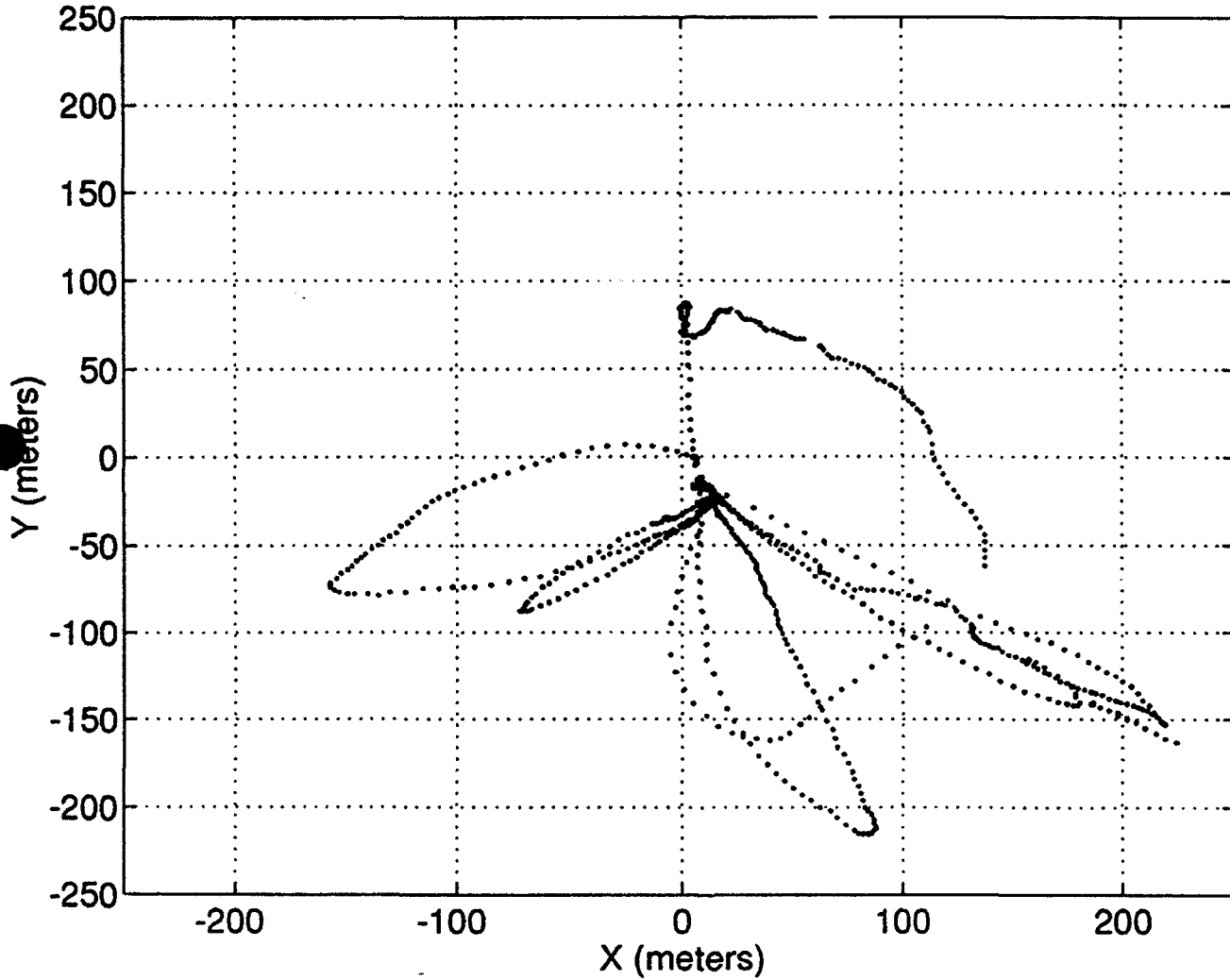
Figure C11:   AUTEC range position data showing location of the
                surface buoy relative to the lower pressure case (at 0,0)
                during the 3-hour test period on April 14, 1994.
                Variations in the pattern are tests with the ship used to
                pull the buoy into different positions with respect to the
                array below.

Figure C12: Task C Schedule

NUM	TASK C	Start Date	Finish Date
C.1	MECHANICAL DESIGN OF CABLE, BOUY AND TERMINATIONS		
	INITIAL DESIGN	4/15/93	8/9/93
	ACCEL LIFE TESTS	8/31/93	4/17/94
	AT SEA TRIALS	9/13/93	1/15/95
	DESIGN REFINEMENTS	3/1/94	3/1/95
C.2	BOUY ELECTRONICS AND NAV SYSTEMS		
	SYSTEM DESIGN	4/15/93	9/1/93
	CONTROLLER /GPS INTERFACE	4/15/93	12/15/93
	ARGOS TELEMETRY	4/11/93	2/27/94
	POWER SYSTEM	4/15/93	12/15/93
	PROTOTYPE TESTS	8/1/93	6/12/94
C.3	DSP SYS ACOUSTIC NAV AND SENSOR MODULE		
	SYSTEM DESIGN	4/15/93	9/1/93
	SENSOR MODULE	4/15/93	12/15/93
	ACOUS NAV MODULE	4/15/93	5/15/94
	DSP MODULE	4/18/93	5/15/94
	DSP SOFTWARE	5/23/93	5/15/94
	TELEMETRY	4/15/93	12/15/93

NUM	TASK C	Start Date	Finish Date
	PROTOTYPE TESTS	8/1/93	6/19/94
	DESIGN REFINEMENTS	3/1/94	3/1/95
C.4	HYDROPHONE ARRAY		
	ARRAY DESIGN	4/15/93	6/10/93
	PROTOTYPE TESTS	10/1/93	6/19/94
C.5	GPS NAV SA CORRECTIONS		
	DATA COLLECTION METHODS	4/15/93	6/12/94
	DEVELOP SOFTWARE	5/1/93	12/15/93
	PROTOTYPE TESTS	12/15/93	6/19/94
C.6	SYSTEM INTEGRATION		
	LAB TESTS	11/15/93	5/15/94
	AT SEA TEST	7/24/94	8/7/94
	DESIGN REFINEMENTS	2/25/94	9/1/94
C.7	FABRICATION OF SSAR		
	BUILD 2 PROTOTYPES	5/1/93	8/30/93
	BUILD & TEST 3 SSARS	1/1/94	6/19/94
	BUILD & TEST 3 SSARS	3/1/94	7/24/94
	BUILD & TEST 4 SSARS	5/1/94	8/30/94

Figure C12: Task C Schedule

NUM	TASK C	Start Date	Finish Date	1993 A M J J A S O N D J F M	1994 A M J J A S O N D J F M	1995 A M J J
C.8	FIELD OPERATIONS					
	DEPLOY 3 SSARS	8/28/94	9/11/94			
	DEPLOY 3 SSARS	10/2/94	10/16/94			
	DEPLOY 4 SSARS	11/6/94	11/20/94			

Figure C12: Task C Schedule

SSAR Recovery Cruise Report
Bermuda, March 9 - 12, 1994

March 9

Alex Bocconcelli and Larry Costello arrived at BBSR at 1300. The
RDF antenna was promptly mounted and the deck gear box loaded.
After receiving an update buoy position from WHOI the ship left
the dock (1500 local time). An SSB communication schedule was
agreed upon with Ed Denton and the SSB link was checked
sucessfully once offshore.

March 10

At 0400 the Argos RDF was switched on and the searchlights turned
on as we approached the buoy estimated position. At 0445 the
first signal was received and seven minutes later the buoy was
spotted on the starboard side at about 50 feet from the bow.
Recovery began at 0640 with daylight and it was concluded at 0745
with all drifting array components on deck. At this time sea and
wind conditions were as follows: wind 25-30 knots from the SE
and sea state 5/6 (SE). At 2245 the ship docked at the BBSR
pier.

March 11

Unloading operations began at 0800 and ended at 0930. After this
we began a close inspection of all the components and testing of
batteries, EM cable and hose (see attached test schedule). The
open circuit was found inside the hose which was therefore
drained and opened in order to recover the faulty EM rope/stopper
rope assembly.
Test results are as follows:
Hose continuity test:
Pin 1 :   15.1 Ohms
Pin 2 :   7.10 KOhms
Pin 3 :   open
EM cable continuity test:
Pin 1 :   10.3 Ohms
Pin 2 :   10.2 Ohms
Pin 3 :   10.3 Ohms
Battery voltages:
Apirb :   13.69 Volts

Top batt: 14.41 Volts
Epack :   14.39 Volts

The batteries were stored in a refrigerator in the BATS
laboratory. Electronics, endcaps and RDF were hand carried back
to WHOI. The buoy, Epack pressure case, EM cable, and hose were
left in storage at BBSR.

March 12

We left BBSR and arrived at WHOI at 1700 and unloaded the hand-
carried equipment. One gear box was airshipped back to Dave
Simoneau lab.

SSAR AUTEC Cruise Report
Andros Island - Tongue of the Ocean
April 8-17, 1994

April 8th, Friday

0700 Depart for Logan, West Palm Beach and Andros Island.

1800 Arrive Andros Island and transport gear to work area in RUB-4 building near docks at AUTEC. Frank Hardy (Program Engineer) and Marc Ciminello (Program Manager) meet group at airport and help with equipment, check-in at housing, base overview, etc.

Unpack and setup computers and lab equipment. Quick checkout of buoy and array electronics.

April 9th Saturday

Finish unpacking of electronics and sensors. Buoy, pressure cases and cable unpacked and checked. Loaded batteries in pressure cases. Ran wires from bottom endcaps through batteries. Tested tilt sensors and calibrated for offset and scale factor corrections. Reviewed all SBL system setup parameters.

Vessel to be used is an LCU, #1647 with bow ramp. Source is deployed off port side near the stern with large crane. Source weighs about 3000 lbs and has Pengo winch for cable. Max depth is 350 feet. Source is bender bar from Honeywell (now Allient Tech) built in about 1983.

April 10th Sunday

Mechanical systems checkout and test assembly complete by mid-day and ready for loading. SBL checkout and testing continues. Built 4 by 6 foot frame for mounting pinger and SBL array for testing dockside.

0900 meeting at CC building to review use of PARGOS real-time range data telemetry system. Desired parameters include x, y and z differences between buoy and array pingers. Data output is in range coordinates (yards). Gear will be installed Tuesday morning by AUTEC technicians.

Carter Ackerman arrives with m-sequence generator on noon flight.

Tomo front-end testing with new analog front-end but old A/D converter card. Baseline equivalent noise is about 75 dB re uPa per root Hertz. Expected ambient noise is about the same so this may be adequate. Encounter problem when installing A/D in target system. Possible software incompatibility with DMA and disk access. Configuration is slightly different than lab tests. Will use a different program (interrupt based) to collect data.

April 11th Monday

Surface electronics loaded in buoy and sealed in RUB-4 building which is air-conditioned. Heavy equipment loaded on LCU: Pengo winch for E/M cable, buoy, electronics pressure case and other mooring gear. Equipment shack loaded on deck and E/M cable spooled to Pengo winch. Packed all electronics and computers and moved into shack aboard the LCU. Vessel moved to dock in front of Marine Operations building and turned winch side out for dockside testing.

Made decision to run tracking test and source data acquisition sequentially without recovering and reconfiguring. This will reduce deck operations considerably. Space aboard LCU-1647 is tight and deployment must be done over the side because other equipment is installed on stern of vessel.

1330 pre-test briefing with range personnel, LCU-1647 crew and technicians for MAXI-SATS acoustic source. Schedule calls for tracking and source ops on Tuesday with Wednesday as contingency. Weather is noted as potential problem. Winds are about 20 knots and seas are 3-6 feet. LCU-1647 has 4 foot draft.

Hiab Seacrane winch used dockside to hang frame with pinger and SBL receive array. Test cables run to electronics package inside van. Testing completed and final parameters programmed for tracking tests. Mounting bracket for WATT pinger installed on subsea pressure case by AUTEC technicians.

M-sequence generator installed in MAXISATS van and connected to acoustic source. Source signal schedule prepared and presented to MAXISATS support group. Signals settled on include 20 ms pulses, 50-100 Hertz up and down FM sweeps, and m-sequences. Most source signals will be m-sequences of varying bandwidths and codes.

April 12th Tuesday

Depart dock for tracking site about 0700. Wind is still about 18-24 knots. Clear of harbor waves are about 3-5 feet. After about 1 hour transit the captain turns into the trough and slows the vessel. Roll is bad enough to bring waves over the side. The captain decides that the weather is too rough for the operation and the ship returns to port before 1000 hours.

Took advantage of delay to continue testing tomo data acquisition system and added data feedback via ARGOS for SBL test.

April 13th Wednesday

Departure delayed because of poor weather. Wind is still about 20 knots and shows no sign of changing. Operations off LCU-1647 not possible under these conditions. Start to make contingency plans for use of another vessel. Meeting with Mark Ciminello and Abe Louis (Program Engineer). Various options considered for carrying out experiments given that the weather may not change for days. Plan decided on is to use the R/V Range Rover

which is a much larger vessel and will also support the MAXISATS source. However, the Range Rover is retrieving a mooring and will not return until after 1630 Wednesday. The mooring gear and a stern roller must be removed before the other equipment can be loaded. Plans are made to remove some of the equipment from the LCU-1647 today, then transfer it to the Range Rover after its gear is off-loaded. Tentative planned departure is 1500 tomorrow.

Buoy, winch, shack and other equipment removed from deck of LCU-1647 in late afternoon.

April 14th Thursday

Range Rover is ready for loading about 1000 hours. Heavy gear moved on board including MAXISATS equipment van and our shack. MAXISATS gear is tested and made ready. PARGOS radio gear and portable computer with tracking software installed and tested. Departure is at 1450 hours with two and half hours transit to weapons range for tracking exercise (the closer acoustic range is only an hour offshore but it is in use).

Arrive on site at 1730 and prep for deployment. Weather is mostly clear with waves 3-5 feet and wind 15-20 knots. Deployment is to be off the side with the Hiab Seacrane to place buoy and hold sheave.

1800 Buoy over the side.

1830 Cable paying out. At range coord 12500, -7590.

1905 Data collection program started.

1910 Connections made at subsea case

1920 Weight drop with slipstick. Waiting for array to settle under buoy.

Switch to Zulu time.

2340 Pickup line on buoy from ship for first pull during 1st test sequence.

0004 Range deltas are: 214, -151, 415. (x-y-z Yards) Allowing to settle

0030 Ship position is 24 22.51 N 77 30.99 W

Range deltas are: 10, -18,493 Manoeuver for second pull

0101 Range deltas are: 89, -236, 416

0141 2nd test sequence begins. Range deltas are: 12, -25, 493 (angle is about 3.5 degrees, deep to shallow).

0156 Ship position is 24 21.90 N, 77 31.05 W.

0207 Range deltas are: 75, -148, 460

0223 Pulling due north.

0234 At rest. Range deltas are 6, 0, 494. Pull again.

0242 Range deltas are -162, -69, 455.

0258 Allowing to drift free. SBL data sequence finished.

Notes: Range origin (0,0) = 24 26' 37.6" N, 77 38' 6.8"

Drift for buoy estimated at 0.23 knots at bearing 160.

Switch to Local Time

2330 MAXISATS acoustic source in the water

2345 Data transmission starts, begin approx 3 hour sequence while drifting. Out of range of Argos RF at about 300-400m. No feedback available.

Ship noise measured at monitor hydrophone at source is 109 dB re uPa per root Hz.

0245 Source off

0315 Source on deck and secure

0320 Begin transit to buoy (3700 yards)

0400 Buoy on deck and cable coming up

0430 Cable in

0445 Array on deck

0450 Under way back to AUTEC base.

0500 Check of data on buoy. All SBL data present on hard disk. Waveform data looks good, high SNR. Computer has stopped after 45 minutes of tomo data collect. Possible hardware problem. Waveforms collected look very corrupted with ship noise (data is ambient only, source was not yet on). Pulses from tracking pingers are also present and clip the receiver.

0730 Dockside. Tom Austin and Alex Bocconcelli depart.

April 15th Friday

0800 Meeting with Marc Ciminello at CC building to check on availability of R/V Range Rover and MAXISATS to redo test for tomo equipment. Possible concern about overlap with submarine ops in range on Saturday. Meeting with another Project Manger about source use on Saturday. Conclude that there is probably no problem. Have go-ahead to do test if we desire.

0900 Discussions with Carter Ackerman about format of experiment and likelihood of success given noise and computer failure. Decide that test is worthwhile despite risks. Request that the Range Rover is to be rigged for quiet ops with 100 KW rubber-tire deck generator. Examine some of the data from the buoy. In period between pings and away from noise bursts the standard deviation is -8.4 dB re volt which is -69 dB at the input to the analog front-end (integrated over the entire band). Equivalent to 98.6 dB in the water, or about 76 dB per root Hz (expected ambient noise level is about 75 dB re uPa per root Hz). Thus basic performance appears OK.

1100 Replace PCMCIA RAM card with 2MB version (was a new 4MB card) and change BIOS to old rev on processor. Replace hard disk, interface and power supply. Install data collect software from old system and begin testing in preparation for next experiment. Battery voltages for bottom side are 13.9 volts for main, 20 volts for analog power (no load).

1230 Give go-ahead to Marc Ciminello to give orders for 12 hour cruise tomorrow, starting at 0700 or 0800 depending on how far they want us away from the range.

1600 Change ARGOS antenna on buoy from patch (flat) antenna to whip (vertical) in hopes of getting additional range. Shipboard antenna is omni so range is limited. Array data collection program is still operating fine. Testing to continue through evening.

April 16th Saturday

0700 Final hardware check complete. Reload bottom electronics in pressure case and put on deck and strap down. Position buoy and make ready.

0750 Depart for 24 55.0 N, 77 43.0 W in Tango 2 area.

0920 On-site, begin prep for deployment. Weather is clear, seas about 3 feet. Wind 10-15 knots.

1000 Buoy in the water, waiting for it to begin drifting away.

1030 Cable all out. Prep for pressure case and array deployment.

1055 Array in water. Flotation released with no problem.

1106 Position is 24 55.382 N 77 44.932 W

1112 Range is opening at about 0.5-1 knots

1135 Engines off, MAXISATS deployment evolution begins. Quiet ship drill with generator on deck.

1200 MAXISATS in water

1230 Source on with first waveform at max power.

1230 - 1545 waveforms changed at least once every 15 minutes to coincide with buoy collection timing (1 8 minute single channel set, 1 2.5 minute 6 channel set starting at 00, 15, 30 and 45 minutes after the hour).

1615 Heading back to buoy (not in sight and out of radio range). Est. range is 4 nmi.

1645 Back at buoy after steaming along drift track. Buoy appears to have drifted about 0.5 mi since launch.

1705 Buoy on deck, cable coming up.

1720 Pressure case on deck, array pulled in.

1730 Under way back to AUTEC base.

1900 Dockside.

1900 - 2200 Packing equipment

April 17th Sunday

0800 Packing equipment continues.

1000 Unload heavy gear with crane. Move to warehouse.

1200 Packing complete. John Bouthillette and Carter Ackerman leave on 1230 plane. Transport gear to be airshipped to shipping-receiving and hand-carry boxes to on-base terminal.

1500 At CC building to pick up data and documents from tests, including range track data. Slight confusion about classification of track data. Data is unclassified and paperwork revised.

1630 Depart for Andros Is. Airport.

1830 Re-group with John Bouthillette at W. Palm Beach Airport for flight to Logan.

Participants: Lee Freitag, Alex Bocconcelli, Tom Austin, John Bouthillette, Carter Ackerman, PSU.

APPLIED RESEARCH LABORATORIES

THE UNIVERSITY OF TEXAS AT AUSTIN

P. O. Box 8029 · Austin, Texas 78713-8029 · (512) 835-3200 · FAX: (512) 835-3259

QUARTERLY PROGRESS REPORT NO. 2

Contract: SC25048

Sponsor: Woods Hole Oceanographic Institution

Project Leader: Mark Leach

Report Period: July, August, September 1993

Applied Research Laboratories, The University of Texas at Austin (ARL:UT), is tasked to provide Woods Hole Oceanographic Institution (WHOI) with a method and system for determining accurate positions of free floating Surface Suspended Acoustic Receivers (SSAR). ARL:UT is to provide guidance in the selection of Global Positioning System (GPS) equipment, and determine the best method of obtaining SSAR positions.

<u>Subtasks 1 and 2</u>: Evaluate Available GPS Technology and Recommend an Appropriate Receiver

In the first report period, the Ashtech Sensor was selected as the optimal GPS receiver for the buoys. During this report period, ARL:UT procured one Ashtech Sensor for test and evaluation purposes. Test results verified that the receiver meets all specifications and requirements. These subtasks have been completed.

<u>Subtask 3</u>: Develop Receiver Control Software

An "alpha" version of the software was delivered to WHOI in mid-July. The software provided full command and control functions for the GPS receiver. These functions included initialization of the receiver at the start of each observation session, receiver queries for necessary data, and writing data to a buffer. Development and testing of the deliverable version 1.0 of the receiver control software will continue during the next quarter. The deliverable software will provide full command and control functions for the receiver in the same way the alpha version did. Additionally, the version 1 software will perform all necessary pre-transmission formatting of the GPS position information. The output will be a single string that the buoy control software can read and incorporate into the transmitted message.

Subtask 4: Modify ARL:UT's Existing Data Correction Capability For WHOI Application

The data correction facility (DCF) is capable of taking RINEX (receiver independent exchange) format as input. Because the Ashtech Sensor data can be easily converted to RINEX via the Ashtech program, ASHTORIN, no functional modifications of the existing DCF were required. Consequently, the focus of effort was to verify the ability of the DCF to process data from the Ashtech Sensor. Converted data collected at ARL:UT and on the test buoys were successfully processed through the DCF to remove the effects of selective availability (SA). The SA free pseudorange data were then used to compute SA free positions. The process is described further in the subtask 5 section of this report.

As part of this effort, WHOI project team members obtained the necessary security approvals and briefings to conduct the processing described above. Additionally, ARL:UT proceeded with planning efforts to move the DCF to a larger area that will also accommodate the Position Correction Facility (PCF).

Subtask 5: Develop Position Correction Model

Typically, the pseudorange data that are needed to apply corrections for the effects of SA are obtained directly from a GPS receiver. Due to severe constraints on telemetry throughput from the buoys, it is not feasible to transmit the pseudorange data. Therefore, the receiver computed buoy position will be sent from the buoy because it requires significantly less data. However, using the position information requires additional satellite orbit information, and additional postprocessing is needed to reconstruct pseudoranges equivalent to those used by the receiver to compute a position. The pseudoranges are needed because SA errors are manifested as range errors, and the SA corrections must be applied to correct the pseudorange values. This reconstruction of pseudoranges is a unique requirement which requires implementation of a new algorithm and development of a software model.

Previously, ARL:UT collected sets of data and began software development of the model to verify that the process was technically sound. During this report period, ARL:UT continued development of the position correction model software. The data flow of the model is illustrated in Fig. 1. The process begins by using observed pseudorange data from the GPS receiver, making the necessary conversions from binary to Ashtech and RINEX format, and computing a SA corrupted position. These position data are equivalent to the receiver output from the operational buoys. The SA corrupted pseudoranges are then computed (reconstructed) using the corrupted position and the satellite ephemerides. Computation of the reconstructed ranges requires determining the satellite position at the time the signal is transmitted and applying corrections for deterministic errors. The satellite's position is known as a function of time from the satellite's ephemeris. The particular time epoch needed is the transmission time of the portion of the GPS signal that is received and used to generate a pseudorange. The GPS signal transmit time is determined by making an initial estimate using the receiver time tag and using an iterative process to determine actual
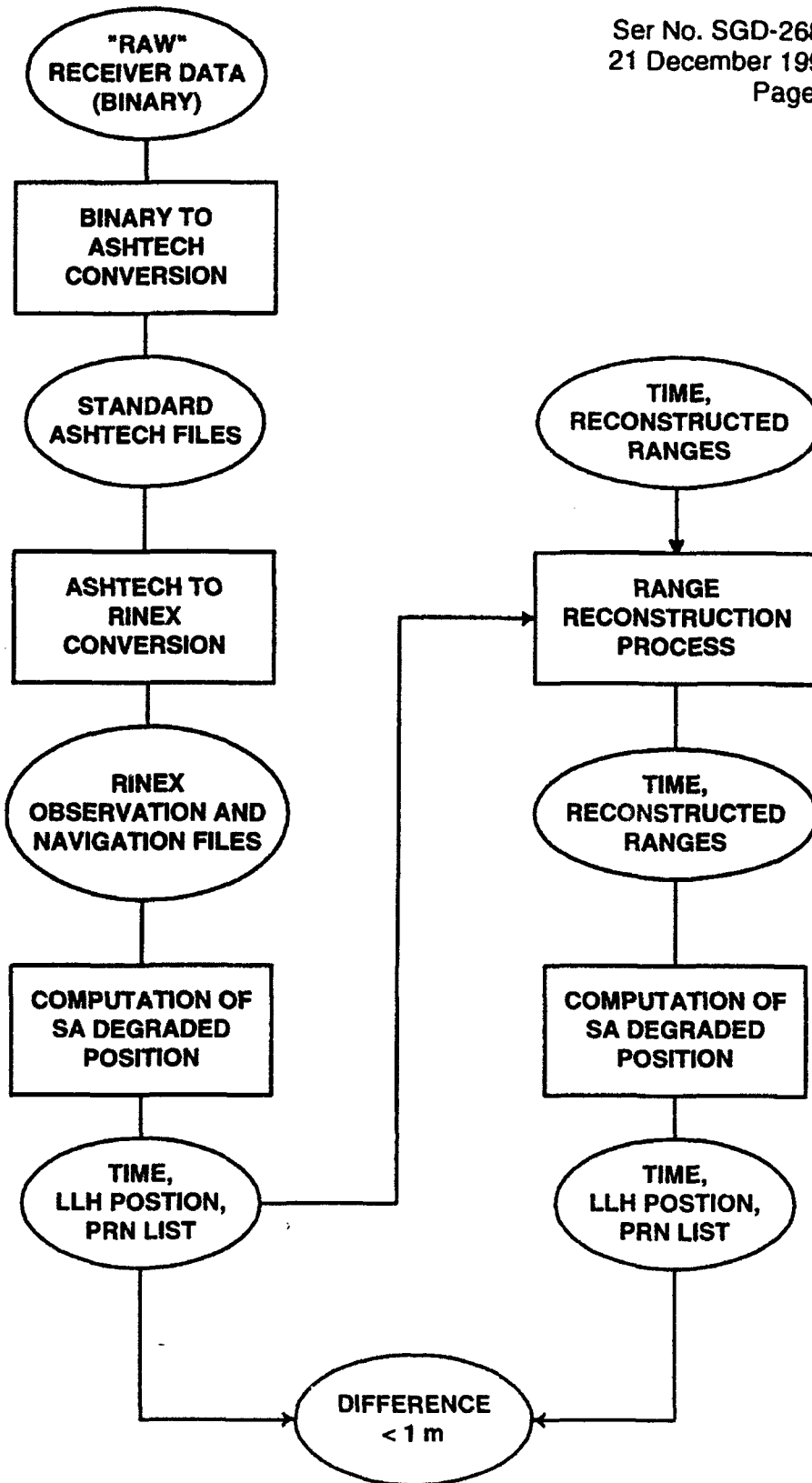
Figure 1: Range Reconstruction Validation Process

transmit time. The satellite position, as well as the slant range between the satellite and GPS receiver, is then computed at the actual transmit time. The deterministic errors include the satellite clock error, earth rotation, and atmospheric effects. To compute the satellite clock error, the drift of each satellite clock is modeled by a polynomial whose coefficients are transmitted as part of the ephemeris (navigation) message. The range reconstruction model applies the satellite clock correction based on the coefficients that are broadcast. The model also corrects for the error in the satellite ranges due to the rotation of the earth during the signal's time of flight. Standard model corrections are also applied for effects of the ionosphere and troposphere on the GPS signal.

After applying all the necessary corrections, the model then solves for the original SA corrupted position with the reconstructed pseudoranges. Data collected at ARL:UT with the Ashtech Sensor were used to evaluate the model. When using the full precision pseudoranges, the position results were identical. The process was also performed using pseudoranges rounded to the meter level. This was done to ensure that reducing the data precision to minimize the number of characters transmitted would not adversely affect the level of accuracy required for the buoys. The differences between the original and re-computed solutions using the rounded, meter level ranges were less than one meter. These results confirm that the critical portion of the algorithm (i.e., transforming position solutions into GPS computed reconstructed pseudoranges) is valid and properly implemented.

Data collected during the sea test were also processed using the model. A sample of the sea test data sets was selected to compute SA corrupted buoy positions. The sample sets were also processed to remove SA from the data using ARL:UT's DCF. SA free positions were then successfully computed using SA free data. The remaining data sets from the sea test will be cleaned to compute SA free positions during the next report period. The positions computed with clean observation data and cleaned reconstructed range data will be compared to validate that the PCF process produces results that are equivalent to the DCF for this application.

In addition to comparing results between the model and the existing DCF, the corrected positions using SA free reconstructed ranges will be compared to true positions. Position solutions computed using data collected at ARL:UT will be compared to known truth positions at ARL:UT. Data collected from the GPS reference receiver on shore will be used to compute differential positions of each buoy, and these differential position solutions will serve as known positions for the buoys. The corrected positions from the buoys will be compared to the differential positions, and an analysis summarizing the results will be presented in the next report.

Subtask 6: Procurement of Microcomputers

ARL:UT initiated procurement of microcomputers for the PCF system. The computers are IBM PC compatible with 80486 processors and all necessary peripherals. The units designated to perform classified processing will use removable

hard disks for enhanced security. The units that will be dedicated to unclassified communication and data storage will have standard hard disk drives. Delivery of all computer systems to ARL:UT is scheduled for early October.

Subtask 7: Integrate and Test the SA Removal Capability Into Position Correction Facility

Once the position error model validation is complete, the software will be enhanced from a prototype process to a fully capable PCF. Testing will be conducted to verify the corrected position solutions are within 30 m, rms, of the true position. Also, ARL:UT's secure facilities will be modified to accommodate equipment dedicated to the WHOI program.

Subtask 8: Implement Capability for Receiving Navigation (Ephemeris) Information

ARL:UT requested broadcast ephemeris data from the Defense Mapping Agency (DMA) for use by WHOI/GAMOT through all phases of the project. DMA has agreed to provide the necessary ephemeris data for processing of buoy positions. The satellite ephemerides are currently collected by DMA's world wide monitor station network, and made available to ARL:UT on a daily basis.

Additional Activities:

The previous report described additional tasking ARL:UT has undertaken beyond the original scope of the subcontract. The progress on this additional tasking is summarized below.

1. September Sea Test

Two prototype buoy designs were evaluated in a sea test conducted by WHOI in September. ARL:UT personnel assisted WHOI during pre-deployment preparations including operational testing of the GPS receiver and data acquisition. While on site, ARL:UT deployed a temporary GPS reference station for data collection. The reference station data will be used to compute post-test differential GPS (DGPS) positions of the buoys. DGPS position solutions in postprocessing for distances under 500 km are typically accurate to within 5 m. Therefore, the utilization of DGPS to compute buoy positions in this test will provide an accurate and independent means of verifying the accuracy of the SA removal technique. ARL:UT personnel remained on site until the departure of WHOI personnel for deployment of the test buoys.

The GPS data from both buoys and the reference station were successfully transferred to ARL:UT upon completion of the test. Archival and conversion of the buoy data from raw format to standard Ashtech format and then to RINEX format were completed. Also, all buoy data has been processed to assess data quality. The processing included determining the number of times in which the receiver lost lock on the signal of an observable satellite, or when a slip occurred in tracking the carrier

phase of a satellite signal (cycle slips). These quantities provide a initial indication of buoy receiver system's tracking ability. Results from this processing indicate that there was no significant difference in performance between the two buoy designs with respect to these parameters.

2. Investigate Feasibility of Using Long Baseline DGPS

ARL:UT initiated an analysis to determine the feasibility of applying DGPS over long baselines up to 7000 km. The purpose of the analysis was to determine whether an unclassified DGPS process could determine buoy positions within 30 m. Data from stations in Canada, Europe, and the United States, including Hawaii and Alaska, were successfully downloaded from the International GPS Geodynamics Service (IGS) database. The database is part of the Crustal Dynamics Data Information System (CDDIS) based at the Goddard Space Flight Center in Greenbelt, Maryland. Compressed GPS data, truth position coordinates, and necessary the decompression tools were obtained. The GPS data were then processed for each site. An ARL:UT DGPS software program was used to compute differential positions. The computed positions were compared to the known station positions. Preliminary results indicate that positions can be determined with an accuracy on the order of three parts per million (3 m over a 1000 km baseline). However, the position solution for two stations had significant errors. The position error for one station was 32 m while the position error for stations at a similar baseline distance were 5 - 7 m. The second anomalous position error was approximately 22 m over a baseline of 3800 km. The position error expected at this distance was approximately 11 - 12 m based on the three parts per million trend described above. Efforts to determine the cause of the errors are continuing. Also, ARL:UT is continuing to assess the overall accuracy and feasibility of applying this technique to future programs requiring precise buoy positioning over long baselines.

3. Interim Processing of Corrected Buoy Positions

The GPS Joint Program Office (JPO) granted approval during this quarter for ARL:UT to perform SA removal during postprocessing of buoy positions for the GAMOT program. ARL:UT is currently reviewing cost requirements to conduct processing of corrected buoy positions until preparations are completed for ARL:PSU to conduct processing. ARL:UT has previously accepted additional tasking (e.g., support of the sea test and LBDGPS analysis) in lieu of deploying reference stations as described in Option 2 of Phase I in the statement of work. Support of the planned Pacific system test in March 1994 will also require additional out-of-scope work. ARL:UT will determine if sufficient funds remain for the processing of SSAR positions and for what length of time.

Shawn Furgason
Research Engineer Associate

MATERIAL INSPECTION AND RECEIVING REPORT

1. PROC. INSTRUMENT IDEN. (CONTRACT) SC 25048	**(ORDER) NO.** **6. INVOICE** N/A	**7.** OF 1 1 **8. ACCEPTANCE POINT** D

2. SHIPMENT NO. EMG-0002	**3. DATE SHIPPED** 93DEC31	**4. B/L** G	**5. DISCOUNT TERMS** N/A

9. PRIME CONTRACTOR CODE N96748	**10. ADMINISTERED BY** CODE
Applied Research Laboratories The University of Texas at Austin P.O. Box 8029 Austin, TX 78713-8029	Woods Hole Oecanographic Institution Office of Sponsored Programs Challenger House Woods Hole, MA 02543

11. SHIPPED FROM (If other than 9) CODE FOB. Same as 9 above.	**12. PAYMENT WILL BE MADE BY** CODE Woods Hole Oceanographic Institution Accounts Payable Office Challenger House Woods Hole, MA 02543

13. SHIPPED TO CODE Woods Hole Oceanographic Institution Woods Hole, Massachusetts 02543	**14. MARKED FOR** CODE Attn: Mr. Daniel Frye

15. ITEM NO.	**16. STOCK/PART NO. DESCRIPTION** (Indicate number of shipping containers - type of container - container number)	**17. QUANTITY SHIP'D/REC'D**	**18. UNIT**	**19. UNIT PRICE**	**20. AMOUNT**
0	A1 Quarterly Progress Report No. 2, July, August, September 1993, under contract SC 25048, entitled, "GPS Based Buoy System."	2	ea.	N/A	N/A

21. PROCUREMENT QUALITY ASSURANCE

A. ORIGIN
☐ PQA ☐ ACCEPTANCE of listed items has been made by me or under my supervision and they conform to contract, except as noted herein or on supporting documents.

B. DESTINATION
☐ PQA ☐ ACCEPTANCE of listed items has been made by me or under my supervision and they conform to contract, except as noted herein or on supporting documents.

22. RECEIVER'S USE
Quantities shown in column 17 were received in apparent good condition except as noted.

DATE ____ SIGNATURE OF AUTH GOVT REP
TYPED NAME AND OFFICE

DATE ____ SIGNATURE OF AUTH GOVT REP
TYPED NAME AND OFFICE

DATE ____ SIGNATURE OF AUTH GOVT REP
TYPED NAME AND TITLE

* If quantity received by the Government is the same as quantity shipped, indicate by ( ) mark. If different, enter actual quantity received below quantity shipped and encircle.

23. CONTRACTOR USE ONLY

This is to certify that shipment of the listed item(s) has been made this date 31 December 1993

SIGNATURE OF ARL:UT CONTRACT OFFICIAL

DD FORM 250
1 Aug 87

GS10023-059

MATERIAL INSPECTION AND RECEIVING REPORT

1. PROC. INSTRUMENT IDEN. (CONTRACT) SC 25048	**(ORDER) NO.**	**6. INVOICE** N/A	**7.** 1 **OF** 1
			8. ACCEPTANCE POINT D

2. SHIPMENT NO. EMG-0002	**3. DATE SHIPPED** 93DEC31	**4. B/L** G	**5. DISCOUNT TERMS** N/A

9. PRIME CONTRACTOR **CODE** N96748	**10. ADMINISTERED BY** **CODE**
Applied Research Laboratories The University of Texas at Austin P.O. Box 8029 Austin, TX 78713-8029	Woods Hole Oecanographic Institution Office of Sponsored Programs Challenger House Woods Hole, MA 02543

11. SHIPPED FROM (If other than 9) **CODE** **FOB.**	**12. PAYMENT WILL BE MADE BY** **CODE**
Same as 9 above.	Woods Hole Oceanographic Institution Accounts Payable Office Challenger House Woods Hole, MA 02543

13. SHIPPED TO **CODE**	**14. MARKED FOR** **CODE**
Woods Hole Oceanographic Institution Woods Hole, Massachusetts 02543	Attn: Mr. Daniel Frye

15. ITEM. NO.	16. STOCK/PART NO. DESCRIPTION *(Indicate number of shipping containers - type of container - container number)*	17. QUANTITY SHIP'D/REC'D*	18. UNIT	19. UNIT PRICE	20. AMOUNT
00●	A1 Quarterly Progress Report No. 2, July, August, September 1993, under contract SC 25048, entitled, "GPS Based Buoy System."	2	ea.	N/A	N/A

21. **PROCUREMENT QUALITY ASSURANCE**		22. **RECEIVER'S USE**
A. ORIGIN ☐ PQA ☐ ACCEPTANCE of listed items has been made by me or under my supervsion and they conform to contract except as noted herein or on supporting documents.	**B. DESTINATION** ☐ PQA ☐ ACCEPTANCE of listed items has been made by me or under my supervsion and they conform to contract, except as noted herein or on supporting documents.	Quantities shown in column 17 were received in apparent good condition except as noted. DATE SIGNATURE OF AUTH GOVT REP TYPED NAME AND OFFICE
DATE SIGNATURE OF AUTH GOVT REP TYPED NAME AND OFFICE	DATE SIGNATURE OF AUTH GOVT REP TYPED NAME AND TITLE	* If quantity received by the Government is the same as quantity shipped, indicate by (✓) mark. If different, enter actual quantity received below quantity shipped and encircle.

23. CONTRACTOR USE ONLY

This is to certify that shipment of the listed item(s) has been made this date <u>31 December 1993</u>

SIGNATURE OF ARL:UT CONTRACT OFFICIAL

DD FORM **250** _{1 Aug 87}

GS10023-059

Ser No. SGD-2713
1 February 1994
SF:ct

QUARTERLY PROGRESS REPORT NO. 3

Contract: SC25048

Sponsor: Woods Hole Oceanographic Institution

Project Leader: Mark Leach

Report Period: October, November, December 1993

Applied Research Laboratories, The University of Texas at Austin (ARL:UT), is tasked to provide Woods Hole Oceanographic Institution (WHOI) with a method and system for determining accurate positions of free floating Surface Suspended Acoustic Receivers (SSAR). ARL:UT is to provide guidance in the selection of Global Positioning System (GPS) equipment, and determine the best method of obtaining SSAR positions. During this quarterly period, the following effort was completed:

Subtask 3: Develop Receiver Control Software

As part of the GPS-based buoy positioning system, ARL:UT is to develop and deliver the GPS receiver control software. During this report period, ARL:UT continued development of the GPS receiver control software. The software is approximately 90% complete. The remaining effort consists of final modifications to the code which prepares the GPS data for transmission. A working version of this code is currently under test. In addition to software functionality tests, program logic and error handling are being tested to ensure reliable performance.

As part of the software development an effort was made to define the optimum message content and format that would meet project requirements, and satisfy operational constraints. ARL:UT has determined that the shortest message consists of a complete three dimensional position for the first fix, followed by position changes (deltas) in time and position components for subsequent fixes. This technique requires 101 bytes for the first full position fix, and 90 bytes for each subsequent fix. ARL:UT recommends collecting and transmitting as many positions as possible for a data collection period, and that a minimum of two position fixes be transmitted per data collection period. Using two position fixes requires a total of 191 bytes and provides a sufficient number of bytes for any potential configuration or changes in the GPS constellation during data collection. This is a reduction of approximately 50% from the initial estimate of 150 bytes per fix previously presented to WHOI. This method does not impose any operational constraints, and it mitigates the risk of relying on a single position which may have significant errors.

It is ARL:UT's understanding that the current goal is 512 bytes of position, sensor, and acoustic data per collection session. Therefore, ARL:UT is continuing to investigate additional methods of reducing the required amount of GPS data. ARL:UT is currently working with WHOI and PSU to implement a bit encoding scheme that may dramatically reduce the number of bytes required for the GPS information.

<u>Subtask 5:</u> Develop Position Correction Algorithm

During this report period, ARL:UT completed development of the position correction algorithm. This algorithm reconstructs the GPS pseudorange observable from the receiver position data. This allows the effects of selective availability (SA) to be removed from the pseudoranges. (A full description of the algorithm is contained in the previous quarterly report.) Data collected with the Ashtech OEM Sensor at ARL:UT, and during a sea test, were processed to test and validate the algorithm. The validation consisted of two parts. The first part of the validation determined how well ranges were reconstructed, and how positions generated from the reconstructed ranges compared to positions generated with ARL:UT's existing data correction facility. Positions were computed using SA-free (cleaned) reconstructed ranges generated by the algorithm. These positions were then compared to reference data positions generated using cleaned raw pseudorange data from the GPS receiver. The three dimensional root sum square (RSS) difference between the solution files was then computed for each data set. The difference is typically less than one meter. As noted in the previous report, this difference is a function of the precision of the reconstructed ranges.

The process was repeated for all data collected during the sea test with the standard and snubber buoys. The overall mean difference was 0.37 m for the standard buoy with a standard deviation of 0.41 m. For the snubber, the mean was 0.58 m, and the standard deviation 0.32 m. These results verify that the range reconstruction algorithm and process is valid and has been successfully implemented.

The second part of verification was to establish the absolute accuracy of the corrected positions. With laboratory data, the position solutions computed from the cleaned reconstructed ranges were differenced from a surveyed position on the ARL:UT roof. The accuracy of the surveyed position is better than 1 m spherical in WGS-84 coordinates. The results show that positions can be corrected to within the 10 m of the surveyed position. Differential GPS (DGPS) positions were computed in post-processing for the buoys to serve as truth. The RSS of the difference between the corrected positions and the DGPS positions was computed to establish the accuracy of the corrected buoy positions in the sea test. The results are presented below in the discussion of the sea test analysis and results.

<u>Subtask 6:</u> Procurement of Microcomputers

ARL:UT took delivery of computers for both position correction facility (PCF) systems. The computers are IBM PC compatible with 80486 microprocessors. All units

are equipped with 16 megabytes of RAM and dual half height floppy drives (one each 3.5 in. and 5.25 in.), super VGA monitors and video cards, DOS 6.0, and Windows 3.1. The computers to be used for classified processing are equipped with two 150 Mb Bernoulli removable hard disk drives. The computers that will handle unclassified data transfer are each equipped with a 200 Mb fixed hard disk.

A faulty motherboard was discovered in one microcomputer during initial checkout. The board was replaced and the computer has subsequently performed without problem. No problems were detected with any of the other computers. Effort on subtask 6, Procurement of Microcomputers, has been completed.

Subtask 7: Integrate and Test the SA Removal Capability into Position Correction Facility

Software required to perform the initial decompression and reformatting of position data was completed during this quarter. Also, the range reconstruction and SA removal process is currently being integrated into a deliverable PCF configuration. Enhancements and modifications to the overall position correction process were identified to streamline data processing. These modifications will be completed during the next report period.

Additional Activity:

ARL:UT has undertaken additional tasking beyond the original scope of the subcontract at the request of WHOI. The progress on these tasks during this report period is summarized below.

September Sea Test

A description of the September test activity and ARL:UT's role in this effort was provided in the previous quarterly report. During this report period, ARL:UT conducted extensive data processing and analysis. A report containing the test results and analysis will be prepared separately during the next reporting period. A preliminary analysis and assessment is presented here.

Two prototype buoy designs (designated as the standard and the snubber) were evaluated in the September sea test conducted by WHOI. A brief additional test was performed in November with the standard buoy design. ARL:UT used these tests as opportunities to satisfy the following objectives: 1) evaluate the performance of the GPS receiver in an operational environment; 2) evaluate the receiver control software; and 3) collect sufficient data in operational conditions to evaluate the range reconstruction and SA removal process.

In general, the receiver performance was very good. The receivers deployed on the buoys operated normally with no apparent equipment malfunctions. Each buoy was equipped with one Ashtech OEM Sensor GPS receiver and Ashtech's low profile micro

strip antenna. The same equipment models were used for a temporary GPS reference station deployed by ARL:UT at the Bermuda Biological Station for Research. The receiver performance was evaluated on the satellite signal to noise ratios (SNR) and satellite tracking performance. The SNR for both buoy receivers were comparable to laboratory conditions.

ARL:UT's receiver control software was used to control the reference station receiver. The software successfully collected 100% of the receiver data when initiated by the computer. There were six sessions during which the computer did not execute the receiver interface software due to a software schedule error that was not related to the interface software. There were several instances in which raw data and satellite ephemerides were not collected from the receiver by the buoy system. The cause of the data collection failures is being investigated and discussed with WHOI. The results of the investigation will be summarized in the test report.

Sufficient data were collected to determine that the performance of the range reconstruction and SA removal process will generate solutions that are significantly more accurate than the specified requirements. DGPS solutions were computed using data collected simultaneously at the reference station and at each buoy. These DGPS positions served as truth for comparison with the corrected positions computed using reconstructed ranges. The DGPS solutions were computed with PPDIFF (post-process differential) which is an Ashtech software application. The typical error in DGPS solutions for the 35 - 40 km baseline between the reference station and buoys is approximately 2 - 5 m. The RSS of both two and three dimensional position differences were computed to determine the residual between the DGPS and buoy positions. Statistics summarizing the overall results for both buoys in the September test are shown in Table 1. The geometric distribution of GPS satellites results in larger vertical than horizontal errors. Consequently the 2D solutions are more accurate than the 3D solutions. Therefore, position accuracy can be increased if the buoy's height is constrained to the geoid.

Table 1: Residual Distribution Statistics by Buoy for All Data

Buoy	2 D		3 D	
	Mean	Std. Dev.	Mean	Std. Dev.
Standard	6.09 m	4.23 m	12.48 m	7.45 m
Snubber	5.68 m	4.67 m	14.63 m	7.29 m

Shawn Furgason
Research Engineer Associate

DRIFTING BUOY SYSTEMS USING
ELASTIC RUBBER STRETCH HOSES

W. Paul, A. Bocconcelli, M. Grosenbaugh

Applied Ocean Physics and Engineering Department
Woods Hole Oceanographic Institution
Woods Hole, MA 02543

ABSTRACT

Most drifting buoy systems require the capability to transmit position and sensor information to satellites. In order to send data from sensors suspended below a drifting surface buoy a reliable electrical conductor path is mandatory. However the long term survivability of conductors in the upper portion of a suspended surface buoy tether is a challenging problem. This paper provides information about the development and testing of drifting buoy systems using highly compliant nylon reinforced rubber hoses to serve as conduit for electrical conductors.

INTRODUCTION

A free drifting acoustic receiver is being developed as part of the Global Acoustic Mapping of Ocean Temperatures (GAMOT) project. It consists of a surface buoy from which an instrument package and vertical hydrophone array are suspended through a cable in about 500 meter water depth. Called the Surface Suspended Acoustic Receiver (SSAR), it is intended to form a lower cost alternative to fixed receiver arrays used to detect changes in sound travel time between an acoustic source and the array hydrophones. Changes in sound travel time, caused by variations in water temperature can be indicative of climatic changes such as global warming. Two prototype SSARs called *Standard* and *Snubber* (Fig. 1) have been developed.

THE NEED OF TETHER COMPLIANCE IN DRIFTING BUOY SYSTEMS

A drifting buoy with a suspended tether and sensor package is a spring mass system responding to the heave motions of the buoy in a sea state with distinct natural frequencies, motions, and tether tensions. Without wave motions and differential current loading the cable or rope-like tether would only experience a static tension equal to the submerged weight of sensor package and tether. Differential current drag or wind generated drift of the surface buoy adds quasi-static drag loads.

Wave motions of the buoy introduce dynamic loading. Tether tensions increase when the surface buoy is lifted by a wave due to the need to overcome hydrodynamic drag and inertial resistance of the accelerated suspended cable and sensor package. When the buoy descends from a wave crest inertia and

SSAR "Standard" Drifting Buoy System

ARGOS & GPS ANTENNAS

ELECTRONICS: GPS, ARGOS,

SURFACE BUOY
Surlyn Foam, 1.2 m Max. Dia.,
1290 lbs Reserve Buoyancy

2.0 m — BATTERY

TENSION CELL
0 - 5,000 lbs.

HOSE COUPLING

15 m (R)
18 m (S)
STRETCH HOSE
(R) = Relaxed
(S) = Stretched
0.12 m Dia.

HOSE COUPLING

ELECTRO-MECHANICAL CABLE
3 Conductor, Jacketed,
Caged Steel Armor,
8,000 lbs. Strength
0.013 m Dia.

500 m

HYDROPHONE

10 m

E.M. CABLE TERMINATION
with Protective Boot

1.8 m
ELECTRONICS PACK
Pressure, Tilt, Battery,
Compass in Aluminum
Housing, 0.23 m Dia.

10 m
WIRE ROPE
Jacketed, 0.005 m Dia.

529 m
SINKER WEIGHT
100 lbs.

SSAR "Snubber" Drifting Buoy System

ARGOS & GPS ANTENNAS

ELECTRONICS: GPS, ARGOS,
6 Axis Accelerometer

SURFACE BUOY
Surlyn Foam, 0.9 m Dia.,
600 lbs. Reserve Buoyancy

~1 m

BATTERY

TENSION CELL
0 - 5,000 lbs.

MOLDED in FLANGE COUPLING
with Electrical Connector,
Calm Water Tension ~200 lb:

75 m (R)
90 m (S)
STRETCH HOSE
3 Hoses @ 25 m
(R) = Relaxed
(S) = Stretched
0.067 m Dia.

NEAR SURFACE BUOY
Syntactic Foam Shell
Around Aluminum
Pressure Cylinder

1.5 m
ELECTRONICS
Pressure, Tilt, Battery

E.M. CABLE TERMINATION

ELECTRO-MECHANICAL CABLE
3 Conductor, Jacketed,
Caged Steel Armor,
8,000 lbs. Strength
0.013 m Dia.

425 m

TEST HYDROPHONE &
3 AXIS ACCELEROMETER

1.8 m
ELECTRONICS PACK
Pressure, Tilt, Battery,
Compass in Aluminum
Housing, 0.23 m Dia.

10 m
WIRE ROPE
Jacketed, 0.005 m Dia.

515 m
SINKER WEIGHT
395 lbs.

**Fig. 1.** *Standard* and *Snubber* prototype SSAR designs as used during the 1993 at-sea tests.

dynamic drag loads act opposite to the static weight load and reduce and possibly eliminate the tether tension. If in this case the dynamic and inertia forces become larger than the static weight load, the cable tether becomes slack, since it can not support compressive forces like a connecting rod. The slack cable allows uncontrolled motion of the sensor package connected to the tether, the next wave lifts the surface buoy and loads the cable. If the mass of the suspended sensor package is considerable or the package has enough time to assume a significant downward speed during the slack cable condition, the unavoidable sudden tensioning of the slack cable can cause significant impact or snap loading (Berteaux, 1989).

A wire rope tether with little compliance can see up to 9 times higher tensions than the static weight during the snap load condition, while in nylon ropes the tensions can quadruple. The maximum snap load occurs at the top of the tether (Goeller, 1969). Snap loads are significantly reduced by the

inclusion of a compliant shock absorber between the surface buoy and the suspended stiff cable, or between the cable and the sensor package.

MECHANICAL SYSTEM MODELING OF BUOY SYSTEM IN WAVES

Static and dynamic analyses have been performed on the SSAR prototype designs to determine their response to steady state current shear and dynamic wave forcing. The static current shear was investigated using a model which derived the shape of the suspended elements based on their drag characteristics. This model was run for the anticipated current shear profiles and predicted the corresponding tilts at the array. The size of the weight located beneath the array was chosen to keep the array tilt below 5° for most anticipated situations.

The dynamic analysis was performed by solving the equations of motion of the array cable in the frequency domain using a finite difference scheme. The input to the program is a specified wave spectra. The surface buoy is assumed to be a wave follower so that the input motion at the top of the array is equal to the wave motion. The hydrodynamic motions are modeled with an "equivalent linearized" coefficient. Since the value of this coefficient depends on the response, the solution must be found by iteration.

The computer codes were checked against data collected during the field trials for the *Standard* (Fig. 2) and *Snubber* (Fig. 3) prototype SSAR buoy systems. The sea conditions during both tests were comparable with a wave-height standard deviation of 0.50 m and a peak frequency of 0.12 Hz. The motion at the bottom of the array is amplified in the *Standard* SSAR (Fig 4). This is explained by the fact that the natural frequency of the system, which is associated with the elastic stiffness of the hose, is 0.3 Hz. For the *Snubber* SSAR, the motion at the bottom of the array is damped (Fig. 5). Here, the natural frequency associated with the hose is approximately 0.09 Hz. Numerical predictions of the tension at the surface buoy for the given wave conditions yield a standard deviation of 200 lbs for the *Standard* SSAR and the 80 lbs for the *Snubber* SSAR.

Also calculations were performed using a sea state corresponding to a strong gale. Inputting a standard deviation of 3.5 m at the surface buoy and a peak frequency of 0.06 Hz, predicted motions at the bottom of the *Standard* SSAR will have a standard deviation of 3.6 m, and the tension at the surface buoy will have a standard deviation of 540 lbs. For the *Snubber* SSAR, the standard deviation of the bottom motion is 1.8 m and the standard deviation of the top tension is 225 lbs.

DEVELOPMENT OF STRETCH HOSE AS ELASTIC TETHER

Reinforced rubber stretch hoses were developed for two SSAR drifting buoy systems to serve as compliant shock absorbers between surface buoy and the suspended electro-mechanical cable, sensor package with acoustic array, and stabilizing sinker weight. In the *Snubber* SSAR the hose is arranged between the surface float and a subsurface buoy. In the *Standard* SSAR the hose connects the surface buoy to the suspended cable and sensor package directly (Fig. 1). Both designs incorporate electrical conductors arranged inside the stretch hose in coiled configurations, allowing them to elongate like a telephone cord without straining the copper conductors. The hoses also contain an initially slack stop rope, which engages when the hose exceeds a certain elongation. The rope with a higher modulus and strength than the hose will dominantly share severe tensions and limit hose load and stretch to safe fractions of its strength.
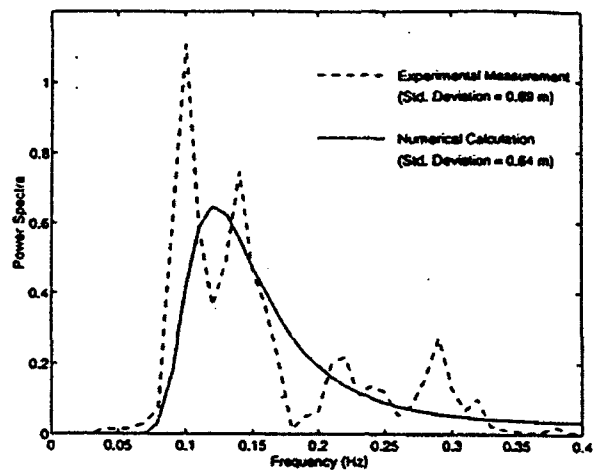
Fig. 2. Measured and calculated power strata
for the motion at the bottom of the
Standard SSAR.
Sea conditions: wave height standard
deviation = 0.5m; peak frequency = 0.12 Hz.
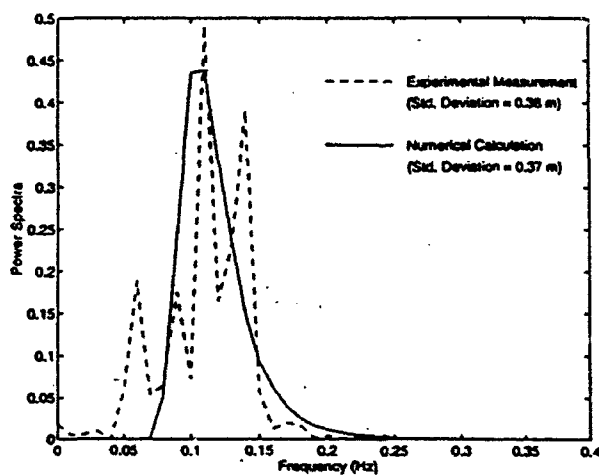
Fig. 3 Measured and calculated power strata
for the motion at the bottom of the
*Snubber* SSAR. Sea conditions same
as Fig. 2.
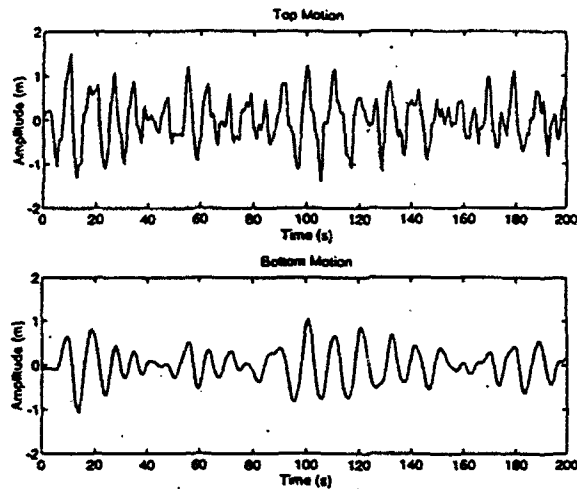
Fig. 4. *Standard* SSAR motions computed from vertical accelerations measured at the surface buoy and the acoustic array at 500m depth.
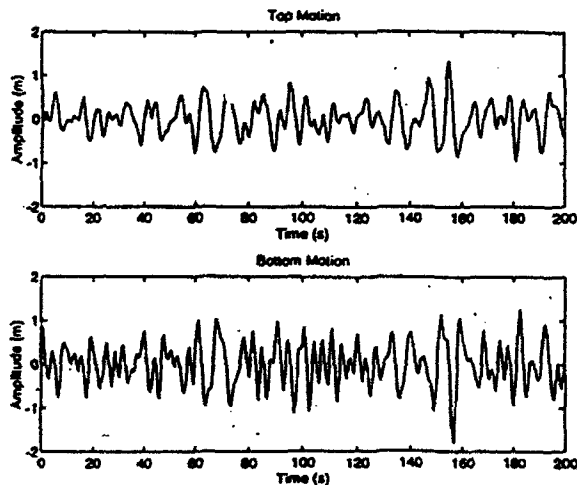

Fig. 5. *Snubber* motions computed from vertical accelerations at the surface buoy and the acoustic array at 500m depth.

Comparison with Offshore Oil Transfer Hoses: The hoses have the external appearance of offshore oil transfer hoses with built in steel flanged couplings. However their construction and mechanical behavior are significantly different. Oil transfer hoses are either built as pressure or suction hoses to allow the safe transport of a large volume of fluid. The pressure hose constrains radial expansion by circumferential arrangement of

unidirectional tire cord fabric, thereby generating the required hoop strength. Service breakdown in suction hoses is prevented by embedding heavy steel wire in the hose wall. The wire is spiraled almost circumferentialy, providing the needed collapse resistance of the hose subjected to vacuum suction of fluids. Additional reinforcement is arranged to add stiffness to the rubber. The oil transfer hoses are tightly controlled under a specification of the Oil Companies International Marine Forum (OCIMF 1991). OCIMF also requires periodic inspection to prevent oil spills through hose failure.

Spiraling of Reinforcement allows Increased Hose Stretch. The shock absorbing hoses for the SSAR drifting buoy systems are designed to provide maximum possible axial stretch within safe working load limits of the nylon tire cord reinforcement. Large axial hose stretch is possible by spiraling the nylon cords in counterhelical layers in the hose wall. The coiling of the reinforcement allows the amplification of the cord elongation in the hose up to 8 times, depending on the selected spiraling or wrap angle (Fig. 6). The spiraling angle is measured between hose axis and cord axis.

CORD ELONGATION AMPLIFICATION THROUGH
HELICAL ARRANGEMENT IN STRETCH HOSE
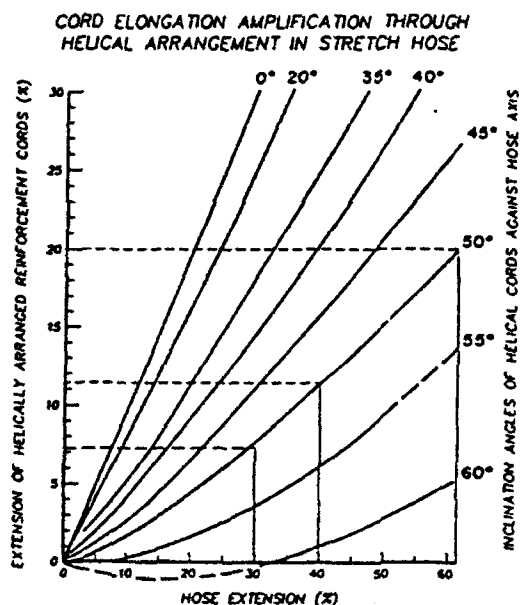
Fig. 6. Cord reinforcement elongation versus hose
elongation as function of helix angle.

The larger the wrap angle, the more stretch is being developed in the hose in response to an applied load. However the more compliant hose response is also coupled with lower safe working loads for the hose with the larger wrap angle.

Stretch Hose Contraction and Fill Fluid Pressure: The counterhelically spiraled nylon reinforcement under tension contracts the stretching hose diameter, the diameter contraction is limited by the presence of fill fluid with assumed constant volume. However the spiraled tensioned cord layers generate fill fluid pressure due to their "chinese finger" contraction, choking the fill fluid inside the hose. The wrap or helix angle of the reinforcement with the hose axis is greatly influencing the load elongation behavior of the stretch hose. Wrap angle and hose size effect the increase of the fill fluid pressure under growing tension.

The Design Process

The hose stretch characteristics are calculated by adapting mechanical modeling developed for textile structures mostly at the University of Manchester in England since 1955 (e.g. Treloar and Riding, 1962). Strain and loading of helically arranged reinforcing cords are determined as a function of their geometry within the hose structure in response to external stretch of the hose. This allows calculation of the load elongation behavior of the reinforced hose, as well as its effect on fill fluid pressure. The procedure is summarized in Fig. 7 and compared with the experimental process.

Comparison with actual built hoses shows reasonable agreement between calculated and experimental behavior (Fig. 8). However typical changes in load elongation behavior due to permanent set and visco-elastic properties of rubber and textile reinforcement have to be considered additionally. Geometric relationship between the stretch of helically applied cords and elongation of a fluid filled hose was shown in Fig. 6, assuming isochoric (constant volume) deformation of the hose filled with incompressible fluid. Fig. 6 shows that at larger cord wrap angles the cord stretch is only a small fraction of the hose elongation. Due to the geometry of the reinforcement hose stretch of up to 35 percent is possible while keeping the cord load below 10 percent of its breaking strength. At cord angles above 55 degrees the cord path goes into compression when the hose is elongated. This is caused by the radial contraction of the hose with applied axial elongation. This poisson ratio effect can be utilized to incorporate materials with much higher elastic moduli into the hose wall. Applied at the proper wrap angle they will not see any stretch or an assigned low stretch over a predetermined elongation range of the hose. Electrical conductors or fishbite resistant layers of high-modulus fibers or metallic wires can be included into the hose design this way. A first test hose with electrical conductors incorporated in its wall has been built and will undergo fatigue testing.
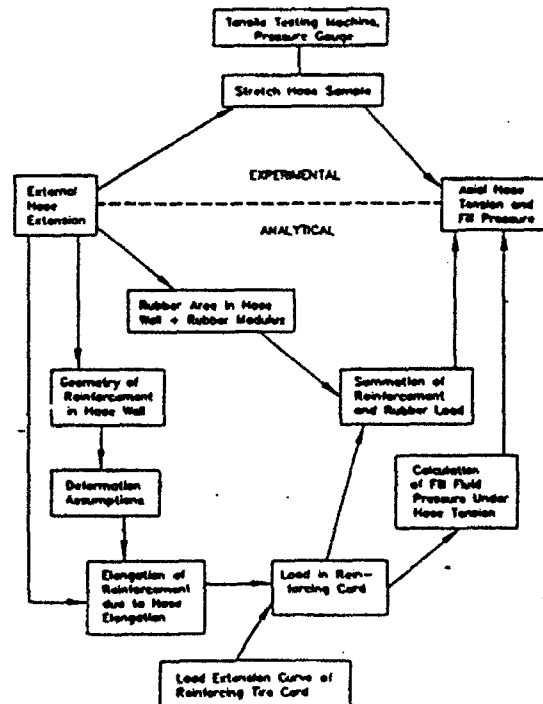

Fig. 7.   Experimental and analytical procedure for load and fill pressure response to hose stretch
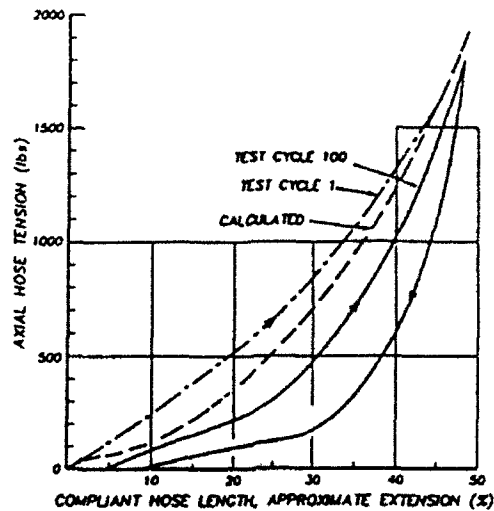
Fig. 8.   Comparison of calculated and tested hose
          tension-elongation behavior.

Hose Construction

The SSAR hose construction combines rubber and reinforcement elements. The reinforcement consists of parallel tire cords, which are evenly and tightly spaced into woven cord fabric. The manufacturing technology was developed and is applied in closely controlled mass production of tire reinforcement. The tire cord fabric, treated with a liquid adhesive, is covered with a thin and even rubber coating on each side. The rubber forms a thin cord containing sheet. Its modulus in the direction of the cord axis is over 250 times that of a cross section made entirely of rubber. Fig. 9a shows the fabric and the fabric containing rubber sheet.

The unreinforced rubber components of the hose consist of thin sheets, rolled with narrow thickness tolerances. Custom compounded rubber materials form the inner tube and outer jacket of the hose.

The hose components are hand laid up over a steel mandrel. Over the inner rubber tube counter-helical layers of rubber covered reinforcement ribbons, sliced to specified widths, are applied similar to the ribbon wrapping around a maypole, (Fig. 9b). This way the reinforcement can be incorporated into the hose structure at specified wrap angles which deliver the required compliance and strength of the hose. Additional reinforcement is built up at each hose end to create low stretch sections with increased axial and bending stiffness.

The hose termination is an internal steel pipe with two spaced apart positioning rings to which a steel flange is welded. The inner rubber tube and the reinforcing layers are built up over the pipe section and locked on by a steel wire wrapped under high tension over the unfinished hose. Subsequently the outer rubber jacket is positioned over the reinforcing layers and temporary textile curing tape is wrapped over the completed hose body. Through pressurized steam treatment (vulcanization) the hose is consolidated and molded to the hose coupling, the vulcanization process creates the extraordinary toughness and cohesion of reinforced rubber structures. The hose end section with its coupling is shown in Fig. 10.

a) Woven cord fabric before and after rubber coating

b) Application of coated reinforcement during construction of stretch hose
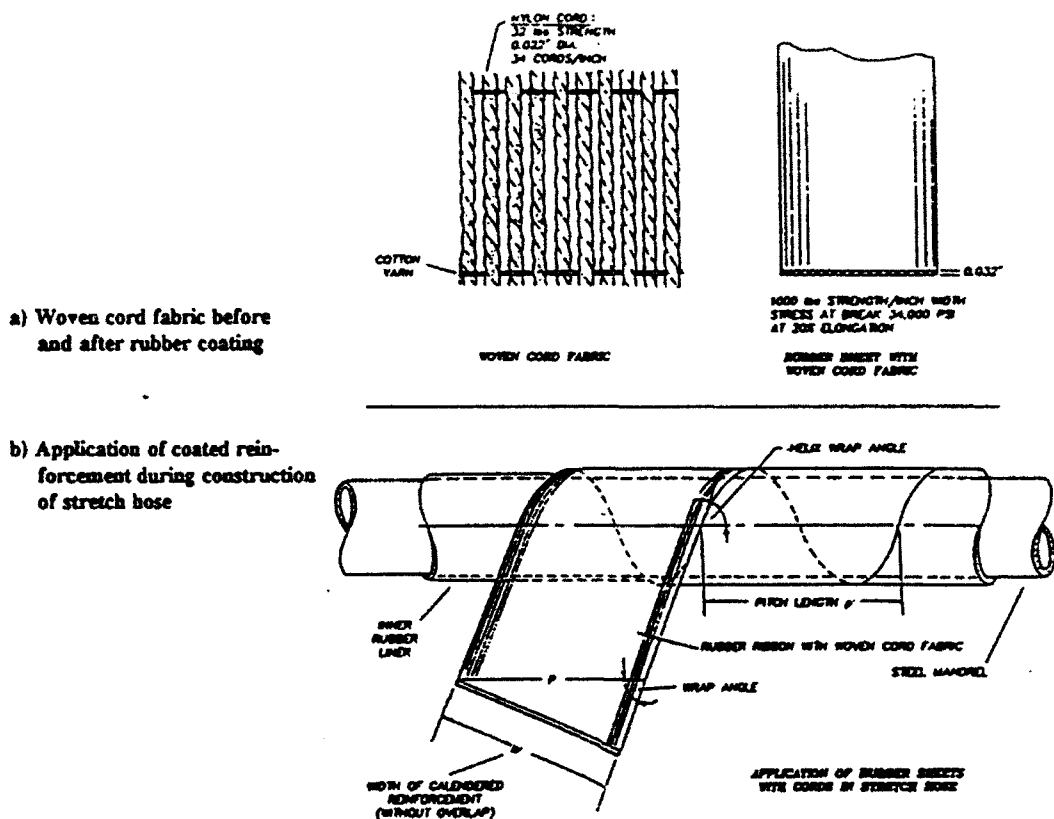
Fig. 9.   Stretch hose reinforcement.

Termination Hardware, Electrical Conductor Path, and Assembly

The electrical conductors in both the *Snubber* and *Standard* hoses were constructed as Electro-Mechanical (EM) ropes. The insulated conductors were stranded around a Very Low Stretch (VLS) polyester rope core, which acts as the strength member. A thin outer braid holds the conductors in position. The EM rope construction allows rope tensioning without elongating the conductors.

The EM ropes were terminated to be longer than the hose assembly. In case of the *Snubber* SSAR the EM rope acts both as a "stop rope" and as the electrical path. In the larger size *Standard* hose assembly a separate 3/4" diameter double braided polyester rope functions as the stop rope, and the EM rope is spliced longer than the stop rope to stay more or less slack all the time in service.

Both hose assemblies were terminated with pressure proof steel endcaps which provide the necessary mechanical connections to fit the surface buoy and the EM cable (or the subsurface buoy in the *Snubber* configuration). The electrical conductors were terminated in glass-epoxy waterproof bulkhead connectors made by Brantner. The top and bottom connectors were mated to electrical pigtails coming from the nearest components in the drifter assembly. The inside faces of the flanges were fitted with a clevis where the stop ropes were terminated with an eye splice protected by a thimble. Once both assemblies were completed they were filled with a non-conductive oil and tested for pressure, electrical continuity, and load elongation behavior.

1. STANDARD OFFSHORE FUEL HOSE COUPLING
2. HOSE BODY WITH EXTRA REINFORCEMENT BUILDUP AT COUPLING
3. BEND LIMITING SECTION OF HOSE
4. STRETCH SECTION OF HOSE
5. COUNTERHELICAL NYLON REINFORCEMENT TO CONTROL HOSE STRETCH
6. FISHBITE PROTECTIVE COUNTERHELICAL LAYER OF KEVLAR FABRIC
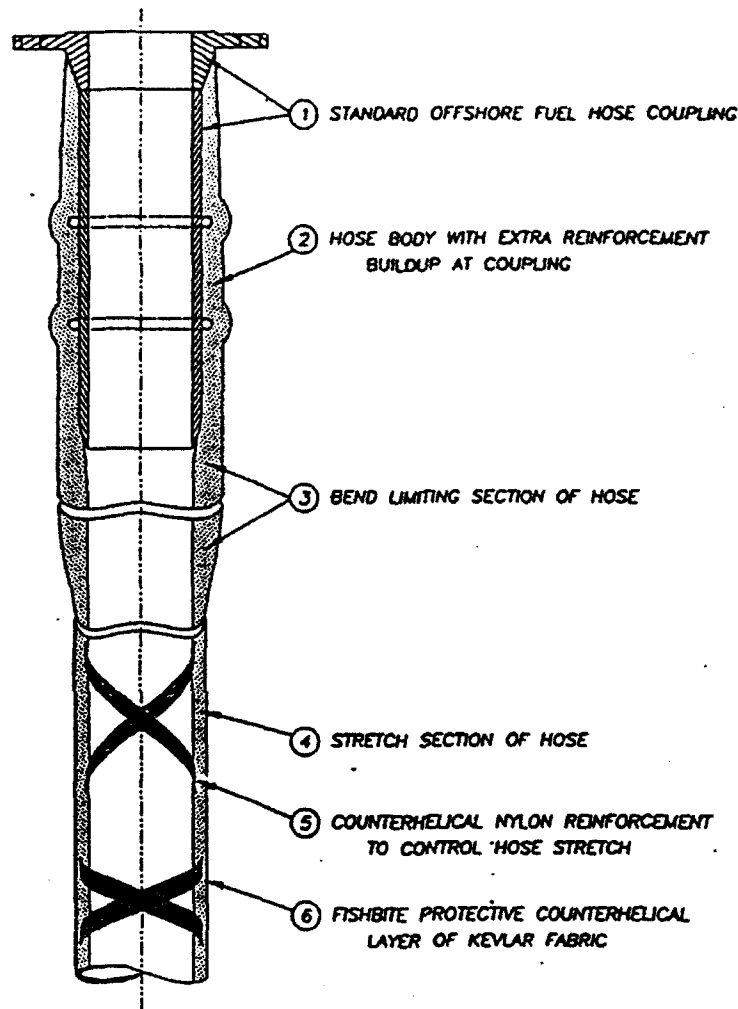
Fig. 10.   Cross section of stretch hose and termination

Laboratory Fatigue Testing of Hose

A special test machine was built by a commercial laboratory to simulate combined axial elongation and flexing cycles experienced by the surface buoy end of the hose in service at sea. Short test hoses were built to fit the machine. One end of the tester stretches and relaxes the hose, while the other end bends it back and forth at a faster frequency. Flex angle, amount of axial stretch, and flex and stretch test frequencies can be adjusted. The hose was marked every inch along its 6 ft overall length to measure the local stretch under applied axial tension, in particular the changes of stretch near the hose terminations caused by the addition of extra reinforcement in those locations (Fig. 11).

Fill pressure and continuity of the electrical conductors were monitored throughout the tests. So far two hoses have been tested and failed by developing rupture areas in the hose wall at the flexing termination, with
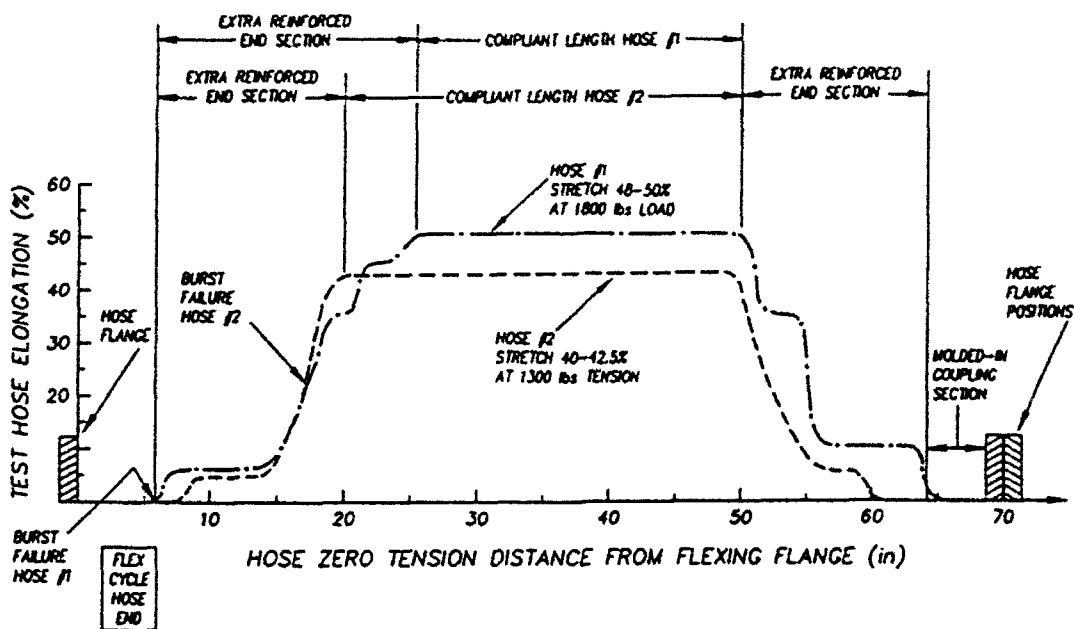
Fig. 11.   Elongation under maximum tension
            of test hoses

no noticeable damage to the reinforcement. Test results are shown in Table 1.
The test conditions were designed to be considerably more severe than those
expected in stormy sea conditions, and future tests will determine the
endurance under lower test tensions. The hose construction near the
terminations is being modified to allow a more gradual reduction of the high
hose extension in its compliant center to the zero stretch condition at the
hose coupling.

BEHAVIOR IN SEA TRIALS

Both the *Standard* and the *Snubber* systems were deployed offshore Bermuda for
an engineering test on September 16, 1993 from the research vessel
Weatherbird. The *Snubber* system was recovered a few days later when the
engineering data telemetered through Argos suggested a loss in buoyancy in the
system. Upon recovery it was discovered that the lower 10-15m of the 80m long
Snubber hose had collapsed. The fill fluid used has only 75% of the density
of seawater and was pushed to the upper portion of the hose mooring. The
lower portion flattened temporarily, causing less displacement and thereby the
loss in system buoyancy. Electrical communication was not affected, and the
hose recovered completely its original round shape. The *Standard* SSAR was
recovered unharmed and redeployed for an endurance test at a site 50 miles
from the southwest shore of the island.

On December 5, 1993, the *Standard* array drifted very close to the reef on the
southwest corner of the island (less than a mile). It was promptly recovered
from the RV Weatherbird and redeployed four days later at a new location, 87
miles from the northeast end of Bermuda (32° 19'N, 63° 14'W). According to the
Pilot chart current data, the prevailing current in this area should prevent
the *Standard* SSAR to drift back to Bermuda. A current (2/17/94) update on
position, trajectory, and engineering data is shown in Fig. 12.

Table 1: Conditions and results of hose flex and
tension fatigue cycling tests.

TEST RESULTS	HOSE SAMPLE #1	HOSE SAMPLE #2
Min and Max Load	0-1,800 lbs	0-1,300 lbs
Load Cycle Duration	10 sec	9.5 sec
Elongation* at Maximum Load	50%	42.5%
Flex Angle	45°	25°
Duration of Flex Cycle	3 sec	2.5 sec
Fill Fluid Pressure at Max Tension	220 psi	105 psi
Load Cycles till Failure	4,152	9,878
Flex Cycles till Failure	13,761	39,546
Failure Type and Localization	Burst failure at end of steel coupling. Reinforcement intact.	1/4" burst at taper of extra rein- forcement; hose otherwise intact.

* Elongation measured in compliant section of test hoses at load cycle 100.

ACKNOWLEDGEMENTS AND SUMMARY

We are at about the midpoint of the development of the SSAR drifting buoy
systems for the GAMOT program. Through system modeling as well as modeling
and fatigue testing of the compliant stretch hose component we seek to gain
sufficient knowledge to achieve at least one year electrical and mechanical
service life of the buoy system.
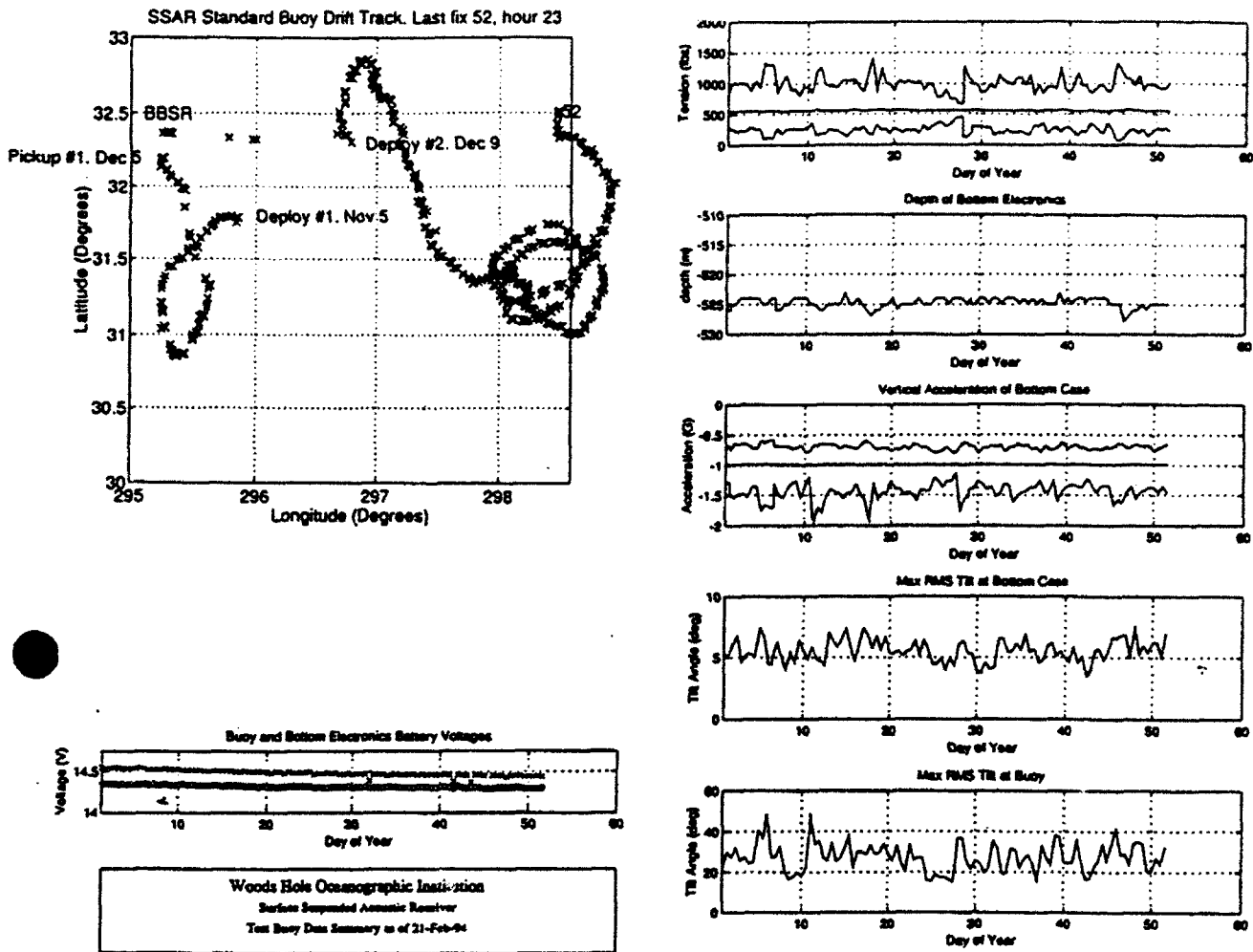
Fig. 12. *Standard* Test buoy data summary as of 2/21/94

REFERENCES

Berteaux, H.O. (1989). Equipment Lowering Mechanics. In: <u>Handbook of Oceanographic Winch, Wire and Cable Technology</u> (A. Driscoll, Ed.), Chapter 9, pp. 9-7, 9-19

Goeller, J.E. (1969). <u>A theoretical and experimental investigation of a flexible cable system subjected to longitudinal excitation</u>. Dissertation, Catholic University, Washington D.C., pp. 83-150

OCIMF Guide to Purchasing, Manufacturing and Testing of Loading and Discharge Hoses for Offshore Moorings (1991). Oil Companies International Marine Forum, 4th ed., Witherby & Co. Ltd, London.

Treloar, L.R.G. and G. Riding (1962). <u>A theory of the stress-strain properties of continuous filament yarns</u>. Shirley Institute Memoirs, Vol. XXXV, 69-83

DELIVERABLES

One deliverable was due during this quarter:
1. Array motion compensation software. Following the sea tests it was determined that the software was not required.

There are three deliverables due during the next quarter:
1. A detailed plan for implementing the investigation of more complex ocean models and providing a prototype design of an experiment for monitoring the North Pacific for climate change and natural variability.
2. SSAR design and test report
3. Delivery of SSARs 1 through 3

Figure:
Fig. 1 GAMOT Deliverable Master Schedule

TASK	DELIVERABLE	Start Date	1993							1994												1995							
			J	J	A	S	O	N	D	J	F	M	A	M	J	J	A	S	O	N	D	J	F	M	A	M	J	J	A
A.1	SOURCE DEPTH, FREQ, LOCATION AND TYPE RECOMMENDATION	11/30/93						◆																					
A.2	RANGE OF ACCEPTABLE SSAR DEPTHS	11/30/93							◆																				
A.3	SIGNAL PROCESSING OF SSAR SIGNAL	6/30/95																										◇	
A.4	ARRAY MOTION COMPENSATION SOFTWARE	3/30/94										◆																	
A.5	SEASONAL MULTIPATH ALGORITHMS	6/30/95																										◇	
A.6	ARGOS RECEPTION ERROR STUDY	6/30/95																										◇	
A.7	ALTERNATIVE SATELLITE SYSTEM EVALUATION	6/30/95																										◇	
A.8	REAL TIME TOMOGRAPHY ALGORITHMS	6/30/95																										◇	
A.9	NEW WORK: SEASONAL CYCLE INFLUENCES ON ACOUSTIC TRAVEL TIMES BASED ON ANALYSIS OF 1987 TOMO DATA	8/30/94																◇											
A.10	NEW WORK: OCEAN MODEL OF TEMPERATURE MAPPING USING SSARS	5/30/95																									◇		
B.1	1980-1991 EQUATORIAL WIND FIELD MODEL STATEMENT OF COMPLETION	6/30/93	◆																										
B.2	EXTRACT THE COASTAL KELVIN SIGNAL FROM THE EQUATORIAL MODEL AND DRIVE THE MID-LATITUDE MODEL FROM 1980-1990 AND PROVIDE A VIDEO OF THE SOLUTION	9/30/93				◆																							

Figure 1: GAMOT Deliverable Master Schedule

TASK	DELIVERABLE	Start Date	1993 (J J A S O N D)	1994 (J F M A M J J A S O N D)	1995 (J F M A M J J A)
B.3	INTEGRATE THE MODEL SOLUTIONS BETWEEN HAWAII AND WEST COAST RECEIVERS AND PROVIDE A GRAPH OF TRAVEL TIME DIFFERENCE AS A FUNCTION OF TIME AND GREAT CIRCLE PATH	9/30/93	◆ (S/O 1993)		
B.4	DRAFT PAPER (AND PROGRESS REPORT) DEMONSTRATING CONNECTION BETWEEN OBSERVED ACOUSTIC DATA AND OCEAN CLIMATE MODEL	12/30/93	◆ (D 1993)		
B.5	PROVIDE DETAILED PLAN FOR IMPLEMENTING INVESTIGATION FOR MORE COMPLICATED MODELS. PROVIDE PROTOTYPE DESIGN OF EXPERIMENT FOR MONITORING THE NORTH PACIFIC FOR CLIMATE CHANGE AND NATURAL VARIABILITY	6/30/94		◇ (J 1994)	
B.6	DOCUMENT RAY TRACING PROGRAMS USED IN OCEAN PHYSICAL MODELING	12/30/94		◇ (D 1994)	
B.7	REPORT ON THE ANALYSIS OF THE RUN OF 1970-1991 NRL MODELS	5/30/95			◇ (M 1995)
B.8	IMPLEMENT DATA ASSIMILATION PLAN USING ADJOINT MODEL	5/30/95			◇ (M 1995)

Figure 1: GAMOT Deliverable Master Schedule

TASK	DELIVERABLE	Start Date	Timeline (1993 – 1995)
B.9	FINAL REPORT EXPLAINING OR NOT EXPLAINING OBSERVED CLIMATE VARIABILITY IN THE NORTH PACIFIC OCEAN	6/30/95	◇ (Jun 1995)
C.1	SSAR PROGRESS REPORT	11/30/93	◆ (Nov 1993)
C.2	SSAR DESIGN AND TEST REPORT	4/30/94	◇ (Apr 1994)
C.3	SSAR UPDATED DESIGN REPORT	3/30/95	◇ (Mar 1995)
	SSAR DELIVERIES		
C.4	TWO PROTOTYPES	8/30/93	◆ (Aug 1993)
C.5	SSARs 1 THRU 3	6/19/94	◇ (Jun 1994)
C.6	SSARs 4 THRU 6	8/14/94	◇ (Aug 1994)
C.7	SSARs 7 THRU 10	10/16/94	◇ (Oct 1994)
	CRUISE REPORTS		
C.8	DEPLOY SSARs 1-3	9/18/94	◇ (Sep 1994)
C.9	DEPLOY SSARs 4-6	10/30/94	◇ (Oct 1994)
C.10	DEPLOY SSARs 7-10	11/27/94	◇ (Nov 1994)
C.11	SSAR FINAL REPORT	6/30/95	◇ (Jun 1995)
D.1	70 HZ SOURCE ASSESSMENT		
D.1	MOORING FABRICATION REPORT		
D.2	AUTONOMOUS MOOR AT SEA TEST AND CRUISE REPORT		

ALL TASK D DELIVERABLES WILL BE RESCHEDULED FOLLOWING THE APPROVAL OF THE PROPOSAL TO INCREASE THE SCOPE OF THIS TASK TO

Figure 1: GAMOT Deliverable Master Schedule

TASK	DELIVERABLE	Start Date
D.3	MOORING DEPLOYMENT CRUISE REPORT	
D.4	MOORING MAINTENANCE CRUISE REPORT	
E.1	DARPA COORDINATION MEETINGS AND PROGRAM BRIEFS	5/20/93 6/7/93 7/1/93 9/16/93 10/15/93 1/16/94
E.2	QUARTERLY PROGRESS REPORTS	7/15/93 10/15/93 1/15/94 4/15/94 7/15/94 10/15/94 1/15/95 4/15/95
E.3	FINAL PROJECT REPORT	6/30/95
F.1	TRANSITION PLAN IMPACT REPORT	6/30/95
F.2	LONG TERM PROGRAM INPUT REPORT	6/30/95
F.3	LONG TERM PROGRAM RISK ANALYSIS REPORT	6/30/95

INCLUDE PROCUREMENT OF A 70 Hz SOURCE.

Figure 1: GAMOT Deliverable Master Schedule